

University of Alberta

MINIMAX APPROXIMATION TO LOGNORMAL SUM DISTRIBUTIONS

by

Qiong Xie



A thesis submitted to the Faculty of Graduate Studies and Research in partial fulfillment of the requirements for the degree of **Master of Science**.

Department of Electrical and Computer Engineering

Edmonton, Alberta

Fall 2002



National Library
of Canada

Acquisitions and
Bibliographic Services

395 Wellington Street
Ottawa ON K1A 0N4
Canada

Bibliothèque nationale
du Canada

Acquisitions et
services bibliographiques

395, rue Wellington
Ottawa ON K1A 0N4
Canada

Your file Votre référence

Our file Notre référence

The author has granted a non-exclusive licence allowing the National Library of Canada to reproduce, loan, distribute or sell copies of this thesis in microform, paper or electronic formats.

The author retains ownership of the copyright in this thesis. Neither the thesis nor substantial extracts from it may be printed or otherwise reproduced without the author's permission.

L'auteur a accordé une licence non exclusive permettant à la Bibliothèque nationale du Canada de reproduire, prêter, distribuer ou vendre des copies de cette thèse sous la forme de microfiche/film, de reproduction sur papier ou sur format électronique.

L'auteur conserve la propriété du droit d'auteur qui protège cette thèse. Ni la thèse ni des extraits substantiels de celle-ci ne doivent être imprimés ou autrement reproduits sans son autorisation.

0-612-81501-3

University of Alberta

Library Release Form

Name of Author: Qiong Xie

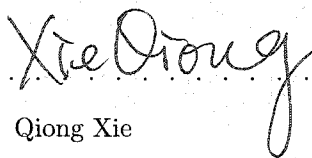
Title of Thesis: Minimax Approximation to Lognormal Sum Distributions

Degree: Master of Science

Year this Degree Granted: 2002

Permission is hereby granted to the University of Alberta Library to reproduce single copies of this thesis and to lend or sell such copies for private, scholarly or scientific research purposes only.

The author reserves all other publication and other rights in association with the copyright in the thesis, and except as hereinbefore provided, neither the thesis nor any substantial portion thereof may be printed or otherwise reproduced in any material form whatever without the author's prior written permission.



Qiong Xie

2nd Floor, ECERF,

University of Alberta

Edmonton, Alberta

Canada, T6G 2V4

Date: Oct. 4, 2002

University of Alberta

Faculty of Graduate Studies and Research

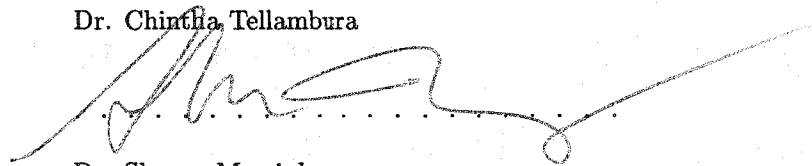
The undersigned certify that they have read, and recommend to the Faculty of Graduate Studies and Research for acceptance, a thesis entitled **Minimax Approximation to Lognormal Sum Distributions** submitted by Qiong Xie in partial fulfillment of the requirements for the degree of **Master of Science**.



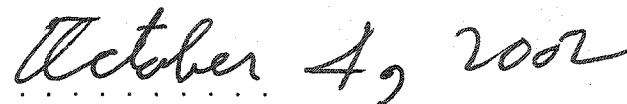
Dr. Norman C. Beaulieu (Supervisor)



Dr. Chintha Tellambura



Dr. Sharon Morsink

Date: 

Abstract

A longstanding problem in wireless engineering is to determine the probability distribution of a sum of independent lognormal random variables. Many approximate solutions to this problem have been developed. But none of them is valid over a wide range of parameters.

A generic approach to find a sum distribution of independent random variables is to use characteristic functions. However the characteristic function of a lognormal random variable is not known. The numerical computation of the characteristic function was even considered to be substantially difficult.

In this thesis, an efficient numerical method is found to evaluate the characteristic function of a lognormal random variable. Then the CDF of a sum of N independent lognormal random variables is obtained by the inverse transform of the characteristic function of the sum evaluated. Based on these numerical data, we compare previous approximate methods and conclude that if a lognormal random variable is used to approximate the sum distribution, neither Schwartz & Yeh's nor Wilkinson's approaches is good. A new paradigm of constructing approximations to lognormal sum distributions, the minimax approximation that minimizes the maximum error, was presented for determining mean values and variances of the corresponding Gaussian distributions. Our work shows that this new method is better than others in the global view.

To my parents

Acknowledgments

I would like to express my sincere appreciation to my supervisor Dr. Norman C. Beaulieu for his insightful guidance, exceptional expertise, continuous encouragement and financial support during the whole course of this work.

I would like to thank my husband Yuan Sha for his encouragement and technical advice in aspect of numerical evaluations. Special thanks to David Young and other people in our iCORE Wireless Communications Lab. for the help on numerical evaluation, documentation and other technical issues.

I thank my parents and my brother for their love and long-time encouragement.

This thesis was financially supported through research assistantships provided by the Alberta Informatics Circle of Research Excellence (iCORE).

Contents

1	Introduction	1
1.1	Overview	1
1.2	Lognormal Shadowing	4
1.3	Lognormal Random Variables	5
1.4	Sums of Lognormal Random Variables	8
1.5	Literature Review	10
1.5.1	Wilkinson's Method	11
1.5.2	Schwartz and Yeh's Method	12
1.5.3	Farley's Method	14
1.5.4	Comparisons of Methods	15
1.6	Thesis Outline and Contributions	16
2	Numerical Computation of the Characteristic Function of a Lognormal	
	Random Variable and the Inverse Transform	17
2.1	The Characteristic Function of a Lognormal Random Variable	18
2.2	Modified Hermite Polynomial Method	20
2.3	Transformed Integral	22
2.3.1	Trapezoidal Rule	26

2.3.2	Simpson's Rule	29
2.3.3	Adaptive Algorithm	32
2.4	Fast Fourier Transform Approach	32
2.4.1	Sampling	35
2.4.2	Truncation	35
2.5	Integration Between the Zeros of the Integrand	37
2.5.1	Division of the interval	40
2.5.2	Integration methods over each subinterval	41
2.5.3	ϵ -algorithm	45
2.6	Comparison of Numerical Methods	47
2.7	Inverse Fourier Transform to PDF and CDF	51
2.7.1	FFT	51
2.7.2	Modified Clenshaw-Curtis	52
3	Minimax Approximation to the Sum Distribution	58
3.1	CDF of the Sum Distribution	58
3.2	Minimax Approximation	64
3.3	Discussion	75
3.4	Minimax approximations of sums with different power means	77
3.5	Minimax approximations of sums with different dB spreads	82
3.6	Conclusion	85
4	Conclusion	86
	References	89

List of Tables

2.1	FFT sizes for the lognormal CF's	37
2.2	Comparison of numerical integration methods	50
3.1	Minimax approximation of the sums of i.i.d lognormal RV's	74

List of Figures

1.1	Frequency reuse of cellular radio systems.	2
1.2	The PDF's of four lognormal distributions $\Lambda(0, \sigma^2)$	8
1.3	The PDF's of three lognormal distributions $\Lambda(m, 1)$	9
2.1	Real and imaginary parts of lognormal CF computed using modified Hermite polynomials for $\sigma = 0.25$	21
2.2	Transformation of the integral.	23
2.3	(a) The transformed integrand in (2.16a). (b) The transformed integrand in (2.16b) for $w = 20$ and $\sigma = 6$ dB.	25
2.4	Real and imaginary parts of a lognormal CF computed using trapezoidal rule ($\sigma = 6$ dB).	27
2.5	Real and imaginary parts of a lognormal CF computed using trapezoidal rule ($\sigma = 12$ dB).	28
2.6	Real and imaginary parts of a lognormal CF computed using Simpson's rule ($\sigma = 6$ dB).	30
2.7	Real and imaginary parts of a lognormal CF computed using Simpson's rule ($\sigma = 12$ dB).	31

2.8	(a) Real and imaginary parts of a lognormal CF computed using an adaptive algorithm for $\sigma = 6$ dB. (b) Magnitudes of the real and imaginary parts of a lognormal CF computed using an adaptive algorithm for $\sigma = 6$ dB.	33
2.9	(a) Real and imaginary parts of a lognormal CF computed using an adaptive algorithm for $\sigma = 12$ dB. (b) Magnitudes of the real and imaginary parts of a lognormal CF computed using an adaptive algorithm for $\sigma = 12$ dB.	34
2.10	Lognormal PDF with different σ	36
2.11	(a) Real and imaginary parts of a lognormal CF computed using FFT for $\sigma = 6$ dB. (b) Magnitudes of the real and imaginary parts of a lognormal CF computed using FFT for $\sigma = 6$ dB.	38
2.12	(a) Real and imaginary parts of a lognormal CF computed using FFT for $\sigma = 12$ dB. (b) Magnitudes of the real and imaginary parts of a lognormal CF computed using FFT for $\sigma = 12$ dB.	39
2.13	(a) Real and imaginary parts of a lognormal CF computed using modified Clenshaw-Curtis method for $\sigma = 6$ dB. (b) Magnitudes of the real and imaginary parts of a lognormal CF computed using modified Clenshaw-Curtis method for $\sigma = 6$ dB.	48
2.14	(a) Real and imaginary parts of a lognormal CF computed using modified Clenshaw-Curtis method for $\sigma = 12$ dB. (b) Magnitudes of the real and imaginary parts of a lognormal CF computed using modified Clenshaw-Curtis method for $\sigma = 12$ dB.	49
2.15	Complementary CDF of a sum of 6 i.i.d. lognormal RV's ($m = 0$ dB, $\sigma = 6$ dB) computed using the FFT.	53

2.16	Comparison of the theoretical PDF and the PDF computed using the numerical inverse transform for $m = 0$ dB and $\sigma = 12$ dB.	55
2.17	Comparison of the theoretical CDF and the CDF computed using the numerical inverse transform for $m = 0$ dB and $\sigma = 12$ dB.	56
3.1	The CDF of the sum of N i.i.d. lognormal RV's ($m = 0$ dB, $\sigma = 6$ dB). . . .	62
3.2	The CDF of the sum of N i.i.d. lognormal RV's ($m = 0$ dB, $\sigma = 12$ dB). . .	63
3.3	Minimax approximation to the CDF.	65
3.4	The CDF of a sum of 2 i.i.d. lognormal RV's ($m = 0$ dB, $\sigma = 6$ dB). . . .	68
3.5	The CDF of a sum of 2 i.i.d. lognormal RV's ($m = 0$ dB, $\sigma = 12$ dB). . . .	69
3.6	The CDF of a sum of 6 i.i.d. lognormal RV's ($m = 0$ dB, $\sigma = 6$ dB). . . .	70
3.7	The CDF of a sum of 6 i.i.d. lognormal RV's ($m = 0$ dB, $\sigma = 12$ dB). . . .	71
3.8	The CDF of a sum of 10 i.i.d. lognormal RV's ($m = 0$ dB, $\sigma = 6$ dB). . . .	72
3.9	The CDF of a sum of 10 i.i.d. lognormal RV's ($m = 0$ dB, $\sigma = 12$ dB). . . .	73
3.10	The CDF of a sum of 6 lognormal RV's with different power means ($m_1 = -3$ dB, $m_2 = -2$ dB, $m_3 = -1$ dB, $m_4 = 1$ dB, $m_5 = 2$ dB, $m_6 = 3$ dB) and the same dB spreads ($\sigma_i = 6$ dB).	78
3.11	The CDF of a sum of 6 lognormal RV's with different power means ($m_1 = -3$ dB, $m_2 = -2$ dB, $m_3 = -1$ dB, $m_4 = 1$ dB, $m_5 = 2$ dB, $m_6 = 3$ dB) and the same dB spreads ($\sigma_i = 12$ dB).	79
3.12	The CDF of a sum of 6 lognormal RV's with different power means ($m_1 = -25$ dB, $m_2 = -15$ dB, $m_3 = -5$ dB, $m_4 = 5$ dB, $m_5 = 15$ dB, $m_6 = 25$ dB) and the same dB spreads ($\sigma_i = 6$ dB).	80

- 3.13 The CDF of a sum of 6 lognormal RV's with different power means ($m_1 = -25$ dB, $m_2 = -15$ dB, $m_3 = -5$ dB, $m_4 = 5$ dB, $m_5 = 15$ dB, $m_6 = 25$ dB) and the same dB spreads ($\sigma_i = 12$ dB). 81
- 3.14 The CDF of a sum of 6 lognormal RV's with different dB spreads ($\sigma_1 = 6$ dB, $\sigma_2 = 8$ dB, $\sigma_3 = 9$ dB, $\sigma_4 = 10$ dB, $\sigma_5 = 11$ dB, $\sigma_6 = 12$ dB) and the same power means ($m_i = 0$ dB). 83
- 3.15 The CDF of a sum of 6 lognormal RV's with different dB spreads ($\sigma_1 = 7.5$ dB, $\sigma_2 = 8$ dB, $\sigma_3 = 8.5$ dB, $\sigma_4 = 9$ dB, $\sigma_5 = 9.5$ dB, $\sigma_6 = 10$ dB) and the same power means ($m_i = 0$ dB). 84

Acronyms

Acronym	Definition
PDF	Probability Density Function
CDF	Cumulative Distribution Function
CF	Characteristic Function
RV	Random Variable
i.i.d	Independently and Identically Distributed
FFT	Fast Fourier Transform

Symbol Notation

Symbol	Definition
\mathcal{A}	Random event A
$E[X]$	Expectation of X
E_n	The maximum deviation in minimax approximation
$f(\cdot)$	Probability density function
$f'(\cdot)$	The first deviative of the function $f(x)$
$f''(\cdot)$	The second deviative of the function $f(x)$
$f^{(n)}(\cdot)$	The n th deviative of the function $f(x)$
f_m	The maximum non-zero frequency
f_0	Frequency resolution in FFT
f_s	Sample frequency in FFT
$f_X(\cdot)$	Probability density function of X
$F(\cdot)$	Cumulative distribution function
$F_X(\cdot)$	Cumulative distribution function of X
$G(\cdot)$	Complementary CDF
$G_X(\cdot)$	Complementary CDF of X
Gn	n -point Gaussian quadrature rule
$g(\cdot)$	A function after some transformation

Im	Imaginary part of a complex number
K_n	n -point Gauss-Kronrod rule
m	Mean value of a Gaussian distribution
m_X	Mean value of a Gaussian distribution X
N	The number of the summands in a sum
	Size of FFT algorithm
$N(m, \sigma^2)$	A normal distribution with mean m and variance σ^2
L_i	The i th summand of a lognormal sum
L_m	The summand with the largest dB spread
L^*	A lognormal RV estimated by minimax approximation
$p_n(x)$	Polynomial of the degree n
P_n	Polynomial space of the degree n
$Q(\cdot)$	Q-function
Re	Real part of a complex number
R_n	Remainder
S_n	Approximation of Simpson's rule with n subintervals
$T_k(\cdot)$	Chebyshev polynomial of the degree k
T_n	Approximation of trapezoidal rule with n subintervals
x_i	Abscissa or node in numerical integration methods
X_t	Truncation length in FFT
ε_{abs}	Absolute tolerance
ε_{rel}	Relative tolerance
$\Lambda(m, \sigma)$	A lognormal RV with the corresponding the Gaussian RV $N(m, \sigma^2)$
$\phi(\cdot)$	Characteristic function

$\phi_0(\cdot)$	Characteristic function of a lognormal RV $\Lambda(0, \sigma)$
$\phi_X(\cdot)$	Characteristic function of X
$\Phi(\cdot)$	CDF of the standard normal distribution $N(0, 1)$
$\Phi^{-1}(\cdot)$	Inverse function of the CDF of the standard normal distribution $N(0, 1)$
σ	Standard deviation of a Gaussian distribution
σ_X	Standard deviation of a Gaussian distribution X

Chapter 1

Introduction

In the first half of 2002, the number of cellular mobile phone subscribers all over the world broke the one billion mark. The sustained growth of the number of cellular mobile users gives the operators impetus to increase the capacities of their systems. An important problem that must be faced is co-channel interference. Co-channel interference can be characterized as a sum of lognormal random variables.

1.1 Overview

In a cellular frequency-reuse radio system, the radio frequencies or channels available for an operator are divided into a number of channel sets, each of which is used to cover a certain cell that is the elemental component of a service area. Channel (frequency) assignment follows the rule that the same frequency set cannot be employed by two adjacent cells but can be reused in two separated cells in a systematic way such that the possible separation (reuse distance) between the same frequency sets is maximized. This system is called frequency reuse. Frequency reuse greatly increases frequency utilization and further increase

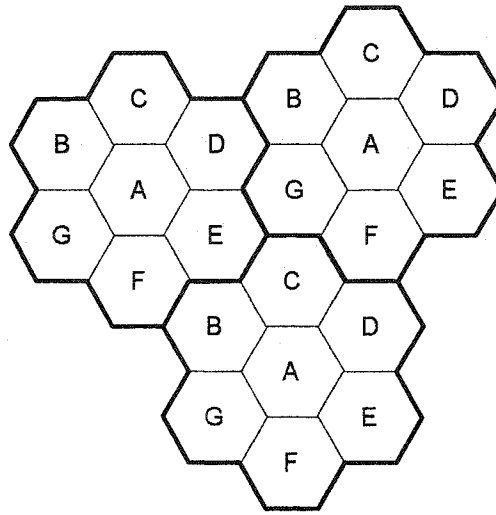


Figure 1.1. Frequency reuse of cellular radio systems (after [1, Fig. 3.1]).

system capacity. However, frequency reuse also introduces co-channel interference arising from distant transmitters using the same frequencies.

For example, in Figure 1.1, the whole available frequencies for a service provider are divided into 7 sets and each set is assigned to one cell. Every 7 cells that uses the complete set of available frequencies form a cluster. The cluster size in this case is 7 and the typical value is 4, 7 or 12. Then the cluster is replicated to cover a certain service area. The cells labeled with the same letter use the same group of channels. They are called co-channel cells. Therefore, co-channel interference occurs between these cells. Co-channel interference cannot be simply combated by increasing the transmit power to improve signal-to-noise ratio (SNR) because the interference to neighboring co-channel cells also increases. In order to reduce co-channel interference, co-channel cells must be physically separated by a sufficient distance so that the interference level in a given cell is below a tolerance due to the radio propagation loss. If the size of a cell is kept constant, a large cluster size is desirable to weaken co-channel interference because a large cluster size implies a large

distance between co-channel cells. On the other hand, the cluster size is important to determine the capacity of a cellular system. This is because if the cluster size is reduced while remaining the same cell size, more clusters are required to cover a given area and hence more users can be served. Thus, there is a trade-off between the capacity and the co-channel interference. Co-channel interference is one of the major factors that limit the capacity of a cellular system.

When a mobile station moves through the service area, the received signal experiences both fading and shadowing. Fading indicates that the envelope of the received signal fluctuates rapidly due to multipath propagation. Shadowing, in contrast, is a phenomenon that the signal envelope gradually changes in the local mean level due to signal blocking by buildings, foliage and hills. Empirical studies have shown that shadowing has a lognormal distribution. Since the effect of fast fading caused by multipath propagation can be mitigated by employing some form of micro-diversity, shadowing of a radio signal can be a more serious transmission impairment than fading. Therefore, co-channel interference becomes strongly dependent on this large scale signal variations originating from shadowing phenomena.

Co-channel interference in cellular telephone systems can be modeled as a sum of lognormal random variables. However, determining the sum distribution of lognormal random variables is a longstanding problem in wireless engineering, even for the case of independent and statistically identical co-channel interference signals. Sums of lognormal random variables also occur in many other important communication problems like the detection of radar targets in clutter and the optimal detection of frequency hopped spread spectrum signals [1].

Studying sum distributions of independent lognormal signals is a good start to the prob-

lem of this kind. Many approximate solutions to the probability distribution of a sum of lognormal random variables such as Wilkinson's [2], Schwartz and Yeh's [2], and Farley's [2] methods have been reported. But none of them is dominant and well-accepted. Many works also focused on the comparison of these methods [1] - [5].

The well-known approach for studying the probability distribution of a sum of independent random variables uses the characteristic function. This approach is totally general because the probability density function of a sum of N independent random variables has a characteristic function equal to the product of the characteristic functions of the summands. However, the characteristic function of a lognormal random variable is unknown.

In this thesis, the numerical computation of lognormal characteristic functions and sum distributions of lognormal random variables are investigated in much greater detail than previously. Moreover, a new paradigm for approximating the distributions of lognormal sums is presented.

1.2 Lognormal Shadowing

Reflection, diffraction and scattering in the radio frequency propagation environment lead to three nearly independent phenomena, fast multipath fading, slow shadowing and pass loss, which correspond to instantaneous signal envelope, local mean and area mean of a received signal, respectively.

In wireless communications, there are usually many radio propagation paths between the transmitter and the receiver due to reflection, diffraction and scattering. The radio waves through different paths possess random amplitudes and phases. The constructive and destructive addition of these radio waves at the receiver leads to rapid fluctuations, called multipath fading or fast fading, in the envelope of the received signal. The main

statistical models for multipath fading include Rayleigh, Ricean, and Nakagami fading.

The mean envelope or power called local mean can be obtained if the fast fluctuation of the envelope is averaged over a distance of 20 to 30 wavelengths. Usually, the local mean will also experience slow variations due to the presence of terrain features such as surrounding buildings, foliage and hills. This phenomenon is called shadowing or slow shadow fading. Experiment observations have confirmed that shadowing follows a lognormal distribution. The signal envelope or power in decibel units of a lognormal shadowed signal is Gaussian distributed about the area mean that is the mean value of the local mean.

The area mean is the average received signal strength over a large area between the transmitter and the receiver. Area mean is directly related to path loss which describes how a signal attenuates with the distance between the transmitter and the receiver. Generally the received power P_r for an arbitrary transmitter-receiver separation d is inversely proportional to the α -th power of the distance d . The quantity α is path loss exponent.

Because some wireless techniques like diversity channel coding can be employed to minimize the effects of the fast multipath fading, the slow signal variations from lognormal shadowing are more serious than rapid fading. For this reason, and to limit the scope of this thesis, our analysis concentrates on the shadowing effect only.

1.3 Lognormal Random Variables

A lognormal random variable (RV) is characterized in that the logarithm of this RV has a Gaussian distribution. Let $X = 10 \log_{10} L$. If X is normally distributed with probability density function (PDF)

$$f_X(x) = \frac{1}{\sqrt{2\pi}\sigma_X} \exp \left[-\frac{(x - m_X)^2}{2\sigma_X^2} \right], \quad (1.1)$$

L is said to be a lognormal RV with PDF

$$f_L(l) = \begin{cases} \frac{1}{\lambda \sqrt{2\pi} \sigma_X l} \exp \left[-\frac{(10 \log_{10} l - m_X)^2}{2\sigma_X^2} \right] & l > 0, \\ 0 & l \leq 0. \end{cases} \quad (1.2)$$

where m_X and σ_X are the mean and standard deviation of the Gaussian RV X , respectively, both of which have decibel units and $\lambda = \ln(10)/10 = 0.23026$ [1]. In a mobile radio environment, the parameter σ_X , sometimes called the dB spread, is typically between 6 dB and 12 dB for practical channels where 6 dB represents a light-shadowed mobile radio environment and 12 dB represents a heavy-shadowed environment.

Generally, the natural logarithm of L is more convenient to handle mathematically. Define the Gaussian RV $Y = \ln L$. The PDF of Y is

$$f_Y(y) = \frac{1}{\sqrt{2\pi} \sigma_Y} \exp \left[-\frac{(y - m_Y)^2}{2\sigma_Y^2} \right] \quad (1.3)$$

with mean m_Y and standard deviation σ_Y , which are related to X by

$$Y = \lambda X, \quad m_Y = \lambda m_X, \quad \sigma_Y = \lambda \sigma_X. \quad (1.4)$$

The PDF of the RV L can be correspondingly given by

$$f_L(l) = \begin{cases} \frac{1}{\sqrt{2\pi} \sigma_Y l} \exp \left[-\frac{(\ln l - m_Y)^2}{2\sigma_Y^2} \right] & l > 0, \\ 0 & l \leq 0. \end{cases} \quad (1.5)$$

The moments of a lognormal RV can be easily computed using the moment generating function of the normal distribution as

$$E[L^n] = E[(e^Y)^n] = e^{nm_Y + \frac{1}{2}n^2\sigma_Y^2}. \quad (1.6)$$

Consequently, the mean value of a lognormal RV is obtained by setting $n = 1$

$$m_L = E[L] = E[e^Y] = e^{m_Y + \frac{1}{2}\sigma_Y^2} \quad (1.7)$$

and the variance is

$$\begin{aligned}\sigma_L^2 &= E[L^2] - m_L^2 = e^{2m_Y + 2\sigma_Y^2} - e^{2m_Y + \sigma_Y^2} \\ &= e^{2m_Y + \sigma_Y^2} (e^{\sigma_Y^2} - 1).\end{aligned}\tag{1.8}$$

The cumulative distribution function (CDF) of a lognormal RV is given by

$$\begin{aligned}F_L(x) &= P(L \leq x) = P(e^Y \leq x) = P(Y \leq \ln x) \\ &= 1 - Q\left(\frac{\ln x - m_Y}{\sigma_Y}\right)\end{aligned}\tag{1.9}$$

where $P(L \leq x)$ is the probability that $L \leq x$ and $Q(x)$ is the complementary CDF of the standard normal distribution written as

$$Q(x) = \frac{1}{\sqrt{2\pi}} \int_x^\infty e^{-t^2/2} dt, \quad x \geq 0.\tag{1.10}$$

The complementary CDF is

$$G_L(x) = 1 - F(x) = Q\left(\frac{\ln x - m_Y}{\sigma_Y}\right).\tag{1.11}$$

Generally a lognormally distributed variable with two parameters m and σ is denoted by $\Lambda(m, \sigma^2)$. The corresponding normal distribution is denoted by $N(m, \sigma^2)$. Figure 1.2 shows the PDF curves of four lognormal RV's $\Lambda(0, \sigma^2)$ for $\sigma = 0.2, 0.5, 1.3816$ (6 dB), 2.3026 (10 dB). Since the PDF of a lognormal RV $\Lambda(m, \sigma^2)$ with non-zero mean can be written as

$$\begin{aligned}f(x) &= \frac{1}{\sqrt{2\pi}\sigma x} \exp\left[-\frac{(\ln x - m)^2}{2\sigma^2}\right] = \frac{1}{\sqrt{2\pi}\sigma x} \exp\left[-\frac{\ln^2(xe^{-m})}{2\sigma^2}\right] \\ &= e^{-m} f_0(xe^{-m})\end{aligned}\tag{1.12}$$

where $f_0(\cdot)$ denotes the PDF of the lognormal RV $\Lambda(0, \sigma^2)$ with zero mean and the same variance, it is seen that the parameter m scales the magnitude and X-coordinate of the

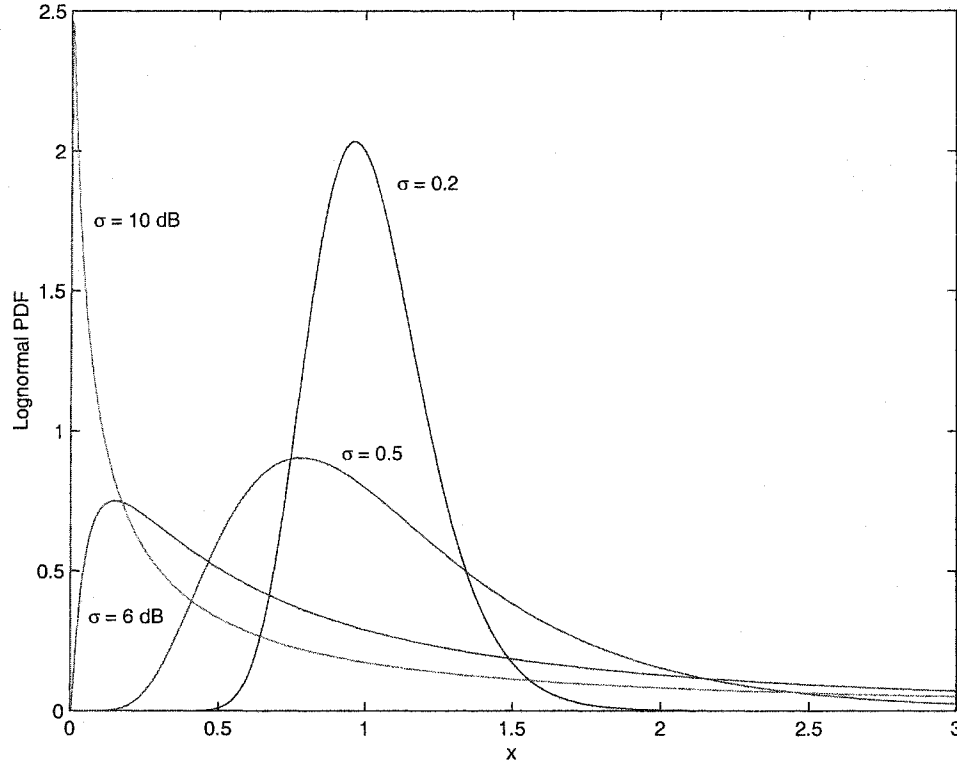


Figure 1.2. The PDF's of four lognormal distributions $\Lambda(0, \sigma^2)$.

PDF of the lognormal RV $\Lambda(0, \sigma^2)$. This parameter can be regarded as a scale factor of a lognormal distribution. Figure 1.3 illustrates the PDF curves of three lognormal variables $\Lambda(m, 1)$ for $m = 0, 1.0, 2.0$.

1.4 Sums of Lognormal Random Variables

A well-known assumption to a sum of lognormally distributed variables is that the sum distribution is well approximated by another lognormal RV, i.e.

$$L = L_1 + L_2 + \dots + L_N = e^{Y_1} + e^{Y_2} + \dots + e^{Y_N} \approx e^Z. \quad (1.13)$$

Here the random variable Z follows a normal distribution.

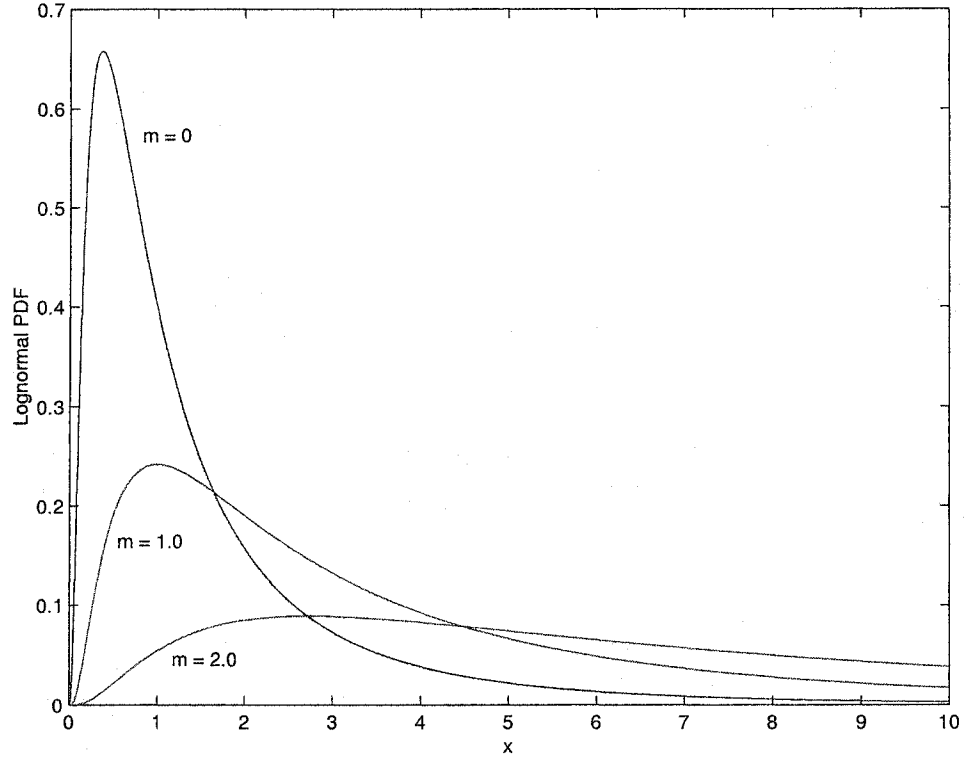


Figure 1.3. The PDF's of three lognormal distributions $\Lambda(m, 1)$.

Estimating outage probabilities in shadowed wireless environments with co-channel interference is one of the important practical applications of sums of lognormal random variables. The outage probability is usually defined in terms of excess co-channel interference; i.e. the resultant interference power is greater than the wanted signal power divided by an appropriate power protection ratio.

Usually, there are N interference signals arriving at the receiver from co-channel mobiles or base stations in a cellular radio system. Both the local mean power level S of the desired signal, $S = e^{Y_0}$, and the local mean power level I_i of the each interference signal, $I_i = e^{Y_i} (i = 1, \dots, N)$, are known as lognormal distributions. The total interference signal

is generally modeled as a sum of N lognormally distributed signals given by

$$I = \sum_{i=1}^N I_i. \quad (1.14)$$

Therefore, the outage probability is defined as [6] [7]

$$\begin{aligned} P_{out} &= P\left(\frac{S}{I} < q\right) = P(I > S/q) \\ &= \int_0^\infty G_I(s/q) f_s(s) da \end{aligned} \quad (1.15)$$

where q is the power protection ratio. This dimensionless quantity depends on modulation techniques and the desired performance. If the assumption (1.13) is used, the outage probability can be written as [1]

$$\begin{aligned} P_{out} &= P\left(\frac{S}{I} < q\right) = P\left(\frac{e^{Y_0}}{e^Z} < q\right) = P(Y_0 - Z < \ln q) \\ &= 1 - Q\left(\frac{\ln q - m_{Y_0} + m_Z}{\sqrt{\sigma_{Y_0}^2 + \sigma_Z^2}}\right) \end{aligned} \quad (1.16)$$

due to the fact that $(Y_0 - Z)$ is a Gaussian distribution.

In practical problems, both values of the CDF and the complementary CDF of the sum less than 10^{-1} are of great interest. To put it another way, the both tails of the CDF are of central concern. For example, outage probabilities in the thermal noise arising from statistical detection problems of radar targets in lognormal clutter involve values of the CDF in the range of 10^{-1} to 10^{-6} . Outage probabilities in co-channel interference are related to the complementary CDF.

1.5 Literature Review

Many approximate solutions have been developed extensively in the past to compute the moments or complementary CDF of a sum of independent lognormal signals. Brief descriptions of these approximations are given in this section.

1.5.1 Wilkinson's Method

Wilkinson's method is based on the widely accepted assumption that the sum of lognormal RV's can be approximated by a lognormal RV. According to Wilkinson's method, the mean value and standard deviation of Z are determined by matching the first and second moments of both sides of (1.13) to give:

$$E[e^Z] = E[L_1 + L_2 + \cdots + L_N], \quad (1.17)$$

$$E[e^{2Z}] = E[(L_1 + L_2 + \cdots + L_N)^2]. \quad (1.18)$$

Combining (1.6) with (1.17) and (1.18), we get

$$\begin{aligned} e^{m_Z + \frac{1}{2}\sigma_Z^2} &= E[L_1] + E[L_2] + \cdots + E[L_N] \\ &= \sum_{i=1}^N e^{m_{Y_i} + \frac{1}{2}\sigma_{Y_i}^2} = u_1 \end{aligned} \quad (1.19)$$

and

$$\begin{aligned} e^{2m_Z + 2\sigma_Z^2} &= \sum_{i=1}^N E[L_i^2] + 2 \sum_{i=1}^{N-1} \sum_{j=i+1}^N E[L_i]E[L_j] \\ &= \sum_{i=1}^N \sigma_{L_i}^2 + u_1^2 = u_2 + u_1^2 \end{aligned} \quad (1.20)$$

where

$$\begin{aligned} \sigma_{L_i}^2 &= E[L_i^2] - E[L_i]^2, \\ u_2 &= \sum_{i=1}^N \sigma_{L_i}^2 = \sum_{i=1}^N e^{2m_{Y_i} + \sigma_{Y_i}^2} (e^{\sigma_{Y_i}^2} - 1). \end{aligned} \quad (1.21)$$

Finally m_Z and σ_Z can be found by solving (1.19) and (1.20) yielding:

$$m_Z = \ln u_1 - \sigma_Z^2/2, \quad (1.22)$$

$$\sigma_Z^2 = \ln \left(\frac{u_2}{u_1^2} + 1 \right). \quad (1.23)$$

1.5.2 Schwartz and Yeh's Method

An exact expression is derived by Schwartz and Yeh for the first two moments of the sum of only two lognormal signals. Based on the assumption that the sum of two lognormal RV's is also a lognormal distribution, Schwartz and Yeh's approach deploys a recursive procedure to calculate the moments of the sum of $N > 2$ lognormal signals, i.e. using the result of the sum of i lognormal signals to obtain the first two moments of the sum of $i + 1$ lognormal signals. This procedure is illustrated as:

$$\begin{aligned} e^Z &= e^{Y_1} + e^{Y_2} + \dots + e^{Y_N} \\ &= e^{Z_2} + e^{Y_3} + \dots + e^{Y_N} = \dots \\ &= e^{Z_{N-1}} + e^{Y_N}. \end{aligned} \tag{1.24}$$

Due to the recursive procedure, we are only interested in the detail of Schwartz and Yeh's method for the case of two components, i.e.

$$e^Z = e^{Y_1} + e^{Y_2} \tag{1.25}$$

where the Gaussian RV's Y_1 and Y_2 have means m_{Y_1} and m_{Y_2} and standard deviations σ_{Y_1} and σ_{Y_2} , respectively.

Define a new Gaussian RV, $Y_d = Y_2 - Y_1$, so that

$$m_{Y_d} = m_{Y_2} - m_{Y_1}, \tag{1.26}$$

$$\sigma_{Y_d}^2 = \sigma_{Y_1}^2 + \sigma_{Y_2}^2. \tag{1.27}$$

After a very long manipulation in [2], the expression for the mean value of the Gaussian RV Z is given by

$$m_Z = m_{Y_1} + G_1 \tag{1.28a}$$

where

$$G_1 = m_{Y_d} \Phi \left(\frac{m_{Y_d}}{\sigma_{Y_d}} \right) + \frac{\sigma_{Y_d}}{\sqrt{2\pi}} e^{-m_{Y_d}^2/(2\sigma_{Y_d}^2)} + \sum_{k=1}^{\infty} c_k e^{k^2 \sigma_{Y_d}^2/2} \left[e^{km_{Y_d}} \Phi \left(\frac{-m_{Y_d} - k\sigma_{Y_d}^2}{\sigma_{Y_d}} \right) + T_1 \right] \quad (1.28b)$$

with

$$T_1 = e^{-km_{Y_d}} \Phi \left(\frac{m_{Y_d} - k\sigma_{Y_d}^2}{\sigma_{Y_d}} \right), \quad (1.28c)$$

$$c_k = \frac{(-1)^{k+1}}{k}. \quad (1.28d)$$

and the variance is given by

$$\sigma_Z^2 = \sigma_{Y_1}^2 - G_1^2 - 2\sigma_{Y_1}^2 G_3 + G_2 \quad (1.28e)$$

where

$$G_2 = \sum_{k=1}^{\infty} b_k T_2 + \left[1 - \Phi \left(-\frac{m_{Y_d}}{\sigma_{Y_d}} \right) \right] (m_{Y_d}^2 + \sigma_{Y_d}^2) + \frac{m_{Y_d} \sigma_{Y_d}}{\sqrt{2\pi}} e^{-m_{Y_d}^2/(2\sigma_{Y_d}^2)} + \sum_{k=1}^{\infty} b_k e^{-(k+1)m_{Y_d} + (k+1)^2 \sigma_{Y_d}^2/2} \Phi \left(\frac{m_{Y_d} - \sigma_{Y_d}^2(k+1)}{\sigma_{Y_d}} \right) - 2 \sum_{k=1}^{\infty} c_k e^{-m_{Y_d} k + k^2 \sigma_{Y_d}^2/2} \left[m_{Y_k} \Phi \left(-\frac{m_{Y_k}}{\sigma_{Y_k}} \right) - \frac{\sigma_{Y_d}}{\sqrt{2\pi}} e^{-m_{Y_k}^2/(2\sigma_{Y_d}^2)} \right], \quad (1.28f)$$

$$G_3 = \sum_{k=0}^{\infty} (-1)^k e^{k^2 \sigma_{Y_d}^2/2} T_1 + \sum_{k=0}^{\infty} (-1)^k T_2 \quad (1.28g)$$

with

$$T_2 = e^{m_{Y_d}(k+1) + (k+1)^2 \sigma_{Y_d}^2/2} \Phi \left(\frac{-m_{Y_d} - (k+1)\sigma_{Y_d}^2}{\sigma_{Y_d}} \right), \quad (1.28h)$$

$$b_k = \frac{2(-1)^{k+1}}{k+1} \sum_{j=1}^k \frac{1}{j}, \quad (1.28i)$$

and

$$m_{Y_k} = -m_{Y_d} + k\sigma_{Y_d}^2. \quad (1.28j)$$

Obviously the computational complexity of this method is much greater than that of Wilkinson's method.

1.5.3 Farley's Method

Farley's approach assumes that the summands are N independently and identically distributed (i.i.d.) RV's each with corresponding Gaussian mean value m_Y and variance σ_Y^2 .

Farley approximated the complementary CDF of the lognormal sum

$$L = \sum_{i=1}^N L_i = \sum_{i=1}^N e^{Y_i} = \sum_{i=1}^N e^Y$$

as

$$P(L > \gamma) \approx 1 - \left[1 - Q\left(\frac{\ln \gamma - m_Y}{\sigma_Y}\right) \right]^N. \quad (1.29)$$

This method was proved by Beaulieu and Abu-Dayya [1] to be a strict lower bound on the complementary CDF of the i.i.d. lognormal sum. Let

$$\mathcal{A} = \{\text{the event that at least one RV} > \gamma\},$$

$$\mathcal{B} = \{\text{the complement of event } \mathcal{A}\}.$$

The mutually exclusive events \mathcal{A} and \mathcal{B} give the computation of the complementary CDF to be

$$\begin{aligned} P(L > \gamma) &= P(L > \gamma, \mathcal{A}) + P(L > \gamma, \mathcal{B}) \\ &= P(\mathcal{A}) + P(L > \gamma, \mathcal{B}) \\ &> P(\mathcal{A}) = 1 - P(L_i \leq \gamma, i = 1, \dots, N) \\ &= 1 - \left[1 - Q\left(\frac{\ln \gamma - m_Y}{\sigma_Y}\right) \right]^N. \end{aligned} \quad (1.30)$$

Farley's method can be easily extended to sums of lognormal RV's that are not i.i.d. The result is

$$P(L > \gamma) > 1 - \prod_{i=1}^N \left[1 - Q\left(\frac{\ln \gamma - m_{Y_i}}{\sigma_{Y_i}}\right) \right]. \quad (1.31)$$

Correspondingly the upper bound of the CDF of a lognormal sum is

$$P(L \leq \gamma) \leq \prod_{i=1}^N \left[1 - Q \left(\frac{\ln \gamma - m_{Y_i}}{\sigma_{Y_i}} \right) \right]. \quad (1.32)$$

1.5.4 Comparisons of Methods

Many works [1] - [5] have discussed comparisons of these methods. Some investigated these approximations to the CDF and complementary CDF while others concentrated on the estimations of the first two moments of the sum distribution. All of these works assessed the accuracies of the methods by comparing results computed using these approximate methods to results from simulation.

In Schwartz & Yeh's paper [2], Wilkinson's method and Schwartz & Yeh's method are compared in terms of their approximations to the first two moments of the lognormal sum distribution. It was stated that the Wilkinson's approach breaks down for $\sigma > 4$ dB which falls in the range of practical values of the dB spread ($6 \text{ dB} \leq \sigma \leq 12 \text{ dB}$).

Beaulieu and Abu-Dayya [1] compared these methods for approximating the CDF and complementary CDF of a sum of i.i.d. lognormal RV's instead of approximating the first two moments. They found that the simpler Wilkinson's approximation may give more accurate results than Schwartz & Yeh's approach for values of the complementary CDF in the range of 10^{-1} to 10^{-6} while Schwartz & Yeh's method, in most cases, provides the most accurate results for values of the CDF less than 0.9. However, Farley's formula gives more accurate estimates than the other two methods for large values of the dB spread $\sigma = 12$ dB.

Cardieri and Rappaport [5] examined the means and standard deviations obtained using Wilkinson's and Schwartz & Yeh's methods for the more general cases when the summands have different mean values and standard deviations in decibel units. It was shown that Schwartz & Yeh's method always provides better accuracy than Wilkinson's method

and is virtually invariant to differences in the mean values and standard deviations of the summands, as well as to the number of summands.

In this thesis, we investigate the assumption that a sum of independent lognormal RV's is also lognormally distributed, which is the basis of Wilkinson's and Schwartz & Yeh's approximations, by numerically computing CDF values of lognormal sums in the range of 10^{-6} to $(1 - 10^{-6})$. This range is much wider than that of previous works. Based on these numerical values of CDF's, we give a more detailed comparison of the above approximate methods and present a new paradigm for constructing approximations to lognormal sum distributions.

1.6 Thesis Outline and Contributions

In this chapter, we give a brief introduction to the background and previous literature on the sum distribution of independent lognormal RV's.

In the next chapter, we investigate the several numerical integration methods for computing the characteristic function (CF) of a lognormal RV for the practical values of dB spread. The curves of the CF's are given and compared for different numerical methods. The CDF values of a sum of independent lognormal RV's are obtained by the inverse Fourier transform of the product of individual CF's.

In Chapter 3, we examine the goodness of the assumption that a sum of independent lognormal RV's is also lognormally distributed and present a new numerical approximation to a lognormal sum distribution based on this assumption. At the same time, we investigate the accuracy of Wilkinson's, Schwartz & Yeh's and Farley's approximations.

In chapter 4, we give a summary and conclusions of the thesis.

Chapter 2

Numerical Computation of the Characteristic Function of a Lognormal Random Variable and the Inverse Transform

The characteristic function (CF) method is a standard approach to determine the probability distribution of a sum of independent RV's. However, the exact form of the CF for a lognormal signal is not known. Computation of the lognormal CF using numerical integration also presents considerable difficulties due to the semi-infinite integration interval, the oscillating behavior of the integrand and the extremely slow decay rate of the tail of the lognormal probability density function (PDF).

In this chapter, we investigate different numerical methods for the lognormal CF's for values of the dB spread of practical interest. The curves of the CF's are given and compared for the different numerical methods to determine the best numerical integration method.

Finally CDF values of a sum of independent lognormal RV's are obtained by the inverse Fourier transform of the product of individual summand CF's.

2.1 The Characteristic Function of a Lognormal Random Variable

The characteristic function is quite useful in determining the probability distribution of a sum because the CF of the sum of independent RV's is equal to the product of the individual CF's. That is, if we have a sum

$$L = \sum_{i=1}^N L_i$$

then the CF of the sum is

$$\phi_L(w) = \prod_{i=1}^N \phi_{L_i}(w) \quad (2.1)$$

where each CF of L_i is actually the Fourier transform (within a minus sign) of its corresponding PDF, $f_{L_i}(x)$, with the form

$$\phi_{L_i}(w) = E[e^{jwx}] = \int_{-\infty}^{\infty} f_{L_i}(x) e^{jwx} dx. \quad (2.2)$$

It is obvious that the PDF can be determined as the inverse Fourier transform of the CF as

$$f_L(x) = \frac{1}{2\pi} \int_{-\infty}^{\infty} \phi_L(w) e^{-jwx} dw \quad (2.3a)$$

$$= \frac{1}{\pi} \int_0^{\infty} \{ \text{Re}[\phi_L(w)] \cos(wx) + \text{Im}[\phi_L(w)] \sin(wx) \} dw. \quad (2.3b)$$

where $\text{Re}[\cdot]$ and $\text{Im}[\cdot]$ denote the real part and the imaginary part, respectively. The last equation is due to the fact that the Fourier transform of a real function has an even real part and odd imaginary part. Using a property of Fourier transform [8, 3.3.7] the CDF of the

sum is obtained as

$$P(L \leq \gamma) = \frac{1}{2\pi} \int_{-\infty}^{\infty} \left[\pi \phi_L(0) \delta(w) - \frac{\phi_L(w)}{jw} \right] e^{-jw\gamma} dw \quad (2.4a)$$

$$= \frac{1}{2} - \frac{1}{2\pi} \int_{-\infty}^{\infty} \frac{\phi_L(w)}{jw} e^{-jw\gamma} dw \quad (2.4b)$$

$$= \frac{1}{2} - \frac{1}{\pi} \int_0^{\infty} \frac{\text{Im}[\phi_L(w)] \cos(w\gamma) - \text{Re}[\phi_L(w)] \sin(w\gamma)}{w} dw. \quad (2.4c)$$

Therefore, the CF provides an general, exact and straightforward approach to find the PDF and the CDF of a sum of independent lognormal random signals. However, no exact expression for the CF of a lognormal RV is known. The Fourier transform of a lognormal RV is very difficult to evaluate even using numerical methods.

In the following sections, several numerical integration approaches are investigated. Because the CF of a lognormal RV is a complex function, numerical computation of the lognormal CF is usually split into two parts, i.e. the real part and imaginary part as

$$\text{Re}[\phi(w)] = \int_{-\infty}^{\infty} f_L(x) \cos(wx) dx = \int_0^{\infty} f_L(x) \cos(wx) dx \quad (2.5)$$

$$\text{Im}[\phi(w)] = \int_{-\infty}^{\infty} f_L(x) \sin(wx) dx = \int_0^{\infty} f_L(x) \sin(wx) dx. \quad (2.6)$$

To simply the computation, let the corresponding Gaussian mean value m equal zero which does not lose generality because, due to (1.12), the CF is expressed by

$$\begin{aligned} \phi(w) &= \int_0^{\infty} f(x) e^{jwx} dx \\ &= \int_0^{\infty} e^{-m} f_0(xe^{-m}) e^{jwx} dx \\ &= \int_0^{\infty} f_0(xe^{-m}) e^{jwx} dx e^{-m} \\ &= \int_0^{\infty} f_0(y) \exp(jwe^m y) dy \\ &= \phi_0(e^m w) \end{aligned} \quad (2.7)$$

where

$$y = e^{-m}x,$$

and $\phi_0(w)$ denotes the CF of the corresponding lognormal RV with zero mean and the same standard deviation in decibel units. Obviously a non-zero mean value only causes a scale factor in frequency.

Due to the spectral symmetry and equations (2.3b) and (2.4c), we only need to evaluate the values of the lognormal CF over the positive frequencies.

2.2 Modified Hermite Polynomial Method

Barakat [9] derived an expression for the CF of a lognormally distributed RV as

$$\phi(w) = e^{jw} e^{-w^2 \sigma^2 / 2} \sum_{n=0}^{\infty} \frac{(j\sigma)^n}{n!} a_n(jw) h_n(\sigma w) \quad (2.8a)$$

where

$$a_n(jw) = \frac{d^n}{dy^n} \exp[jw(e^y - y - 1)]_{y=0} \quad (2.8b)$$

and the Taylor-series coefficients and

$$h_n(x) \equiv H_{e_n}(x) = (-1)^n e^{x^2/2} \frac{d^n}{dx^n} e^{-x^2/2} \quad (2.8c)$$

are defined as modified Hermite polynomials which are different from the normal Hermite polynomials. The relationship with the normal Hermite polynomial is

$$H_{e_n}(x) = 2^{-n/2} H_n\left(\frac{x}{\sqrt{2}}\right). \quad (2.9)$$

Figure 2.1 gives the real and imaginary parts of the lognormal CF for $\sigma = 0.25$. This figure is a replication of [9, Fig.1]. To the best of the authors' knowledge, this is the only graph of the real and imaginary parts of the CF of a lognormal RV published in the literature.

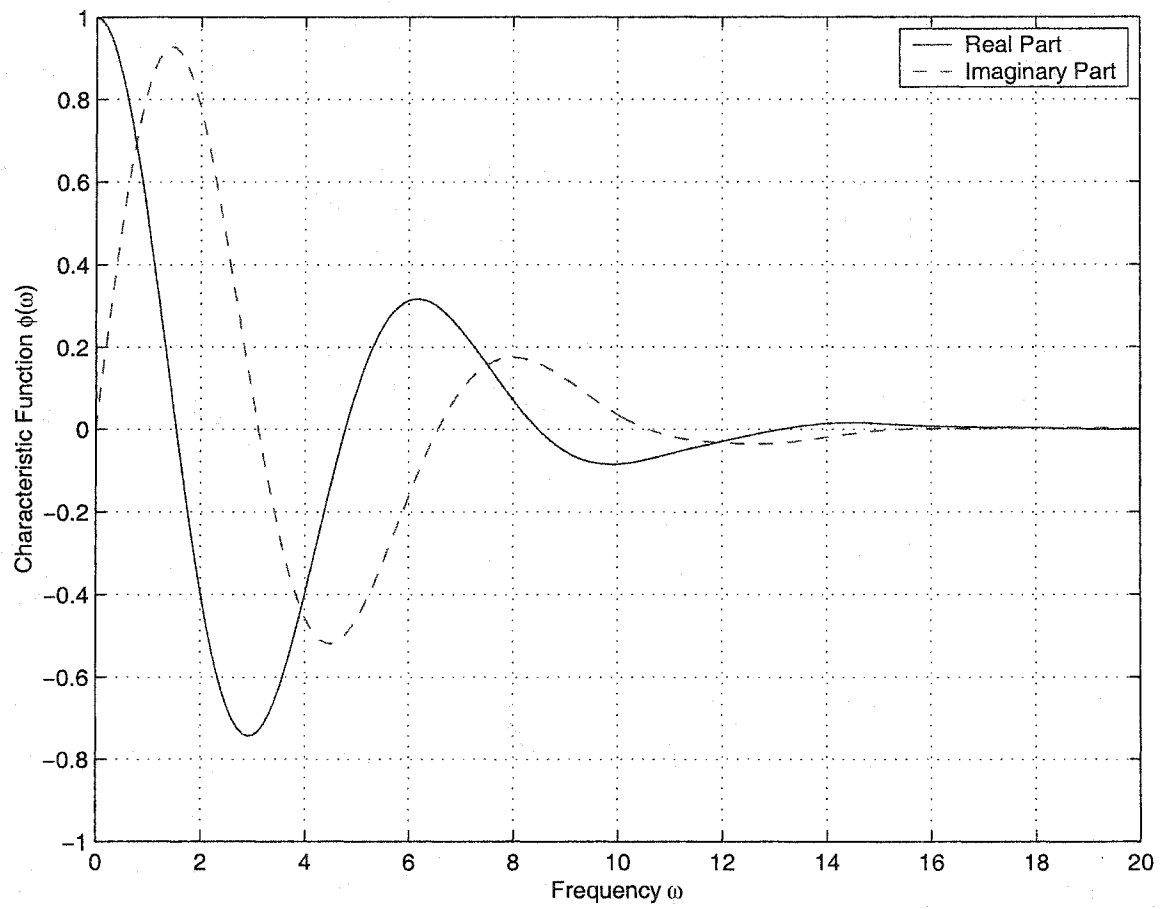


Figure 2.1. Real and imaginary parts of lognormal CF computed using modified Hermite polynomials for $\sigma = 0.25$ (after [9, Fig.1]).

Note the $\sigma = 0.25$ or $\sigma^2 = 0.0625$ corresponding to 1.09 dB spread. Practical problems in wireless communication involve lognormal RV's with values of dB spread ranging from 6 dB to 12 dB. Our empirical tests indicate that the expansion (2.8) can only be used for small values of σ and small values of w . For example, for $\sigma = 1.0$ and $w = 5$, or for $\sigma = 0.25$ and $w = 30$, the series did not converge. These tests were done using MATLAB on a Linux system. We note from Figure 2.1 that the real and imaginary components exhibit oscillatory behavior.

2.3 Transformed Integral

As mentioned in the previous section, the major difficulties encountered in working with numerical integration of the lognormal CF are the following:

- Semi-infinite integration interval;
- Slow decay rate of the lognormal PDF;
- Oscillation behavior of the Fourier integral.

A common approach for dealing with the infinite or semi-infinite integration interval is to make some transformation to change the interval to be finite.

According to the behavior of the lognormal PDF which is a positive-valued function with only one local maximum (unimodal function), its Fourier transform can be performed by evaluating the area below the PDF curve in horizontal strips instead of in vertical strips, if one has knowledge of the inverse PDF function [10]. The following are the details.

Since the lognormal distribution has only one maximum value

$$Y_m = \frac{1}{\sqrt{2\pi}\sigma} e^{\sigma^2/2} \quad (2.10)$$

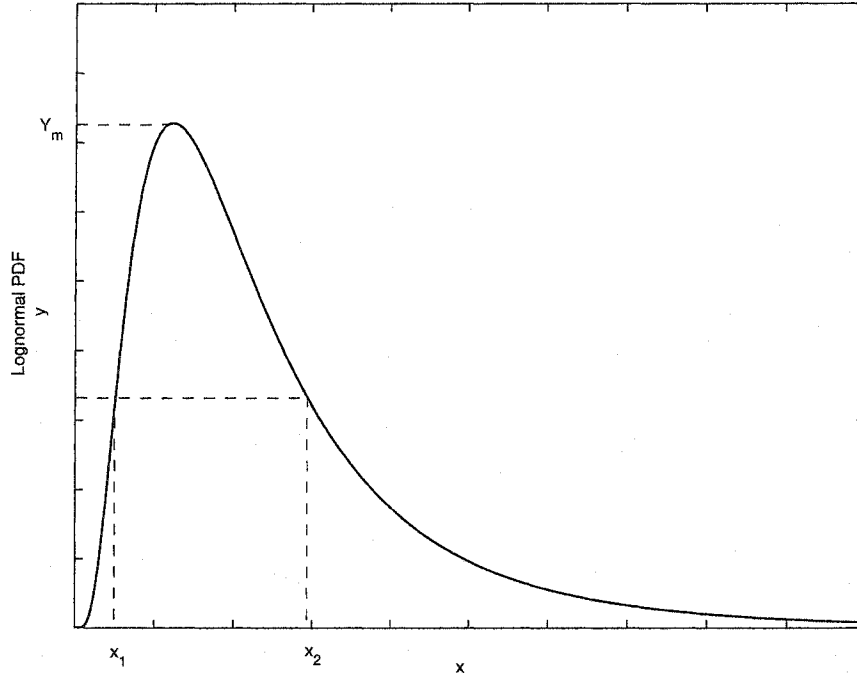


Figure 2.2. Transformation of the integral.

at $x = e^{-\sigma^2}$, the Fourier integral can be transformed to be

$$\begin{aligned}
 \phi(w) &= E[e^{jwx}] = \int_0^\infty f(x) e^{jwx} dx \\
 &= \int_0^\infty \int_0^{f(x)} dy e^{jwx} dx = \int_0^{Y_m} \int_{x_1(y)}^{x_2(y)} e^{jwx} dx dy \\
 &= \int_0^{Y_m} \frac{e^{jwx}}{jw} \Big|_{x_1(y)}^{x_2(y)} dy = \int_0^{Y_m} \frac{e^{jwx_2(y)} - e^{jwx_1(y)}}{jw} dy
 \end{aligned} \tag{2.11}$$

where $x_1(y)$ and $x_2(y)$ are the inverse functions of the lognormal PDF which can be obtained by solving the PDF equation

$$\begin{aligned}
 y &= f(x) = \frac{1}{\sqrt{2\pi}\sigma x} \exp\left(-\frac{\ln^2 x}{2\sigma^2}\right) \\
 \sqrt{2\pi}\sigma y &= \exp\left(-\frac{\ln^2 x}{2\sigma^2} - \ln x\right) \\
 (\ln x)^2 + 2\sigma^2 \ln x + 2\sigma^2 \ln(\sqrt{2\pi}\sigma y) &= 0.
 \end{aligned} \tag{2.12}$$

Solving the equation (2.12), the inverse functions are

$$\begin{aligned} x_1(y) &= \exp(-\sigma^2 - \sigma \sqrt{\sigma^2 - 2 \ln(\sqrt{2\pi}\sigma y)}) \\ &= \exp(-\sigma^2 - \sigma \sqrt{-2 \ln(y/Y_m)}) \end{aligned} \quad (2.13)$$

$$\begin{aligned} x_2(y) &= \exp(-\sigma^2 + \sigma \sqrt{\sigma^2 - 2 \ln(\sqrt{2\pi}\sigma y)}) \\ &= \exp(-\sigma^2 + \sigma \sqrt{-2 \ln(y/Y_m)}). \end{aligned} \quad (2.14)$$

Substituting (2.13) and (2.14) into (2.11) and after some manipulations, the Fourier integral is transformed to be

$$\phi(w) = \frac{Y_m}{jw} \int_0^1 (e^{jwu_2(y)} - e^{jwu_1(y)}) dy \quad (2.15a)$$

where

$$u_1(y) = \exp(-\sigma^2 - \sigma \sqrt{-2 \ln y}) \quad (2.15b)$$

$$u_2(y) = \exp(-\sigma^2 + \sigma \sqrt{-2 \ln y}). \quad (2.15c)$$

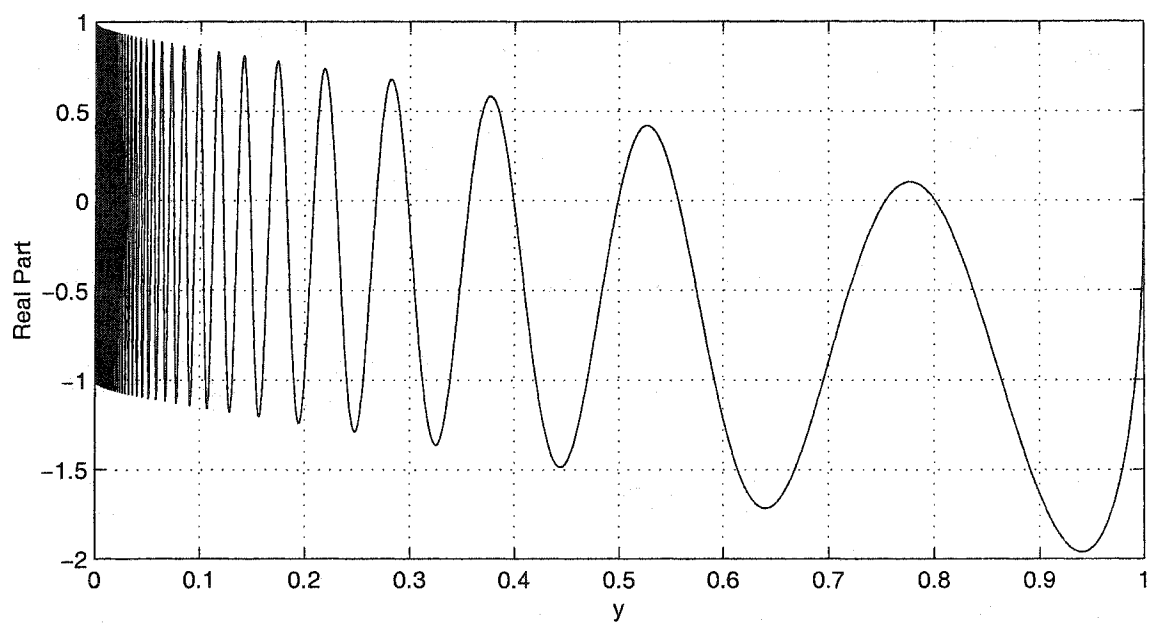
The real part and imaginary part of the transformed integral are given, respectively, by

$$\text{Re}[\phi(w)] = \frac{Y_m}{w} \int_0^1 \{\sin[wu_2(y)] - \sin[wu_1(y)]\} dy \quad (2.16a)$$

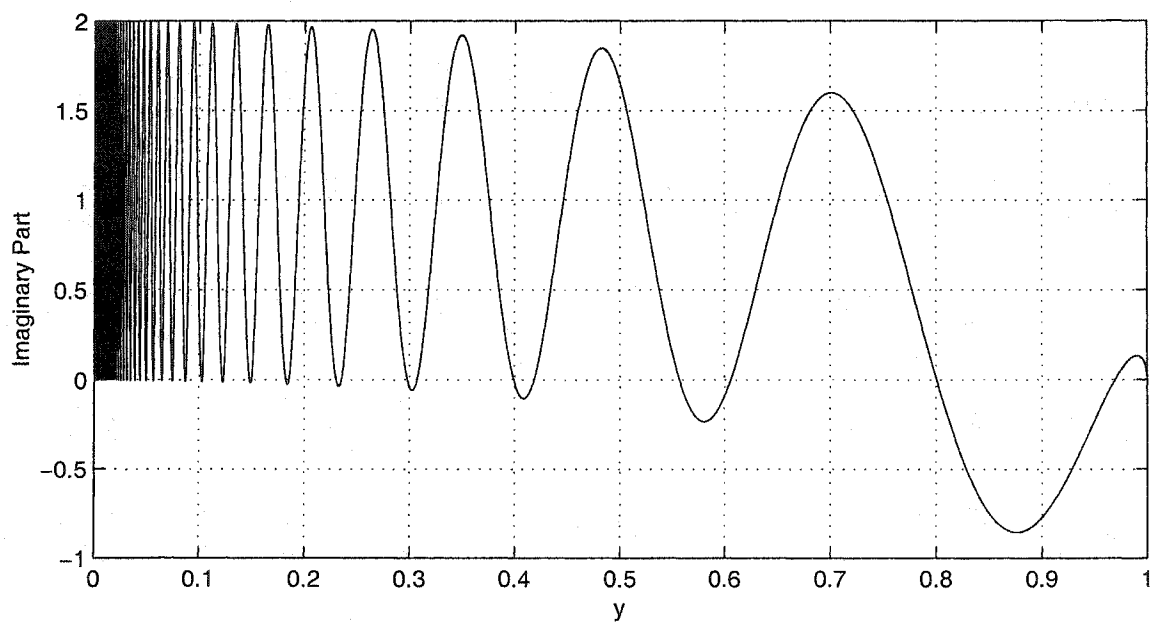
$$\text{Im}[\phi(w)] = \frac{Y_m}{w} \int_0^1 \{\cos[wu_1(y)] - \cos[wu_2(y)]\} dy. \quad (2.16b)$$

These are definite integrals, each with a finite interval that is free of the truncation error that occurs for a semi-infinite integral. Moreover, the form of this transformed integral is quite interesting. However, this integral has a singular point at $y = 0$ which cannot be evaluated in computer systems. Thus, the actual integration interval has to be $[\delta, 1]$ where δ is very small. In addition, it is found that the transformed integrands are still oscillatory functions with irregularly located zeros. They are illustrated in Figure 2.3 for $w = 20$ and $\sigma = 6$ dB.

Figure 2.3 shows that the integrand oscillates more rapidly as y approaches zero and that the envelope is not constant. These features may make the transformed integral inefficient



(a)



(b)

Figure 2.3. (a) The transformed integrand in (2.16a). (b) The transformed integrand in (2.16b) for $w = 20$ and $\sigma = 6$ dB.

to evaluate numerically. In the following subsections, we use the trapezoidal rule and Simpson's rule to compute the transformed integral.

2.3.1 Trapezoidal Rule

In this subsection, we apply the trapezoidal rule to the transformed integral developed in the previous section and use an automatic integration technique that will continue to bisect the subintervals until a preset absolute tolerance ε_{abs} or relative tolerance ε_{rel} is satisfied.

The integration interval $[a, b]$ is divided into n equal subintervals, let $a = x_0 < x_1 < \dots < x_n = b$, $x_i = a + ih$, $h = (b - a)/n$, and the trapezoidal rule is applied to each subinterval.

Then the extended or composite trapezoidal formula [11] is given by

$$T_n = h \left[\frac{1}{2}f(x_0) + f(x_1) + \dots + f(x_{n-1}) + \frac{1}{2}f(x_n) \right]. \quad (2.17)$$

The remainder is

$$R_n = -\frac{(b-a)^3}{12n^2}f''(\xi), \quad a < \xi < b \quad (2.18)$$

for some ξ . But it is not easy to choose the step h or n perfectly at the beginning if the bound of $f''(\xi)$ cannot be found. Therefore, the trapezoidal rule can be implemented in an iterative way. First we set an initial n , calculate T_n , then double the number of subintervals by equally dividing each original subinterval. Then

$$T_{2n} = \frac{1}{2}T_n + \frac{h}{2} \sum_{k=0}^{n-1} f\left(x_k + \frac{h}{2}\right). \quad (2.19)$$

The algorithm (2.19) does not lose the benefit of the previous work. If $|T_{2n} - T_n| < \varepsilon_{abs}$, the iteration stops and T_{2n} is the integration approximation. If not, the iteration will continue until the tolerance is achieved.

The plots of the CF's computed using trapezoidal rule are given in Figure 2.4 for 6 dB spread and Figure 2.5 for 12 dB spread. In Figure 2.5 we found three small abrupt

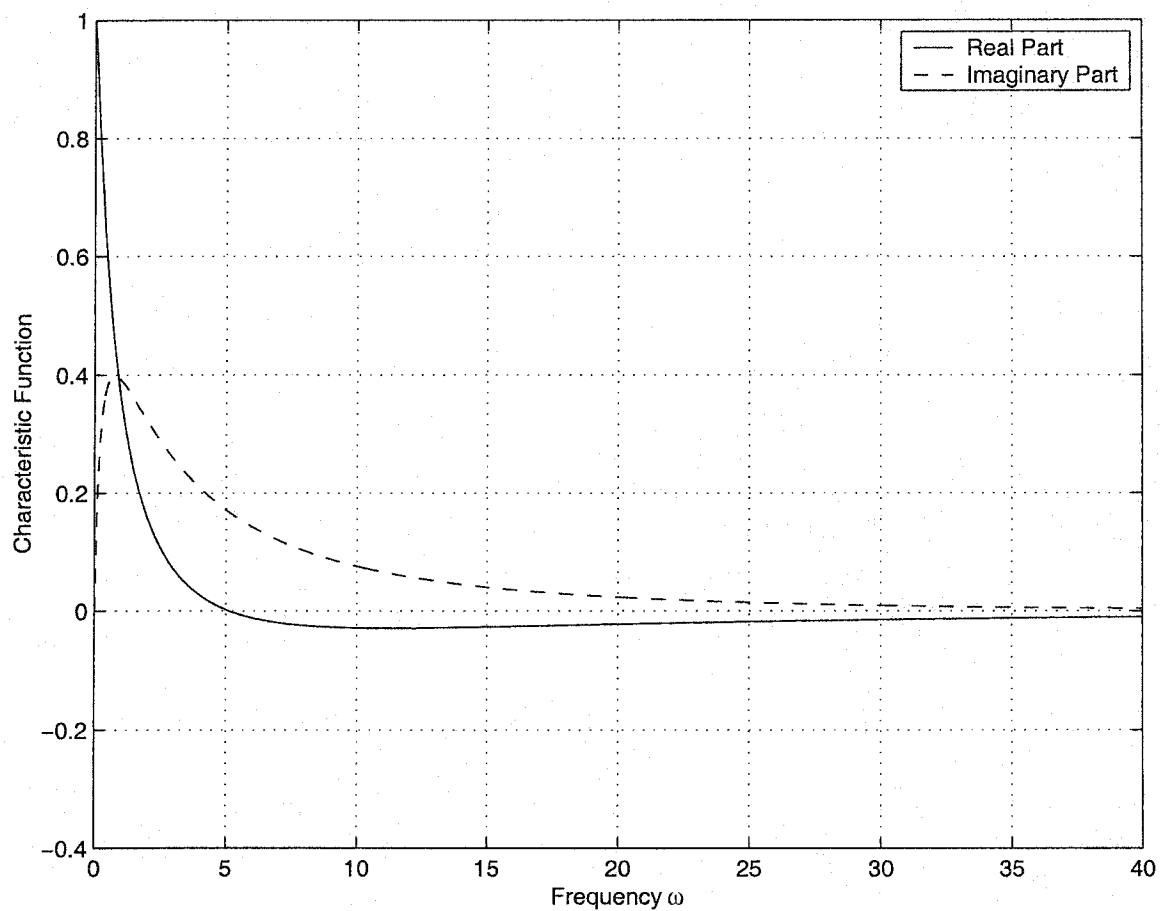


Figure 2.4. Real and imaginary parts of a lognormal CF computed using trapezoidal rule ($\sigma = 6$ dB).

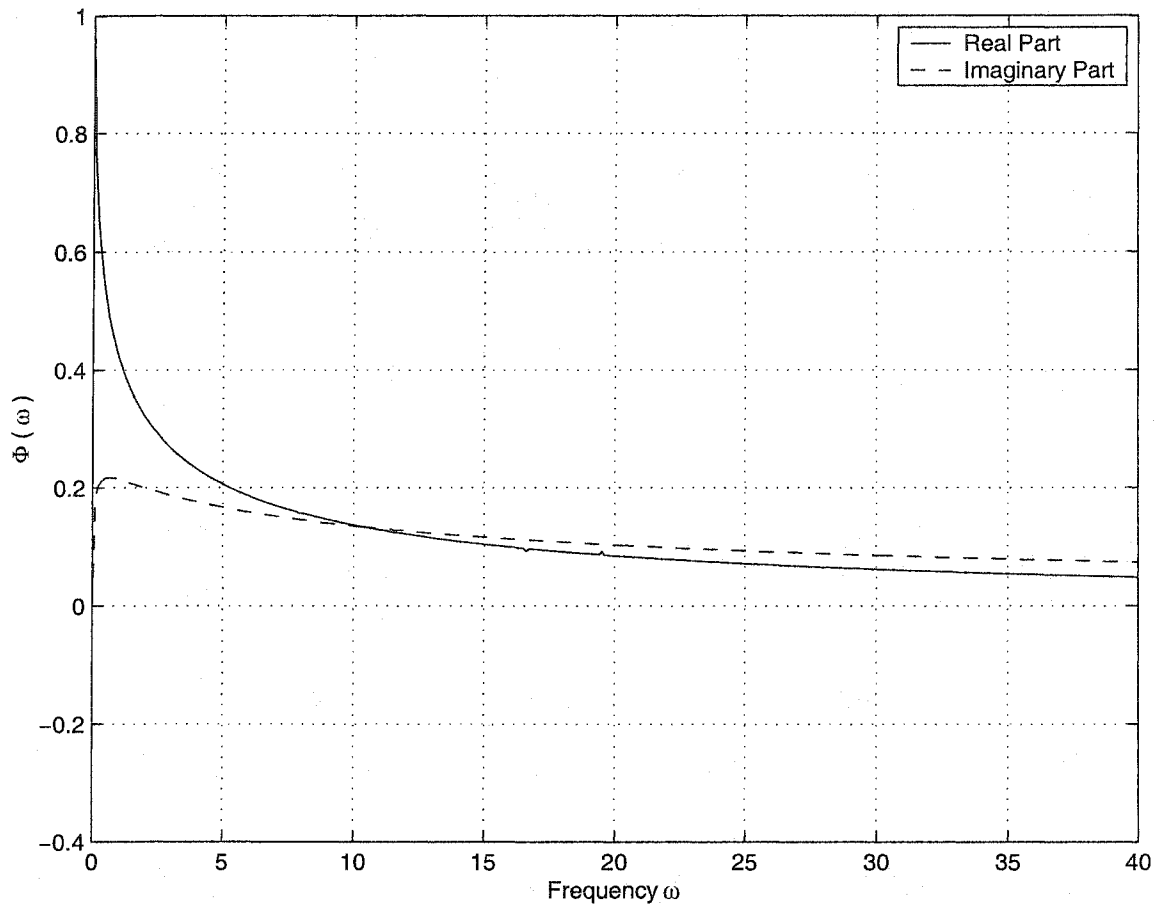


Figure 2.5. Real and imaginary parts of a lognormal CF computed using trapezoidal rule ($\sigma = 12$ dB).

convexities along the curve of the real part of the CF on $w \in [0, 40]$ that illustrates that the use of the trapezoidal rule to compute the transformed integral is not fully stable so that there are some inaccuracies occurring in its evaluation.

2.3.2 Simpson's Rule

Simpson's rule is very frequently used in approximating integrals [11], [12]. This rule approximates $f(x)$ with a quadratic polynomial and, in general, is more efficient and more accurate than the trapezoidal rule when the integrand function has a finite 4th derivative.

The composite Simpson's rule is given as

$$S_{2n} = \frac{h}{3} \left[f(a) + f(b) + 2 \sum_{i=1}^{n-1} f(x_{2i}) + 4 \sum_{i=1}^{n-1} f(x_{2i-1}) \right] \quad (2.20a)$$

where

$$h = \frac{b-a}{2n}, \quad (2.20b)$$

$$x_i = a + ih, \quad i = 1, 2, \dots, 2n-1. \quad (2.20c)$$

The remainder is

$$R_{2n} = -\frac{(b-a)^5}{2880n^4} f^{(4)}(\xi), \quad a < \xi < b. \quad (2.21)$$

An interesting and useful observation is that Simpson's approximation can be calculated from the trapezoidal rule by

$$S_{2n} = \frac{4T_{2n} - T_n}{3}. \quad (2.22)$$

As a result, Simpson's rule can reuse most of the computational effort and programming code of the trapezoidal rule.

The plots of the CF's using Simpson's rule are given in Figure 2.6 for 6 dB spread and Figure 2.7 for 12 dB spread. Similar to the trapezoidal rule, there is a small glitch happening to the imaginary part curve in Figure 2.7 for 12 dB spread.

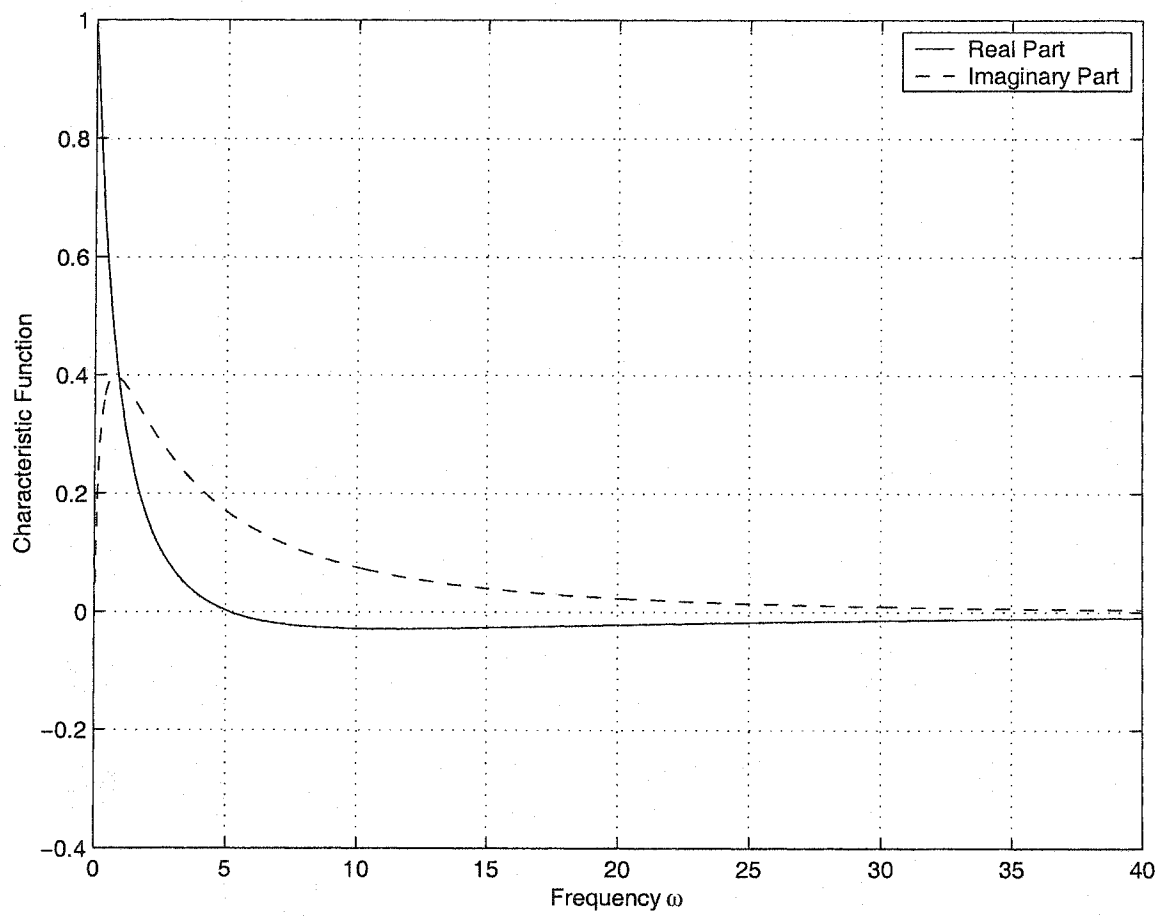


Figure 2.6. Real and imaginary parts of a lognormal CF computed using Simpson's rule ($\sigma = 6$ dB).

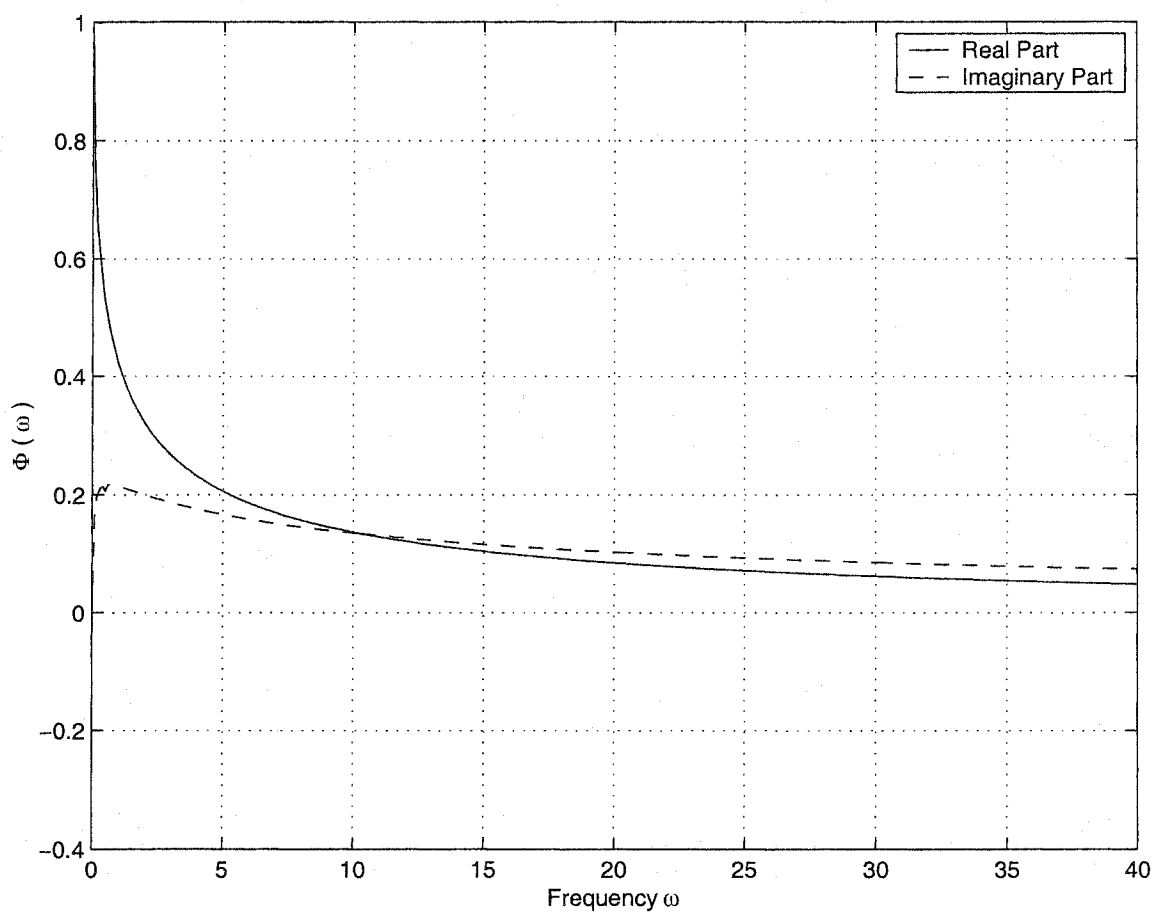


Figure 2.7. Real and imaginary parts of a lognormal CF computed using Simpson's rule ($\sigma = 12$ dB).

Both trapezoidal rule and Simpson's rule are simple numerical techniques to implement but they are not the most efficient. As w increases, the integration becomes extremely time-consuming.

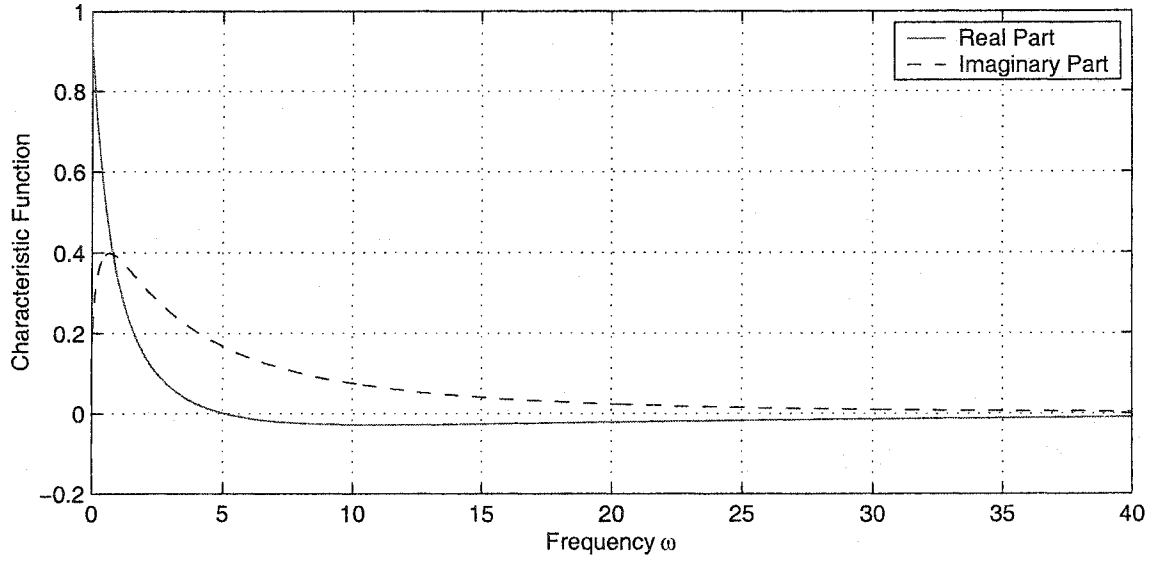
2.3.3 Adaptive Algorithm

Observing the transformed integrand in Figure 2.3, we conjecture that an adaptive algorithm might be helpful because the integrand changes more rapidly when $y \rightarrow 0$. An adaptive algorithm partitions the original subintervals based on the estimated error on each subinterval for each iteration, such that many points are located in the neighborhood of local difficulties of the integrand.

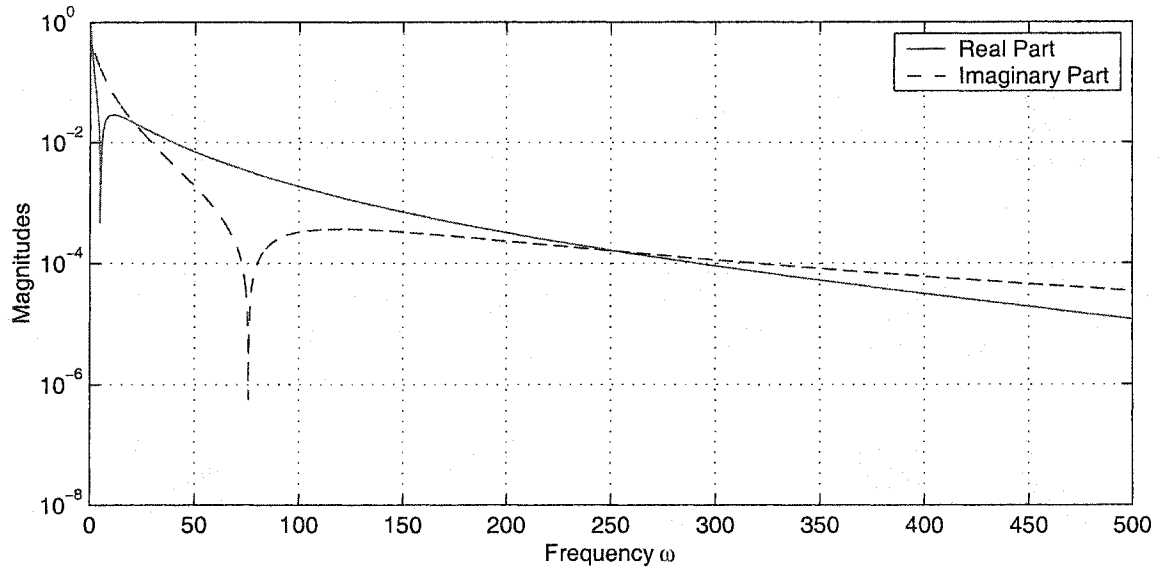
We utilize an adaptive subroutine from GNU Scientific Library (GSL). The algorithm is based on Gauss-Kronrod rule. The curves obtained by this adaptive algorithm, which are illustrated in Figure 2.8 and 2.9 for 6 dB and 12 dB, respectively, are almost the same as those we have obtained using the trapezoidal and Simpson's rules but the computation time is reduced greatly and the curves are smooth without any glitches or cusps. Since the CF values become very small and change slowly beyond the point $w = 40$, we also plot the absolute values of the real and imaginary parts of CF's over a large interval to see how the CF's decay with the frequency w .

2.4 Fast Fourier Transform Approach

The fast Fourier transform (FFT) usually provides an efficient approach to the spectral analysis of a signal. The FFT also can be used to evaluate the Fourier integral of a function. However, the PDF of a lognormal RV is a continuous function with a long slowly-decaying

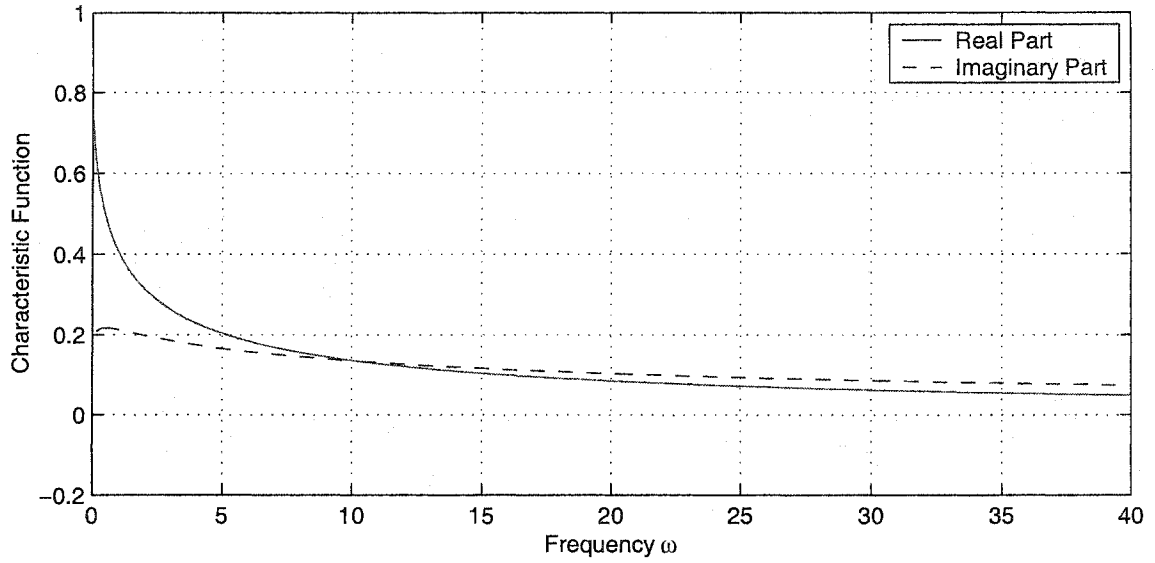


(a)

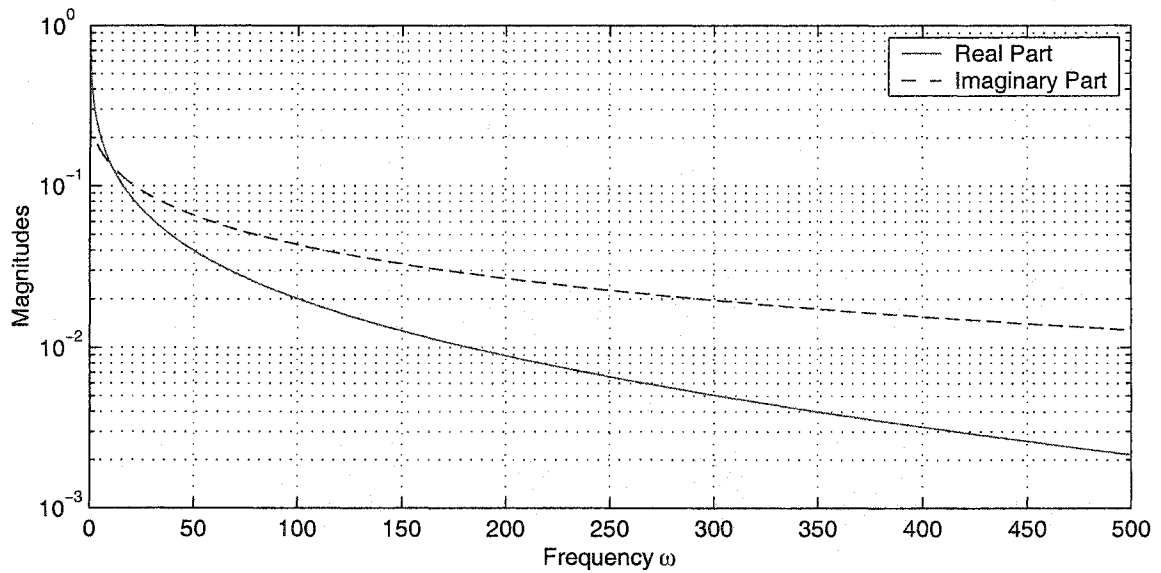


(b)

Figure 2.8. (a) Real and imaginary parts of a lognormal CF computed using an adaptive algorithm for $\sigma = 6$ dB. (b) Magnitudes of the real and imaginary parts of a lognormal CF computed using an adaptive algorithm for $\sigma = 6$ dB.



(a)



(b)

Figure 2.9. (a) Real and imaginary parts of a lognormal CF computed using an adaptive algorithm for $\sigma = 12$ dB. (b) Magnitudes of the real and imaginary parts of a lognormal CF computed using an adaptive algorithm for $\sigma = 12$ dB.

tail that requires special treatments before applying the FFT algorithm. Sampling and truncation are necessary steps in the FFT approach.

2.4.1 Sampling

The PDF of a lognormal RV is a continuous function that has to be converted to a discrete value sequence via sampling. The sampling rate must be carefully chosen to avoid or minimize the aliasing effect.

The theoretical sampling frequency required to eliminate the aliasing effect must be equal to or greater than two times the maximum non-zero frequency [13], i.e.

$$f_s \geq 2f_m. \quad (2.23)$$

However, the spectrum of the lognormal distribution is not known. From the CF plots gotten in last section, it seems to be not zero over a large range of the frequency, especially for greater σ . This feature makes eliminating the aliasing effect impossible. From another point of view, the location of the PDF mode may give us a reference point. The peak value of a lognormal PDF happens at $x_0 = e^{-\sigma^2}$ which decreases exponentially with the square of the dB spread. Thus, f_s must at least be on the order of that value. For example, for $\sigma = 12$ dB, $x_0 = 0.00049$ so that f_s must be greater than 10^4 . In this work, the values of f_s are decided by the empirical data. We continuously increase f_s until it reaches a point that the CF curve does not change greatly any more.

2.4.2 Truncation

The lognormal distributions possess long tails that have low values but nonzero probabilities. This character is more obvious for the larger dB spreads as demonstrated in Figure

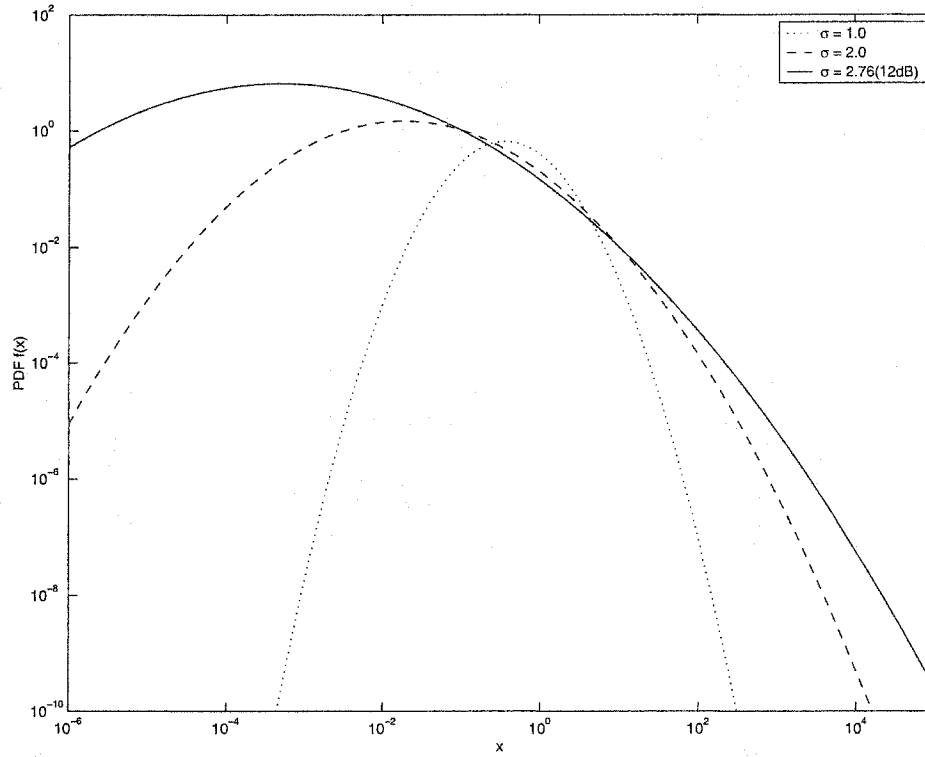


Figure 2.10. Lognormal PDF with different σ .

2.10. Before applying the FFT algorithm, the PDF must be truncated to be a sequence with a finite length. Truncation operation actually multiplies a rectangular window function with the lognormal PDF which will introduce high frequency components into the spectrum. This is the effect referred to as frequency leakage. Therefore, a new source of error in addition to aliasing error is triggered. We inevitably have to take it into consideration.

The number of points in the FFT is also important in determining the frequency resolution. Fortunately it is determined by the truncation length since

$$f_0 = \frac{f_s}{N} = \frac{f_s}{X_t f_s} = \frac{1}{X_t} \quad (2.24)$$

in which X_t denotes the truncation length. Equation (2.24) shows that if the truncation length is large enough, the frequency resolution can be made very small.

In this thesis, We choose N to be a power of 2 because then the FFT algorithm is the

fastest and most efficient. The explicit values of N are determined by the truncation points at which the PDF values start to be less than 10^{-4} .

Table 2.1. FFT sizes for the lognormal CF's

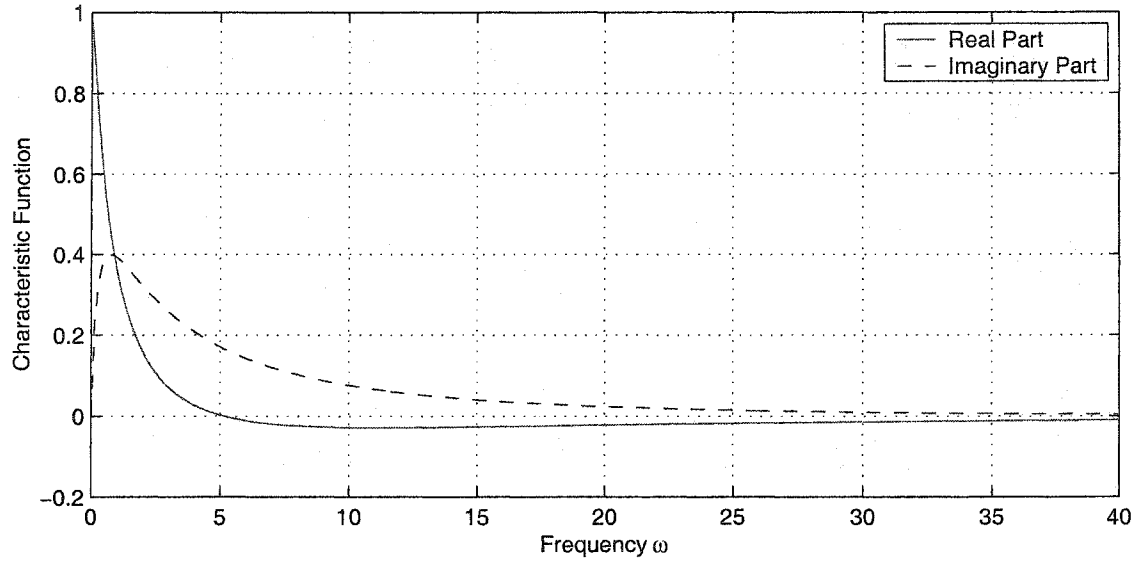
$\sigma(\text{dB})$	$e^{-\sigma^2}$	f_s	X_t	N (Power of 2)
6	0.1483	1000	32.77	2^{16}
8	0.0336	3000	87.38	2^{18}
10	0.0050	10000	209.72	2^{21}
12	0.0005	20000	419.43	2^{23}

Table 2.1 provides some data about the parameters used for the FFT algorithm in evaluating the lognormal CF's. Figure 2.11 and 2.12 are CF plots obtained by FFT methods. The analysis above shows that the errors derived from aliasing and frequency leakage cannot be estimated due to the limited knowledge of the CF so that the accuracy of the FFT approach can not be rigorously guaranteed. Error control is only roughly implemented by increasing f_s to reach a point that the curve will not change significantly.

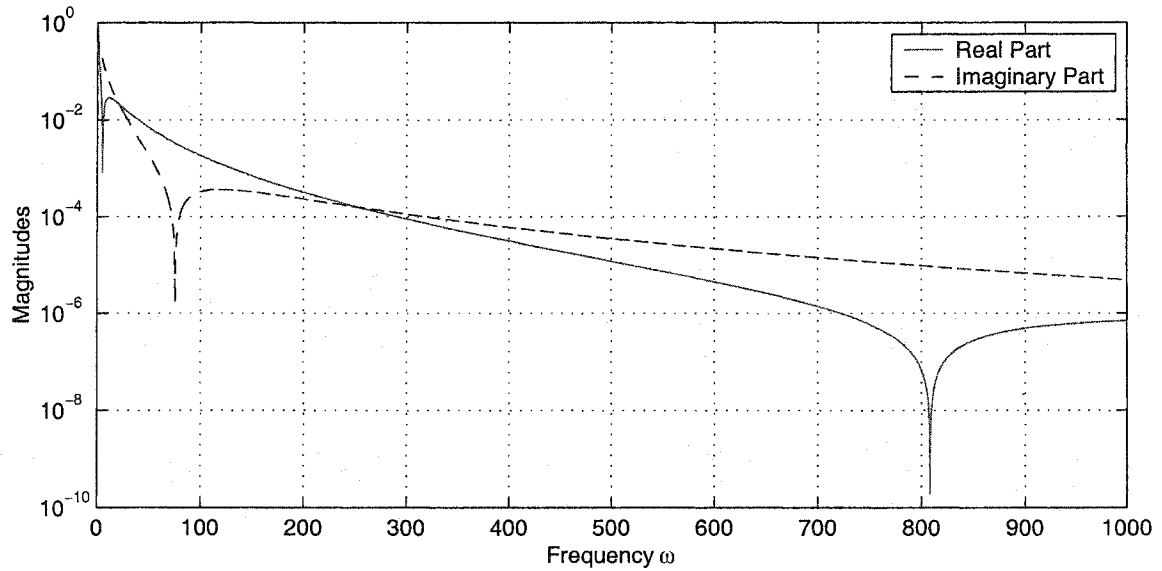
2.5 Integration Between the Zeros of the Integrand

The method of the transformed integral shows that it is very difficult to change the oscillatory character of the integrand no matter how the integration is transformed. In general, the regular rules for numerical integration are not effective for oscillatory functions [12]. A simple method for oscillatory functions is to integrate between the zeros of the integrand function and sum up the resultant infinite series.

The algorithms used in this section are based on those in QUADPACK [14]. A subrou-

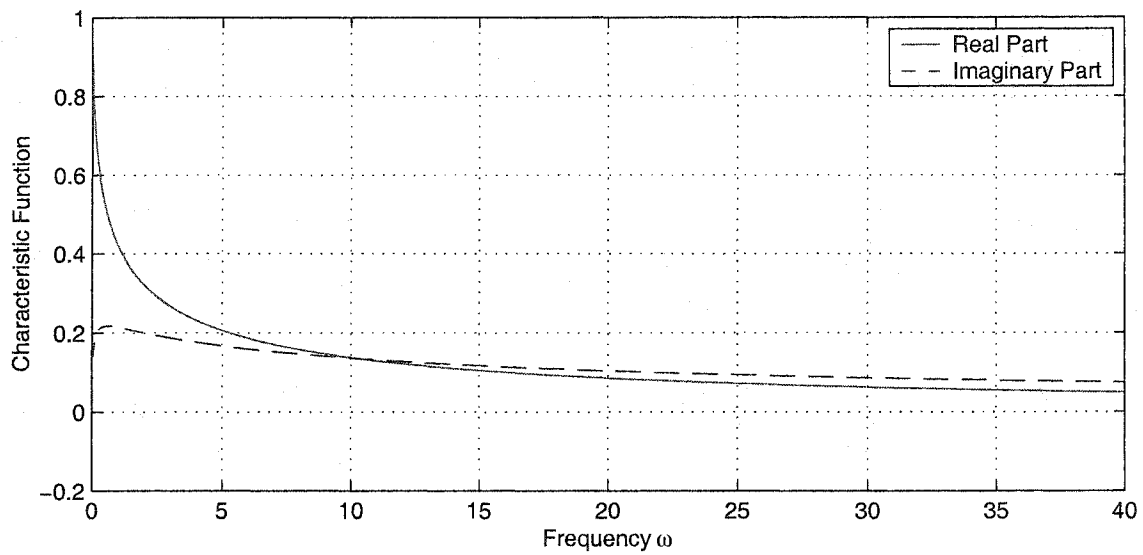


(a)

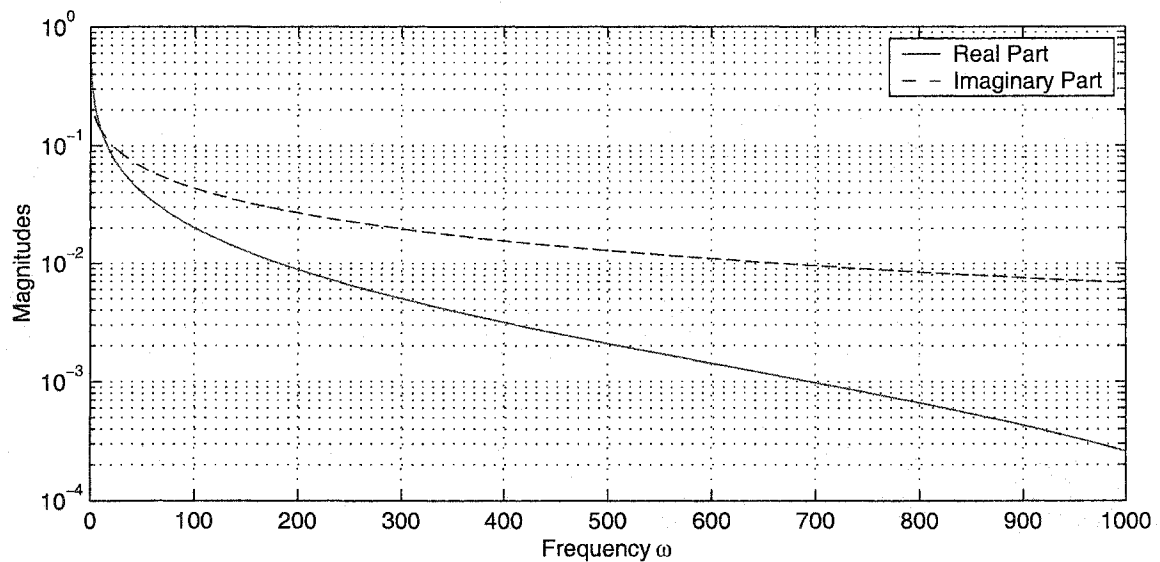


(b)

Figure 2.11. (a) Real and imaginary parts of a lognormal CF computed using FFT for $\sigma = 6$ dB. (b) Magnitudes of the real and imaginary parts of a lognormal CF computed using FFT for $\sigma = 6$ dB.



(a)



(b)

Figure 2.12. (a) Real and imaginary parts of a lognormal CF computed using FFT for $\sigma = 12$ dB. (b) Magnitudes of the real and imaginary parts of a lognormal CF computed using FFT for $\sigma = 12$ dB.

tine from GSL, qawf, is utilized to compute the lognormal CF's for the practical parameters.

In this method, the integration is evaluated by three steps:

1. Divide the semi-infinite Fourier integration interval into the consecutive subintervals by the zeros of the integrand. Note that the zeros of the integrand are those of $\cos(wx)$ or $\sin(wx)$ as the zeros are not displaced by the multiplication by the PDF.
2. Apply the modified Clenshaw-Curtis algorithm to the integral over each subinterval. If w in (2.5) and (2.6) is too small, the Gauss-Kronrod rule instead of the modified Clenshaw-Curtis rule is used to evaluate the integral over each subinterval.
3. The contributions from the consecutive subintervals form a series. The summation of this series is speeded up using a series acceleration technique, ε -algorithm.

Because the step 2 is the key procedure in this method, we simply call this integration method as “modified Clenshaw-Curtis” method in the remainder of this thesis.

2.5.1 Division of the interval

The entire semi-infinite interval is divided into the consecutive subintervals as

$$C_k = [(k-1)T, kT], \quad k = 1, 2, \dots, \quad (2.25a)$$

where T is the length of each subinterval

$$T = \frac{(2[|w|] + 1)\pi}{|w|}. \quad (2.25b)$$

The quantity $[|w|]$ represents the largest integer that is smaller than or equal to $|w|$. The formula (2.25b) makes the width of the subintervals contain an odd number of half circles and prevents the width of the subintervals from varying greatly with the value of w . Since the

subinterval length T is chosen to be an odd number of half periods, the contributions from the consecutive subintervals will have alternative signs when the function to be integrated is positive and monotonically decreasing.

The whole integration works on an overall absolute error tolerance (ε_{abs}). On each subinterval C_k the algorithm tries to achieve the tolerance

$$\varepsilon_k = (1 - p)p^{k-1} \cdot \varepsilon_{abs}, \quad k = 1, 2, \dots, \quad (2.26)$$

with $p = 0.9$ such that the overall absolute tolerance can be guaranteed in the entire process since

$$\begin{aligned} \varepsilon_{total} &= \sum_{k=1}^{\infty} \varepsilon_k = (1 - p) \left(\sum_{k=1}^{\infty} p^{k-1} \right) \varepsilon_{abs} \\ &= \varepsilon_{abs}. \end{aligned}$$

2.5.2 Integration methods over each subinterval

The modified Clenshaw-Curtis procedure is applied to the integral over each subinterval. If w in (2.5) and (2.6) is too small, the Gauss-Kronrod rule instead of the modified Clenshaw-Curtis rule is used to evaluate the integral over each subinterval. In the following, we give brief introductions to the modified Clenshaw-Curtis algorithm and Gauss-Kronrod integration. The details are given in [15].

2.5.2.1 Modified Clenshaw-Curtis method

Clenshaw-Curtis integration approximates the integrand $f(x)$ by a truncated Chebyshev expansion which can be integrated exactly. That is, if $f(x)$ is a continuous and bounded function in $[a, b]$, then it can be expanded as Chebyshev polynomials as [15]

$$f(x) = g(t) = \frac{1}{2}c_0 + \sum_{k=1}^{\infty} c_k T_k(t) \approx \sum_{k=0}^N c_k T_k(t) \quad (2.27a)$$

where

$$g(t) = f \left[\frac{(b-a)t + (b+a)}{2} \right], \quad t \in [-1, 1], \quad (2.27b)$$

and \sum'' indicates that the first and last terms are to be halved. The Chebyshev polynomial of degree k is given by

$$T_k(t) = \cos(k \cos^{-1} t), \quad (2.28)$$

and the coefficients are obtained by

$$c_k = \frac{2}{\pi} \int_0^\pi f(\cos \theta) \cos(k\theta) d\theta. \quad (2.29)$$

The Chebyshev polynomials of up to degree five are expressed as

$$\begin{aligned} T_0(t) &= 1, & T_3(t) &= 4t^3 - 3t, \\ T_1(t) &= t, & T_4(t) &= 8t^4 - 8t^2 + 1, \\ T_2(t) &= 2t^2 - 1, & T_5(t) &= 16t^5 - 20t^3 + 5t. \end{aligned}$$

Then the integral becomes

$$\begin{aligned} \int_a^b f(x) dx &= \frac{b-a}{2} \int_{-1}^{+1} g(t) dt \\ &\approx \frac{b-a}{2} \sum_{k=0}^N'' c_k \int_{-1}^{+1} T_k(t) dt \end{aligned} \quad (2.30)$$

which can be integrated exactly.

The coefficients c_k in (2.29) can be approximated by means of the trapezoidal rule

$$c_k = \frac{2}{N} \sum_{l=0}^N'' f \left[\cos \left(\frac{\pi l}{N} \right) \right] \cos \left(\frac{\pi l k}{N} \right), \quad k = 0, 1, 2, \dots, N. \quad (2.31)$$

In the subroutine based on QUADPACK, a 25-point modified Clenshaw-Curtis rule is used to evaluate the integration over each subinterval. Piessens *et al* [14] gives an extended method for calculating these 25 coefficients efficiently.

For the integrand with the weight functions $\sin(wx)$ and $\cos(wx)$, the integration changes to be

$$\begin{aligned}\int_a^b w(x)f(x)dx &= \frac{b-a}{2} \int_{-1}^{+1} w \left(\frac{b-a}{2}t + \frac{b+a}{2} \right) \sum_{k=0}^N c_k T_k(t) dt \\ &= \frac{b-a}{2} \sum_{k=0}^N c_k \int_{-1}^{+1} w \left(\frac{b-a}{2}t + \frac{b+a}{2} \right) T_k(t) dt.\end{aligned}\quad (2.32)$$

Then

$$\begin{aligned}\int_a^b \sin(wx)f(x)dx &= \frac{b-a}{2} \cos \left(\frac{b+a}{2}w \right) \sum_{k=0}^N c_k \int_{-1}^{+1} \sin(\lambda t) T_k(t) dt \\ &\quad + \frac{b-a}{2} \sin \left(\frac{b+a}{2}w \right) \sum_{k=0}^N c_k \int_{-1}^{+1} \cos(\lambda t) T_k(t) dt\end{aligned}\quad (2.33a)$$

and

$$\begin{aligned}\int_a^b \cos(wx)f(x)dx &= \frac{b-a}{2} \cos \left(\frac{b+a}{2}w \right) \sum_{k=0}^N c_k \int_{-1}^{+1} \cos(\lambda t) T_k(t) dt \\ &\quad - \frac{b-a}{2} \sin \left(\frac{b+a}{2}w \right) \sum_{k=0}^N c_k \int_{-1}^{+1} \sin(\lambda t) T_k(t) dt\end{aligned}\quad (2.33b)$$

where

$$\lambda = \frac{b-a}{2}w. \quad (2.33c)$$

Consequently the sine and cosine Chebyshev moments are calculated by

$$S_k(\lambda) = \int_{-1}^{+1} \sin(\lambda t) T_k(t) dt, \quad k = 0, 1, \dots, N, \quad (2.34)$$

$$C_k(\lambda) = \int_{-1}^{+1} \cos(\lambda t) T_k(t) dt, \quad k = 0, 1, \dots, N, \quad (2.35)$$

respectively. It is noticed that

$$S_{2k}(\lambda) = C_{2k+1}(\lambda) = 0, \quad k = 0, 1, \dots. \quad (2.36)$$

And some recurrence relationships are used to obtain these moments, that is,

$$\begin{aligned}\lambda^2(k-1)(k-2)S_{k+2}(\lambda) - 2(k^2-4)(\lambda^2-2k^2+2)S_k(\lambda) \\ + \lambda^2(k+1)(k+2)S_{k-2}(\lambda) = -8(k^2-4)\sin(\lambda) - 24\lambda\cos(\lambda)\end{aligned}\quad (2.37a)$$

with initial values

$$S_1(\lambda) = 2(\sin(\lambda) - \lambda \cos(\lambda))\lambda^{-2}, \quad (2.37b)$$

$$S_3(\lambda) = \lambda^{-2} \sin(\lambda)(18 - 48\lambda^{-2}) + \lambda^{-1} \cos(\lambda)(48\lambda^{-2} - 2) \quad (2.37c)$$

and

$$\begin{aligned} \lambda^2(k-1)(k-2)C_{k+2}(\lambda) - 2(k^2-4)(\lambda^2-2k^2+2)C_k(\lambda) \\ + \lambda^2(k+1)(k+2)C_{k-2}(\lambda) = 24\lambda \sin(\lambda) - 8(k^2-4)\cos(\lambda) \end{aligned} \quad (2.38a)$$

with initial values

$$C_0(\lambda) = 2\lambda^{-1} \sin(\lambda), \quad (2.38b)$$

$$C_2(\lambda) = 8\lambda^{-2} \cos(\lambda) - \lambda^{-3}(2\lambda^2 - 8) \sin(\lambda), \quad (2.38c)$$

$$C_4(\lambda) = 32\lambda^{-4}(\lambda^2 - 12) \cos(\lambda) + 2\lambda^{-5}(\lambda^4 - 80\lambda^2 + 192) \sin(\lambda). \quad (2.38d)$$

Therefore, the numerical computation of the Fourier integral can be easily and efficiently accomplished using the modified Clenshaw-Curtis method.

In this thesis, a 25-point modified Clenshaw-Curtis integration rule is applied to evaluate the integral over each subinterval. Then an iterative computation similar to that in the trapezoidal rule or Simpson's rule is executed. For small values of λ , there is no need to take special care regarding the weight function because the function does not oscillate greatly. A 15-point Gauss-Kronrod formula instead is used in this case for directly computing the integrals.

2.5.2.2 Gauss-Kronrod Integration

In the general Gaussian quadrature formula

$$G_n = \sum_{i=1}^n w_i f(x_i), \quad (2.39)$$

the nodes x_i and the weights w_i for the different n -point Gaussian formulae do not overlap. That means that the computation of m -point ($m > n$) Gaussian quadrature cannot reuse the previous results of n -point rules. But this is particularly important when some specified degree of accuracy is required and the number of points needed to achieve this accuracy is not known ahead of time.

Kronrod found a way to expand Gaussian quadrature to allow the duplication of nodes. The Gauss-Kronrod rule uses the original n nodes and adds $n + 1$ new nodes to form a higher order $2n + 1$ Kronrod rule. But this required new weights to be calculated again. The expression of Kronrod rule is

$$K_{2n+1} = \sum_{i=1}^n u_i f(x_i) + \sum_{j=1}^{n+1} v_j f(y_j) \quad (2.40)$$

where u_i and v_j are the new weights, x_i are the original Gaussian nodes, and y_j are the new added nodes. Consequently G_n and K_{2n+1} share n nodes.

In the automatic integration, a Gauss-Kronrod rule starts from a classical n -point ($n = 7, 10, 15, 20, 25$ or 30) Gaussian quadrature rule over each subinterval. Then this is extended to be $2n + 1$ order Kronrod rule. The difference between the two rules is regarded as an error estimate in the approximation of the integral. If the required tolerance is not achieved, the subintervals will be continuously bisected and the same procedure is then applied to the new and smaller subintervals.

2.5.3 ε -algorithm

The summation of the contributions from the consecutive subintervals in the previous subsection is speed ed up using ε -algorithm. The ε -algorithm [12] is a device for accelerating the convergence of slowly convergent sequences or determining a limit for divergent se-

quences. The fundamental relationships of the ε -algorithm is

$$(\varepsilon_{s+1}^{(m)} - \varepsilon_{s-1}^{(m+1)})(\varepsilon_s^{(m+1)} - \varepsilon_s^{(m)}) = 1 \quad (2.41)$$

that also can be rearranged as

$$\varepsilon_{s+1}^{(m)} = \varepsilon_{s-1}^{(m+1)} + (\varepsilon_s^{(m+1)} - \varepsilon_s^{(m)})^{-1}. \quad (2.42)$$

A two-dimensional array can be used to demonstrate the procedure of the ε -algorithm in which the subscript s of the quantity $\varepsilon_s^{(m)}$ indicates a column number and the superscript m a diagonal.

$$\begin{array}{ccccccc} & & & & \varepsilon_0^{(0)} & & \\ & & & & & & \\ \varepsilon_{-1}^{(1)} & & & & \varepsilon_1^{(0)} & & \\ & & & & & & \\ & & \varepsilon_0^{(1)} & & \varepsilon_2^{(0)} & & \\ \varepsilon_{-1}^{(2)} & & & & \varepsilon_1^{(1)} & & \varepsilon_3^{(0)} \\ & & & & & & \\ & & \varepsilon_0^{(2)} & & \varepsilon_2^{(1)} & & \\ \varepsilon_{-1}^{(3)} & & & & \varepsilon_1^{(2)} & & \vdots \\ & & & & & & \\ & & \varepsilon_0^{(3)} & & \vdots & & \\ \vdots & & & & \vdots & & \\ & & & & \vdots & & \end{array}$$

The relationship in (2.42) can be applied to a fundamental component in this two-dimensional array in a general form as

$$\begin{array}{ccc} & \varepsilon_s^{(m)} & \\ \varepsilon_{s-1}^{(m+1)} & & \varepsilon_{s+1}^{(m)} \\ & \varepsilon_s^{(m+1)} & \end{array}$$

If we set the initial conditions

$$\varepsilon_{-1}^{(m)} = 0, \quad m = 1, 2, \dots, \quad (2.43a)$$

$$\varepsilon_0^{(m)} = S_m, \quad m = 0, 1, \dots, \quad (2.43b)$$

in which S_m are the elements of the slowly convergent series to which the ε -algorithm applies, equations (2.43a) and (2.43b) give the values in the first two columns of this two-dimensional array and then the rest of the array is constructed from left to right, column by column, using the relationship (2.42).

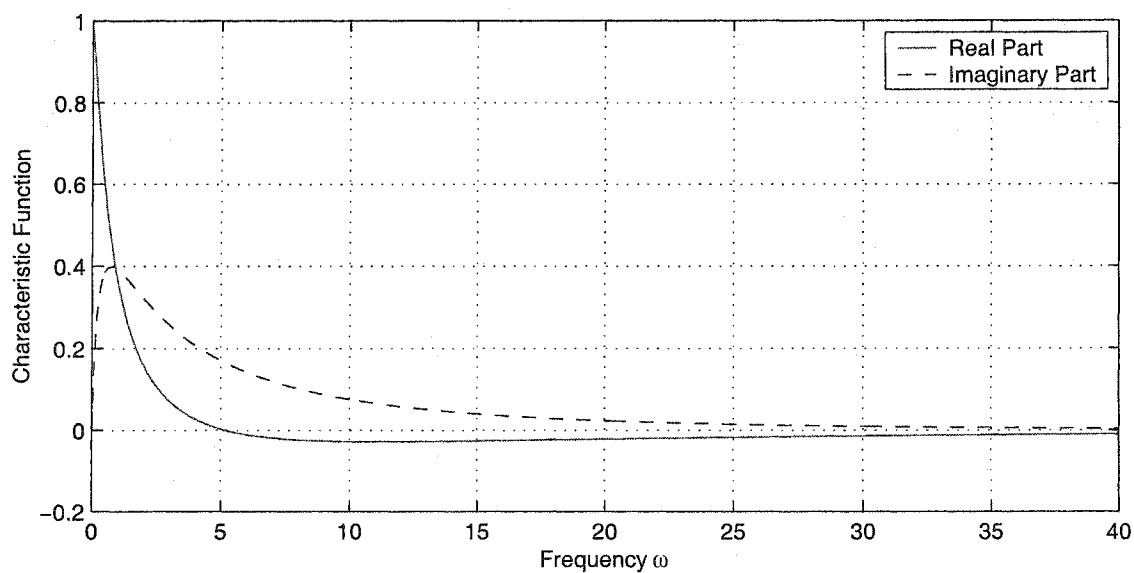
It is often found that the quantities $\varepsilon_{2s}^{(m)}$ approach more rapidly to the limit of the sum of the sequence $\{S_m\}$ than partial sums of the original sequence [15]. That is also the property that enables the ε -algorithm to be a convergence accelerating transformation.

Figure 2.13 and Figure 2.14 are CF plots obtained using the third method, the modified Clenshaw-Curtis integration. The curves obtained in this section are more smooth than those obtained from the transformed integral using the trapezoidal and Simpson's rules.

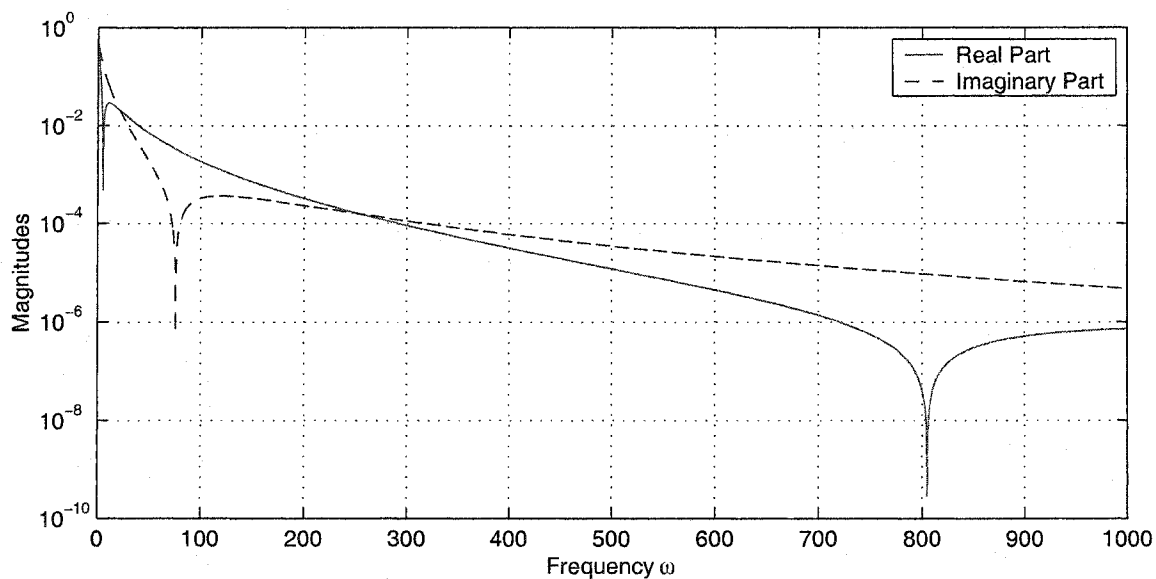
2.6 Comparison of Numerical Methods

Based on the graphs obtained using the three different numerical methods, these methods give us almost the same results. But their efficiencies are different.

A comparison of these numerical methods is made on a specific machine to identify their efficiencies. The numbers of multiplications, function evaluations, integrand functions evaluation and computing time are used as the criteria. Function evaluation here is referred to as the evaluation of all involved elementary functions, such as $\sin(x)$, $\cos(x)$, $\ln(x)$, e^x and so on, while the integrand function evaluation regards the entire integrand as a function. So the integrand evaluation gives us an idea about how many data points a specific algorithm needs to achieve the tolerance. In this thesis, the transformed integral (trapezoidal, Simpson's, adaptive algorithm), FFT and modified Clenshaw-Curtis methods are compared in calculating the lognormal CF for 12 dB spread for $\omega \in [0, 40]$. When the step size $\Delta\omega$ is 0.1 rad/s, there are 400 frequency points to be evaluated. The absolute tolerance in the CF

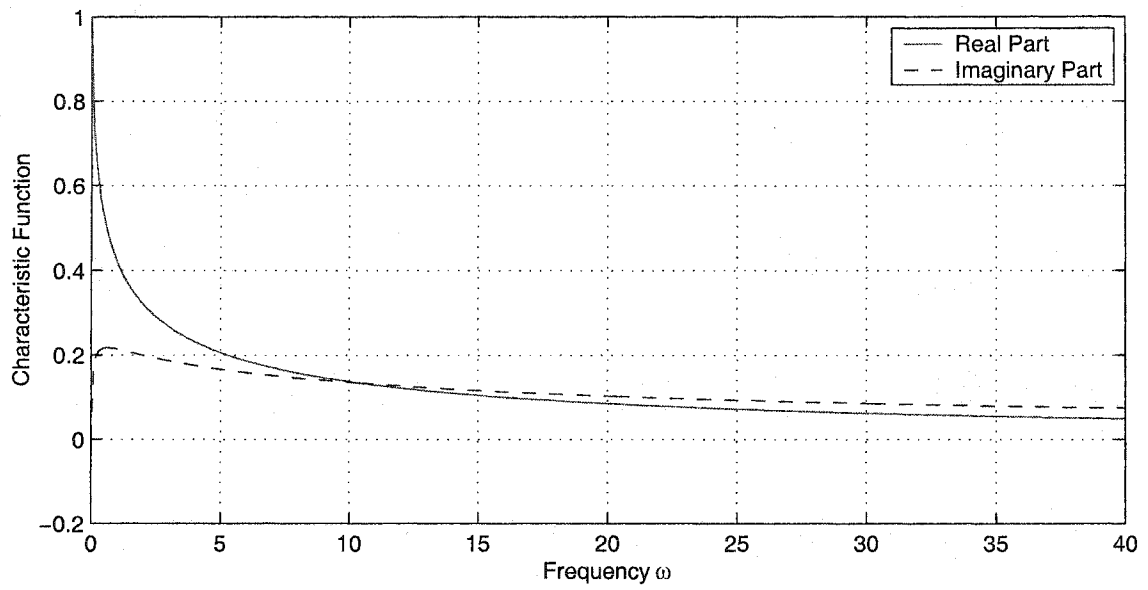


(a)

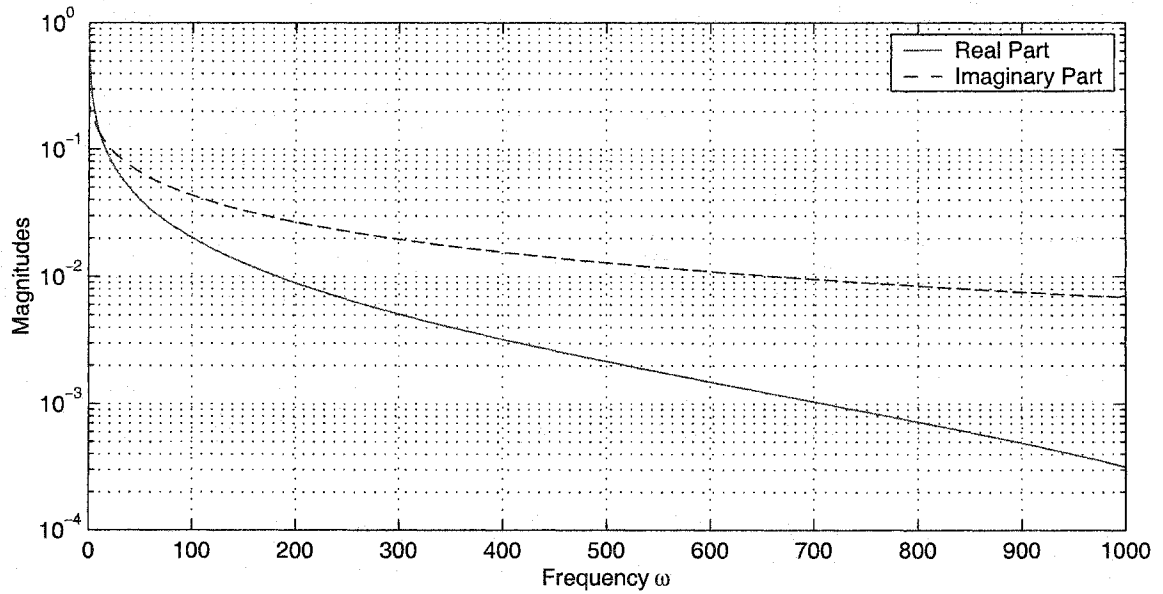


(b)

Figure 2.13. (a) Real and imaginary parts of a lognormal CF computed using modified Clenshaw-Curtis method for $\sigma = 6$ dB. (b) Magnitudes of the real and imaginary parts of a lognormal CF computed using modified Clenshaw-Curtis method for $\sigma = 6$ dB.



(a)



(b)

Figure 2.14. (a) Real and imaginary parts of a lognormal CF computed using modified Clenshaw-Curtis method for $\sigma = 12$ dB. (b) Magnitudes of the real and imaginary parts of a lognormal CF computed using modified Clenshaw-Curtis method for $\sigma = 12$ dB.

is set to be 10^{-5} .

Table 2.2. Comparison of numerical integration methods

Methods	Multiplication	Func. Eval.	Integ. Eval.	Time(sec)
Trapezoidal	6.84E+9	4.56E+9	0.76E+9	749
Simpson's	10.03E+9	6.68E+9	1.11E+9	1099
Adaptive	54.97E+6	36.64E+6	6.11E+6	7
FFT	40.94E+6	24.12E+6	1,048,576	5
Clenshaw-Curtis	19.01E+6	2.67E+6	495,075	1

Table 2.2 summarizes the approximate number of operations required in these methods. It is concluded that the modified Clenshaw-Curtis is the most efficient in terms of all the criteria while the transformed integral is the worst. Among the three algorithms for the transformed integral, the performance of the adaptive algorithm is better than the others by 2 to 3 orders of magnitude. Simpson's rule is a little worse than the trapezoidal rule consistent with published results that the trapezoidal rule is well suited for Fourier integrals [16]. Furthermore, the difficulties of the trapezoidal and Simpson's rules becomes more and more severe with increasing ω .

The FFT differs from the other methods in that it has to hold the whole data set in the memory at the same time which leads to large storage requirements. If the size of the FFT is determined, the computation complexity of the FFT method is always determined as $O(N \log_2 N)$ no matter what the spectral range being evaluate. In other words, evaluating a CF over the ranges of $[0, 40]$ and $[0, 100]$ require the same amount of time. However, the errors coming from aliasing and sequence truncation are difficult to estimate due to the lack of knowledge of the exact form of the lognormal CF. In order to minimize these errors,

f_s is set to be as great as possible.

2.7 Inverse Fourier Transform to PDF and CDF

As mentioned in Section 2.1, the characteristic function of a sum of independent RV's is the product of the characteristic functions of the summands. The sum distribution can be obtained by evaluating the inverse Fourier transform of the CF of the sum based on equations (2.3b) and (2.4c). In this section, we give a method to evaluate these inverse transforms numerically. The numerical computation of the inverse transform is actually a two-dimensional integration without the exact form of the CF of a lognormal RV.

Since the inverse Fourier transform is a similar procedure to the Fourier transform, we applied the same numerical methods to it. We found that the transformed integral method is not valid for the inverse transform because the computation efficiency of the transformed integral is extremely low. Our efforts mainly concentrate on the FFT method and the modified Clenshaw-Curtis integration method.

2.7.1 FFT

It is straightforward to find the PDF of the sum via the IFFT. Then the CDF is obtained through accumulating the discrete values of the PDF. But it is found that the resources of computer systems might not be able to implement the FFT for some parameters to obtain the desired CDF values. For instance, the CDF for a sum of 6 lognormal RV's with 12 dB spread converges to unity slowly. Its value is not above $(1 - 10^{-6})$ until $\gamma \approx 10^6$. If the CDF value of $(1 - 10^{-6})$ is desired, we need to carry out the FFT with a size of

$$N = 10^6 \times f_s = 10^6 \times 20000 = 2 \times 10^{10} < 2^{34}$$

which demands $8 \times 16\text{G}$ bytes memory in a computer system supposing that a double-type variable occupies 8 bytes. This is because the FFT algorithm requires storing N variables in memory at the same time. Obviously, the FFT method is not practical in evaluating CDF values for large dB spreads that require great sampling frequencies. But it is well suited for small dB spreads like 6-8 dB. Figure 2.15 gives a complementary CDF plot obtained using the FFT method.

2.7.2 Modified Clenshaw-Curtis

When using the modified Clenshaw-Curtis approach, it is noticed that the function cannot be evaluated at $w = 0$ in the formula (2.4c) because the denominator is $w = 0$. If we evaluate the integration starting from a small δ instead of zero, truncation error will be introduced. An alternative way that avoids truncation error is to use the limiting value of the integrand function at $w = 0$. Fortunately the limiting value at $w = 0$ can be found using l'Hospital's rule because $\text{Re}[\phi(0)] = 1$ and $\text{Im}[\phi(0)] = 0$ in all cases, i.e.

$$\begin{aligned}
\lim_{w \rightarrow 0} \frac{\text{Im}[\phi_L(w)] \cos(w\gamma)}{w} &= \lim_{w \rightarrow 0} \{\text{Im}[\phi_L(w)]\}' \cos(w\gamma) - \lim_{w \rightarrow 0} \text{Im}[\phi_L(w)] \sin(w\gamma) \gamma \\
&= \lim_{w \rightarrow 0} \frac{1}{2j} [\phi_L(w) - \phi_L(-w)]' \cos(w\gamma) \\
&= \sum_{i=1}^N E[L_i] = \sum_{i=1}^N e^{m_i + \sigma_i^2/2},
\end{aligned} \tag{2.44}$$

and

$$\begin{aligned}
\lim_{w \rightarrow 0} \frac{\text{Re}[\phi_L(w)] \sin(w\gamma)}{w} &= \lim_{w \rightarrow 0} \{\text{Re}[\phi_L(w)]\}' \sin(w\gamma) + \lim_{w \rightarrow 0} \text{Re}[\phi_L(w)] \cos(w\gamma) \gamma \\
&= \lim_{w \rightarrow 0} \frac{1}{2} [\phi_L(w) + \phi_L(-w)]' \sin(w\gamma) + \gamma \\
&= \gamma
\end{aligned} \tag{2.45}$$

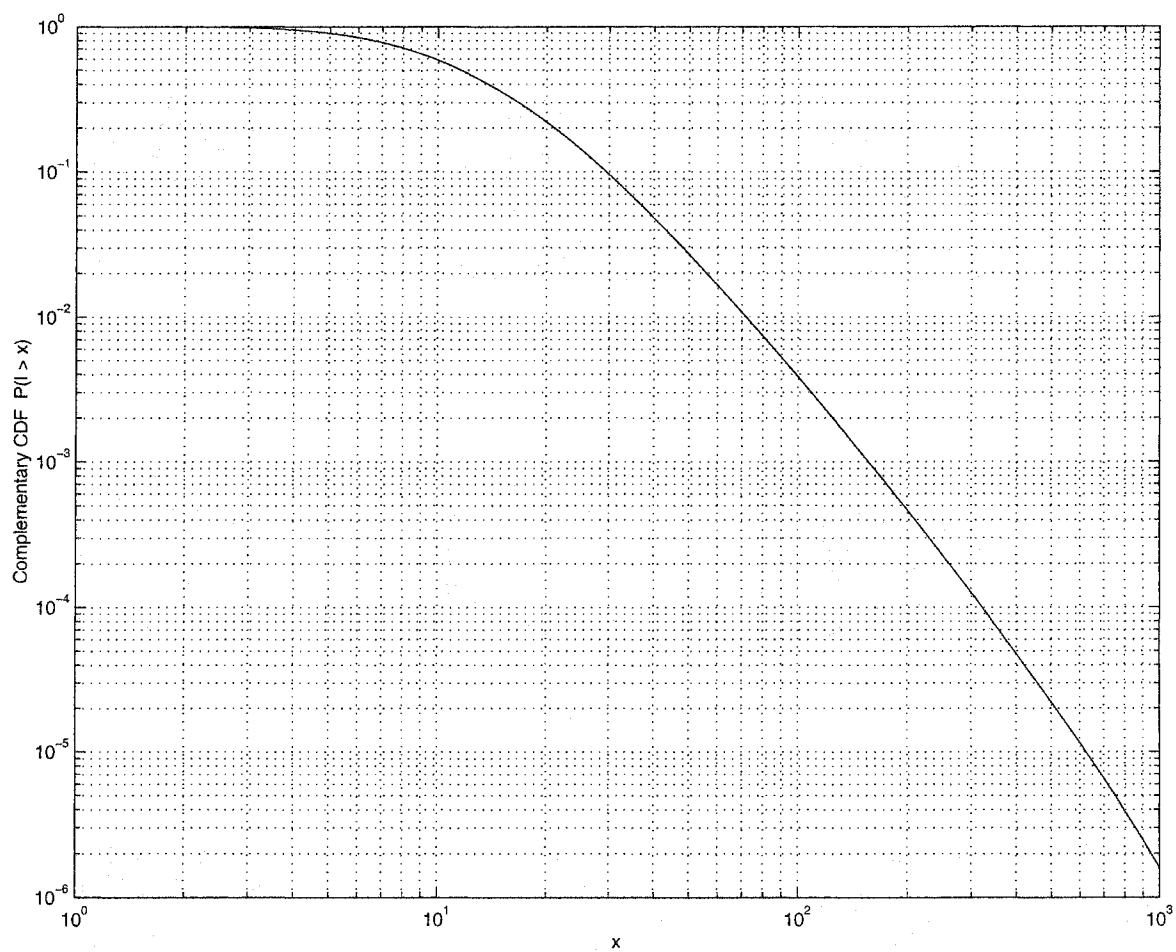


Figure 2.15. Complementary CDF of a sum of 6 i.i.d. lognormal RV's ($m = 0$ dB, $\sigma = 6$ dB) computed using the FFT.

where

$$\begin{aligned}\phi_L^*(w) &= \phi_L(-w), \\ \phi_L(w) &= \prod_{i=1}^N \phi_{L_i}(w), \\ \left. \frac{d\phi_{L_i}(w)}{dw} \right|_{w=0} &= jE[L_i].\end{aligned}$$

Consequently the limiting value of the function in (2.4c) is

$$\lim_{w \rightarrow 0} \frac{\text{Im}[\phi_L(w)] \cos(w\gamma) - \text{Re}[\phi_L(w)] \sin(w\gamma)}{w} = \sum_{i=1}^N e^{m_i + \sigma_i^2/2} - \gamma. \quad (2.46)$$

In the special case of i.i.d. RV's and $m_i = 0$ for all i , the right side of (2.46) becomes $Ne^{\sigma_i^2/2} - \gamma$.

In implementing the inverse transform, the subroutine we utilized from GSL often broke down. It was found that this was caused by evaluating the CF at some extremely small frequencies ($w < 10^{-6}$). In such situation, we changed to use the Gauss-Kronrod rule directly after making the variable change

$$x = \frac{1-t}{t} \quad (2.47)$$

to transform the semi-infinite range to a finite range $(0, 1]$ because when the w in the integrands $f(x) \sin(wx)$ and $f(x) \cos(wx)$ becomes too small, the integrand functions do not oscillate quickly and can be treated normally.

Although there is no closed-form expression for the sum distribution of independent lognormal RV's, the numerical methods for computing the PDF and CDF can be tested through the case of $N = 1$ by comparing the quantities after Fourier transform and inverse transform with the theoretical data. The CDF of a single lognormal RV is evaluated as

$$P(L \leq \gamma) = 1 - Q\left(\frac{\ln(\gamma) - m}{\sigma}\right). \quad (2.48)$$

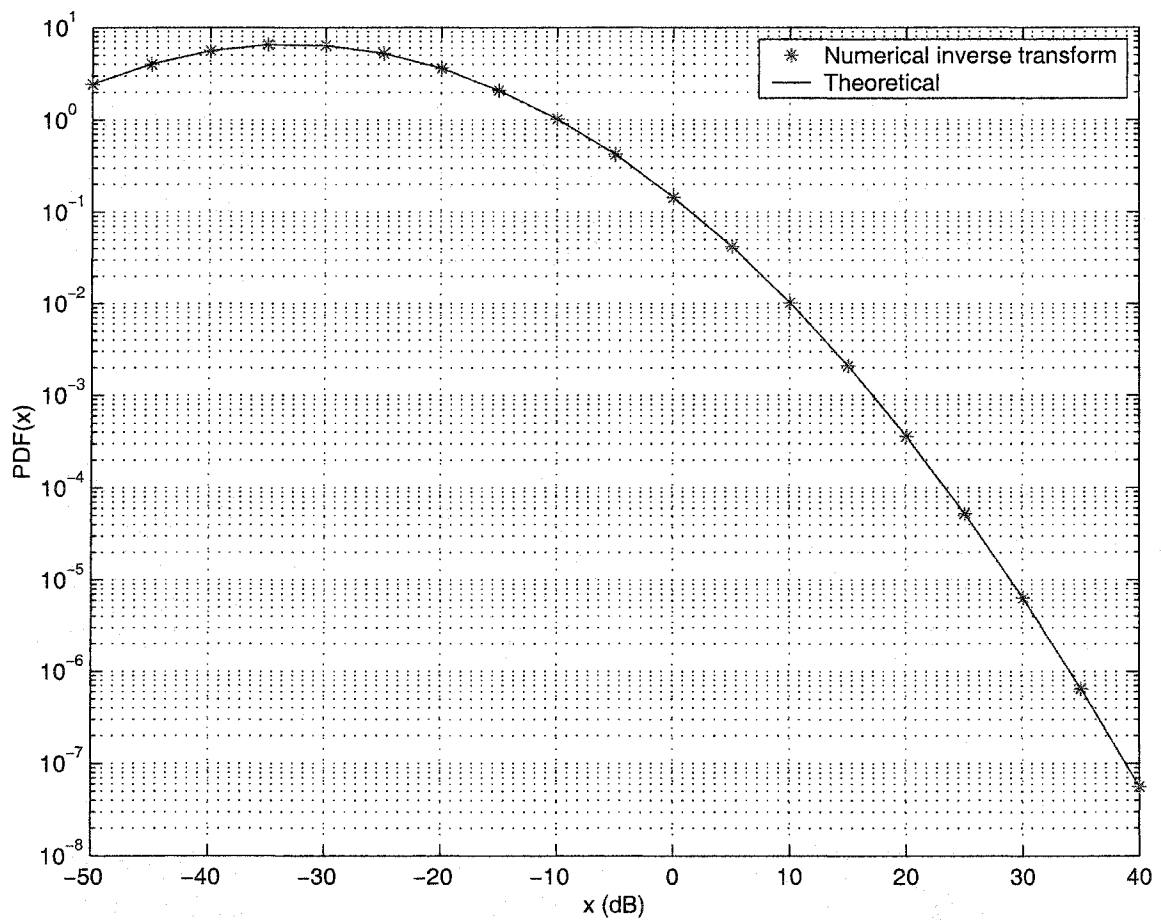


Figure 2.16. Comparison of the theoretical PDF and the PDF computed using the numerical inverse transform for $m = 0$ dB and $\sigma = 12$ dB.

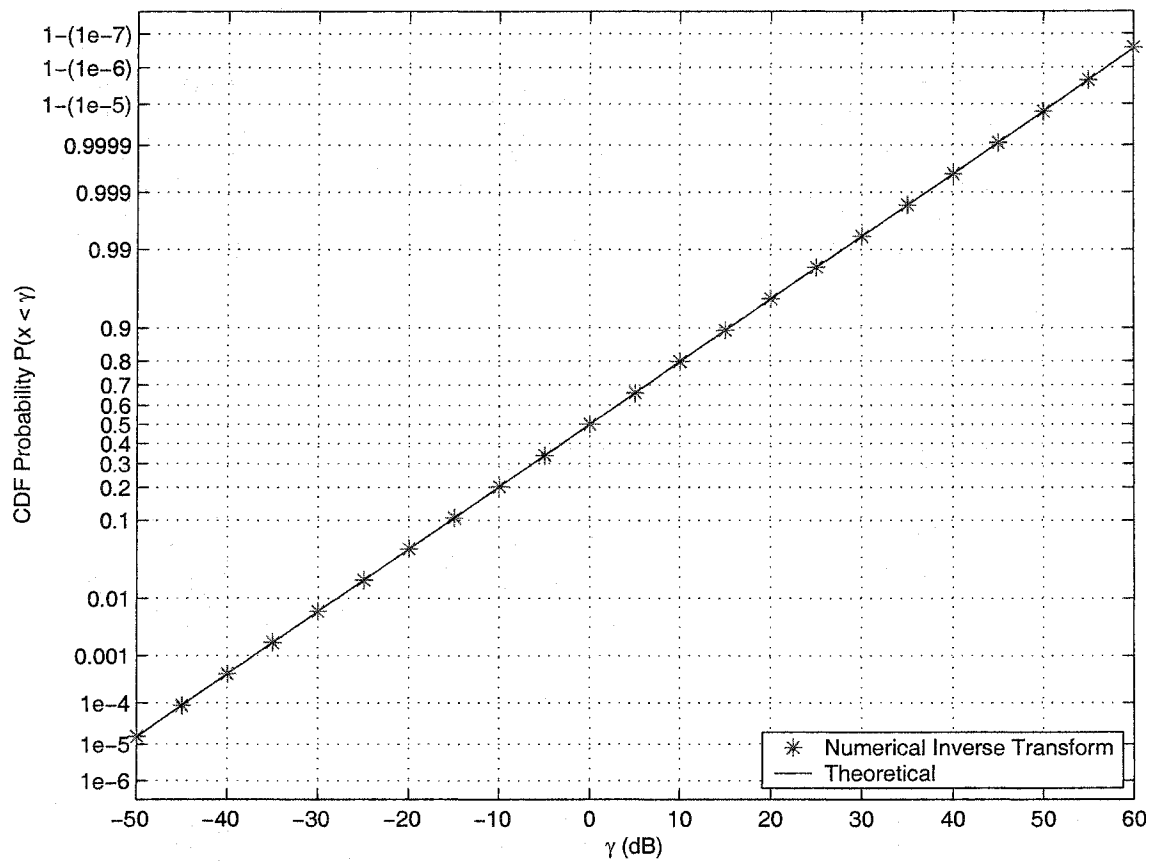


Figure 2.17. Comparison of the theoretical CDF and the CDF computed using the numerical inverse transform for $m = 0$ dB and $\sigma = 12$ dB.

The comparison results are illustrated in Figure 2.16 and 2.17. In Figure 2.17 we plot the data on the lognormal probability paper in which the lognormal CDF is plotted as a straight line. It is observed in both figures that the results from the numerical computations are in excellent agreement with the theoretical values. Therefore, we gain confidence that our numerical method is suitable for computing the sum distributions of independent lognormal RV's for probabilities in the range of practical interests and that the plots of the lognormal CF are correct.

In conclusion, three numerical integration methods for the lognormal CF and the inverse transform have been investigated in this chapter. The modified Clenshaw-Curtis approach was seen to be well suited to this computation. We can further in the next chapter calculate the sum distribution of $N > 1$ i.i.d. lognormal RV's and examine their behaviors. To the best knowledge of the author's, these numerical results about lognormal CF's and sum distributions are new. Moreover, we present a new approach, based on our numerical values, to approximate a sum as a lognormal RV. The details are given in the next chapter.

Chapter 3

Minimax Approximation to the Sum Distribution

Both two well-known approximations, Wilkinson's and Schwartz & Yeh's methods, are based on the assumption that the sum of independent lognormal variates is approximated by another lognormal variate. But the question as to whether such an assumption is good or just acceptable is still not clear. In this chapter, we examine this assumption and further presents a new paradigm for constructing approximations to lognormal sum distributions.

3.1 CDF of the Sum Distribution

A lognormal distribution $L \sim \Lambda(m, \sigma^2)$ where two parameters m and σ denote the mean value and standard deviation of the corresponding normal distribution $N(m, \sigma^2)$, respectively, can be written as a scaled lognormal random variable with only one parameter σ .

Let

$$V = e^{-m}L, \tag{3.1}$$

then, due to (1.12), the PDF of V is

$$\begin{aligned} f_V(v) &= f_L(l) \cdot \left| \frac{dl}{dv} \right| \\ &= e^{-m} f_0(le^{-m}) e^m = f_0(v). \end{aligned} \quad (3.2)$$

We can see that V here is a lognormal variable with zero mean and the same standard deviation, i.e. $\Lambda(0, \sigma^2)$, which only has one parameter σ . The non-zero parameter m can be regarded as a scaling factor in the lognormal distribution.

The above relationship can be applied to a sum of N independent lognormal variables with different mean values m_i and standard deviations σ_i . Both the mean and standard deviations here refer to the corresponding Gaussian distribution. Thus, the sum

$$L = \sum_{i=1}^N L_i \quad (3.3)$$

can be expressed as a weighted sum of N independent lognormal variables with zero means but the same dB spreads as

$$L = \sum_{i=1}^N a_i V_i \quad (3.4)$$

where the weights are

$$a_i = e^{m_i} \quad (3.5)$$

and V_i denotes the lognormal distribution $\Lambda(0, \sigma_i^2)$. The characteristic function of the sum in (3.3) is [17]

$$\phi_L(w) = \prod_{i=1}^N \phi_{L_i}(w) = \prod_{i=1}^N \phi_{V_i}(a_i w). \quad (3.6)$$

The same result can be obtained from equation (2.7). The scaling factor e^{m_i} only affects the frequency for a CF. Setting m_i to be zero would not lose the generality. Thus, this section focuses on sums of i.i.d. lognormal variates with zero power mean m_i . We will discuss the cases of non-i.i.d. and non-zero power mean in section 3.4 and 3.5.

One way of examining whether or not a random variable is lognormally distributed is to plot the curve of the CDF on the lognormal probability paper and to see whether it acts as a straight line. A probability plot [18] is a graphical technique for assessing whether or not a data set is approximately a certain distribution. The data are plotted against a theoretical specific distribution in such a way that the points should form an approximate straight line. Departures from this straight line indicate departures from that distribution. Therefore, the lognormal probability paper is used in this thesis to assess to what extent the lognormal sum behaves like a lognormal variable.

The CDF of a sum of N independent lognormal RV's except for $N = 2$ is evaluated using the numerical inverse transform of the characteristic function by the modified Clenshaw-Curtis method described in Chapter 2. In the case of $N = 2$, it is found that numerical convolution is more efficient than the numerical inverse transform because the convolution for $N = 2$ is a one-dimensional integration as

$$F_L(z) = f_{L_1}(z) * F_{L_2}(z) = F_{L_1}(z) * f_{L_2}(z) \quad (3.7)$$

where $f(x)$ denotes the PDF and $F(x)$ denotes the CDF of the summands. Equation (3.7) is proved [17] by letting

$$Z = X + Y,$$

then

$$\begin{aligned} F_Z(z) &= \int_{-\infty}^{\infty} \int_{-\infty}^{z-y} f_{X,Y}(x,y) dx dy \\ &= \int_{-\infty}^{\infty} \int_{-\infty}^{z-y} f_X(x) dx f_Y(y) dy \\ &= \int_{-\infty}^{\infty} F_X(z-y) f_Y(y) dy \\ &= F_X(z) * f_Y(z). \end{aligned}$$

The examined range of CDF in this thesis is from 10^{-6} to $1 - 10^{-6}$. This range is much wider than those of the simulations in previous works. The previous work [2] studied the CDF of a sum of independent lognormal RV's in the interval of [0.001, 0.999]. Reference [3] only gave simulation results for values of the complementary CDF greater than 10^{-4} for 12 dB spread, while [19] did not provide simulation data for dB spreads greater than 8 dB.

We plot on the same graph the CDF's of the sum of i.i.d. lognormal RV's with different numbers N of summands and compare their behaviors. Figures 3.1 - 3.2 illustrate the CDF's of the sum distribution for 6 dB and 12 dB spread, respectively. Even though the CDF's of the i.i.d. lognormal sum over the range of [0.1, 0.9] are close to straight lines, the CDF's in $[10^{-6}, (1 - 10^{-6})]$ form an approximate quadratic pattern on the lognormal probability paper and are left-skewed relative to the lognormal distribution. It is observed that the larger the number N of the summands is, the more severely the CDF curve bends and deviates from a straight line. The numerical data in our work shows that the sum distribution increasingly deviates from a lognormal distribution as N grows when plotted on the scales used here.

The number of the summands does not seem to affect the tail of complementary CDF too much but significantly influences the tail value of CDF. Examining these graphs, we found that the tails of complementary CDF with different summation numbers approach that of the single lognormal RV with the identical m and σ as $\gamma \rightarrow \infty$. This phenomenon can be explained by the asymptotic character of sum distributions given by Janos [20]. Janos indicated that the tail of a sum distribution asymptotically displays the lognormal behavior of its members with the largest dB spreads.

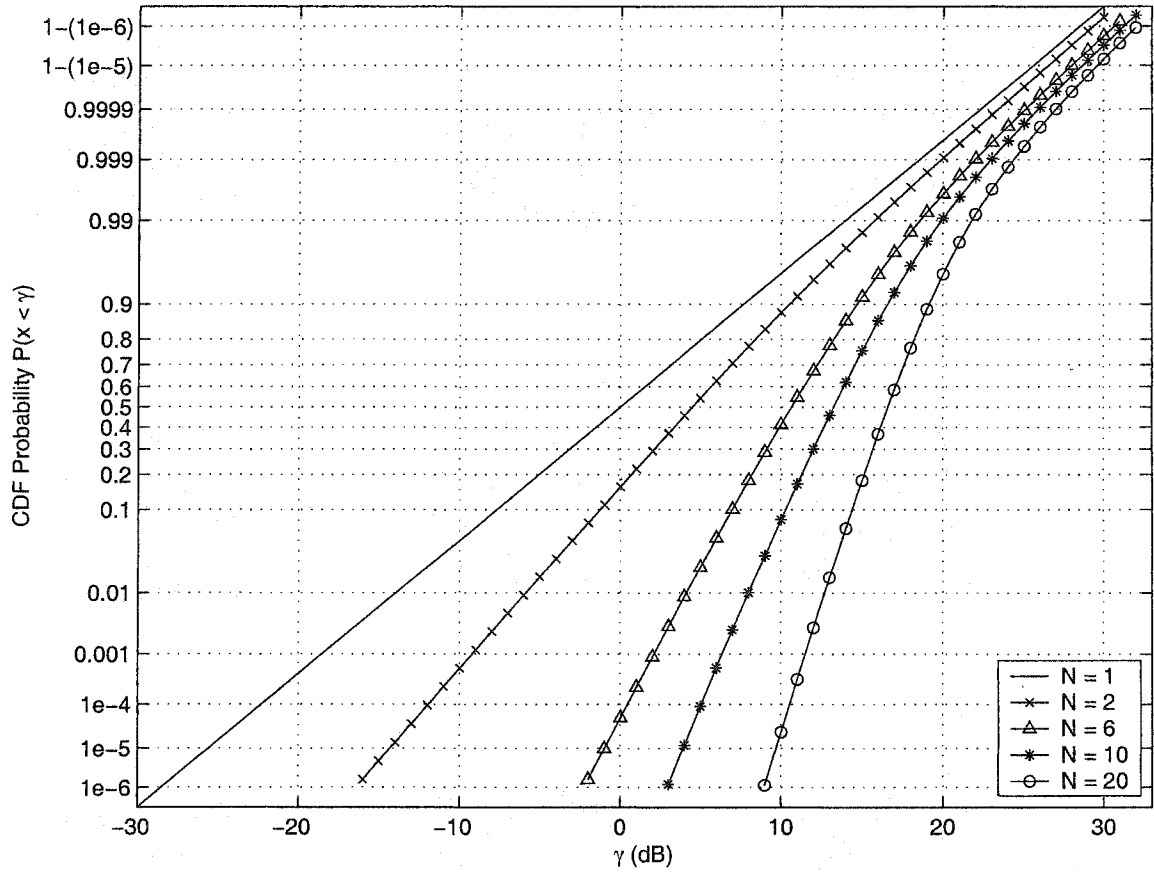


Figure 3.1. The CDF of the sum of N i.i.d. lognormal RV's ($m = 0$ dB, $\sigma = 6$ dB).

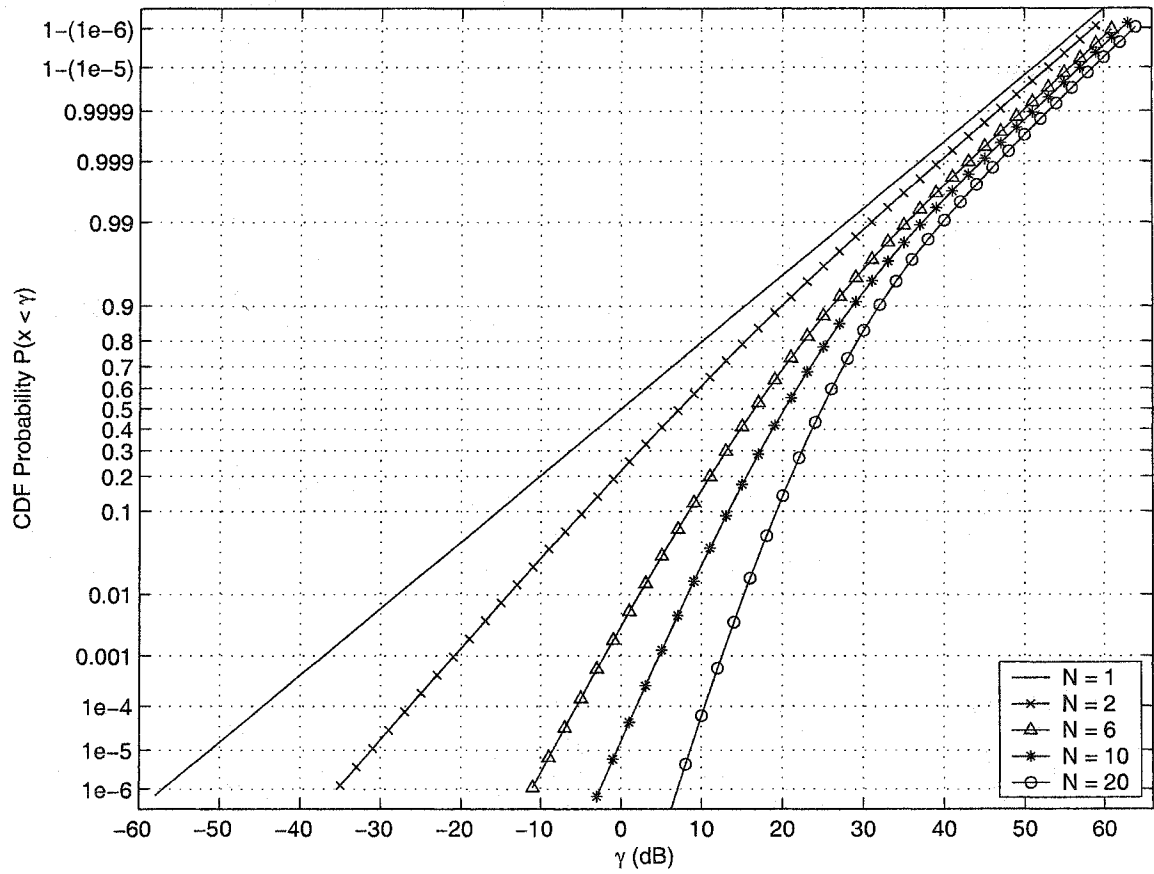


Figure 3.2. The CDF of the sum of N i.i.d. lognormal RV's ($m = 0$ dB, $\sigma = 12$ dB).

3.2 Minimax Approximation

If we use a lognormal distribution to approximate the sum distribution, a straight line need to be found to fit the numerical data set for the CDF on $[10^{-6}, 1 - 10^{-6}]$ on the lognormal probability paper. Because minimax approximation [21] is an approximation that minimizes the maximum deviation from the true function, namely, makes best performance in the worst case, this approximation presents better estimation than others. Let $f(x)$ be continuous on $[a, b]$ and $p_n(x)$ be any polynomial with degree n . If there exists a polynomial $p_n^*(x) \in P_n$ that satisfies the expression of the form

$$\|f - p^*\|_\infty = \max_{a \leq x \leq b} |f(x) - p_n^*(x)| \leq \max_{a \leq x \leq b} |f(x) - p_n(x)| \quad (3.8)$$

or

$$\|f - p^*\|_\infty = \max_{1 \leq i \leq m} |f(x_i) - p_n^*(x_i)| \leq \max_{1 \leq i \leq m} |f(x_i) - p_n(x_i)| \quad (3.9)$$

then $p_n^*(x)$ is called the *best uniform approximation* or *minimax approximation* of degree n to $f(x)$. For the more general approximation problem, the monomials $1, x, x^2, \dots, x^n$ in $p_n(x)$ are replaced by other fixed functions g_0, g_1, \dots, g_n such as $g_0 = \ln(x), g_1 = \sin(x)$ and so on. The form $\sum_{i=0}^n c_i g_i$ is called the generalized polynomials.

It was already proved that such a solution *exists and uniquely exists* for any continuous function $f(x)$ defined on a finite interval [22]. In addition, the alternation theorem [21] provides a necessary and sufficient condition for the minimax approximation.

Alternation Theorem:

Let $f(x) \in C[a, b]$ and $p(x)$ be a polynomial of degree n . Let $E_n = \max_{a \leq x \leq b} |f(x) - p(x)|$ and $\varepsilon(x) = f(x) - p(x)$. A necessary and sufficient condition that $p(x)$ be the unique best uniform approximation to $f(x)$ is that there are at least

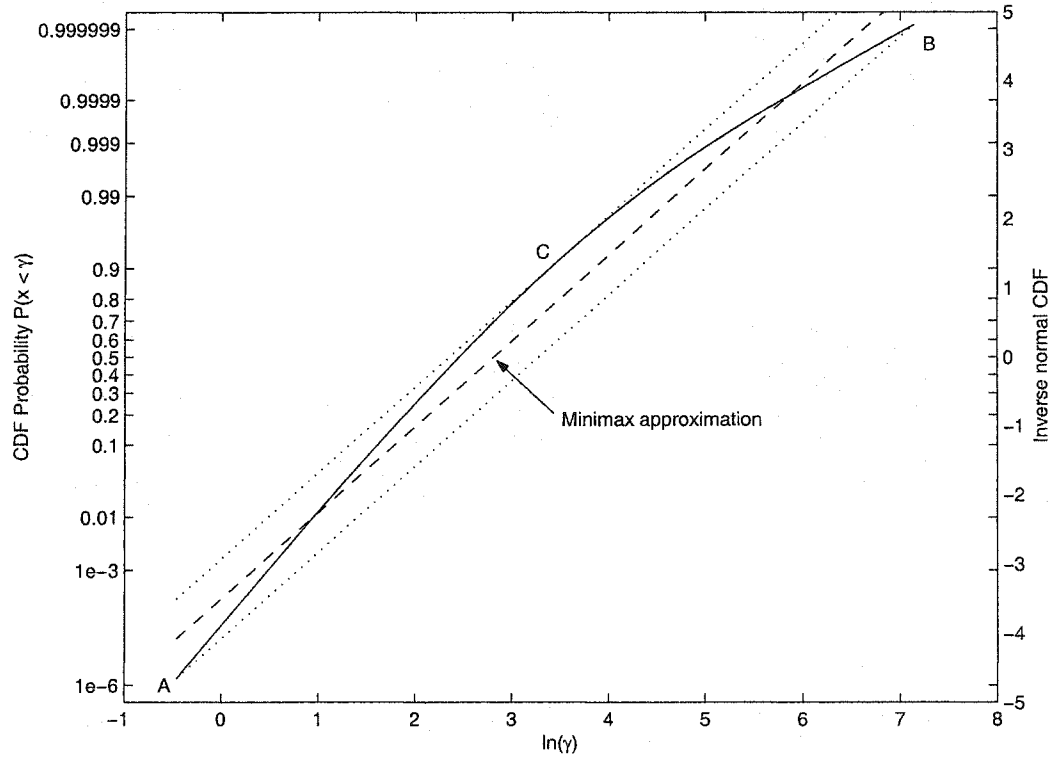


Figure 3.3. Minimax approximation to the CDF.

$n + 2$ points $a \leq x_1 < x_2 < \cdots < x_{n+2} \leq b$ where $\varepsilon(x)$ assumes the values $\pm E_n$ and with alternating signs:

$$\varepsilon(x_i) = \pm E_n, \quad i = 1, 2, \dots, n+2,$$

$$\varepsilon(x_i) = -\varepsilon(x_{i+1}), \quad i = 1, 2, \dots, n+1.$$

This theorem is very important for the numerical determination of best uniform approximation. But before determining minimax approximations to the sum distributions, we first describe how to construct a lognormal probability paper. In order to create a lognormal probability paper, the CDF $F(x)$ of a RV is transformed to

$$g(x) = \Phi^{-1}(F(x)) \quad (3.10)$$

where $\Phi^{-1}(x)$ is the inverse function of the standard normal CDF with the form

$$g(x) = \Phi^{-1}(F(x)) = \frac{1}{\sigma}x - \frac{m}{\sigma} \quad (3.11)$$

for any normal distribution, or

$$g(x) = \Phi^{-1}(F(x)) = \frac{1}{\sigma} \ln x - \frac{m}{\sigma} \quad (3.12)$$

for any lognormal distribution. Then we plot the data pairs $\ln(x)$, $g(x)$ on a two dimensional coordinate system and label manually the corresponding probability values on the vertical axis. Such lognormal probability plot is demonstrated in Figure 3.3 where we notice that the horizontal axis is a log-scale. Therefore, if the $F(x)$ is the CDF of a lognormal variate, the points of $g(x)$ will definitely form a straight line.

Now with $m > 2$ distinct values of the CDF $F^*(x)$ of a sum of lognormal RV's, a straight line, i.e. $p(x) = c_0 + c_1 g_1$ with $g_1 = \ln x$, on the lognormal probability paper is to be found in the sense of

$$\min_{c_0, c_1} \max_{1 \leq i \leq m} |g(x_i) - (c_0 + c_1 \ln x_i)| \quad (3.13)$$

where $g(x)$ is the function after the transformation (3.10) of $F^*(x)$.

According to the alternation theorem [21], there are at least 3 distinct points $a \leq x_1 < x_2 < x_3 \leq b$ which have maximum deviation E_1 . Through observing the shape of the CDF of a sum, we find that the CDF of a sum is a concave function with $g'' < 0$. So g' is monotonic function. Since

$$g(x_k) - p(x_k) = \pm E_1 \quad k = 1, 2, 3,$$

there is only one root on $[a, b]$ for the equation

$$g'(x_k) - p'(x_k) = g'(x_k) - c_1 = 0.$$

That is

$$g'(x_2) = c_1.$$

The other two maximum discrepancy points must occur at the two ends of the interval, i.e.

$x_1 = a, x_3 = b$. Then the coefficients are found by the expressions [22]

$$c_1 = \frac{g(b) - g(a)}{b - a}, \quad (3.14a)$$

$$c_0 = \frac{1}{2}[g(a) + g(x_2)] - \frac{a + \ln(x_2)}{2} \frac{g(b) - g(a)}{b - a} \quad (3.14b)$$

where x_2 is the unique solution of

$$g'(\ln x_2) = \frac{g(b) - g(a)}{b - a}. \quad (3.14c)$$

The numerical procedure for the minimax approximation shown in Figure 3.3 is described as follows:

1. Connect the two ends of the curve to form a line AB. The slope of $p(x)$, i.e. c_1 , is the slope of the line AB.
2. Find a point C on the curve whose derivative is c_1 , i.e. its tangent is parallel to the line AB or a parallel line to AB passing this point is the most far away to the line AB;
3. Then $p(x)$ should be in the middle position between the tangent of point C and the line AB;
4. The mean m^* and the standard deviation σ^* approximated by minimax approximation are given by (3.12), i.e.

$$m^* = -c_0/c_1, \quad (3.15)$$

$$\sigma^* = 1/c_1. \quad (3.16)$$

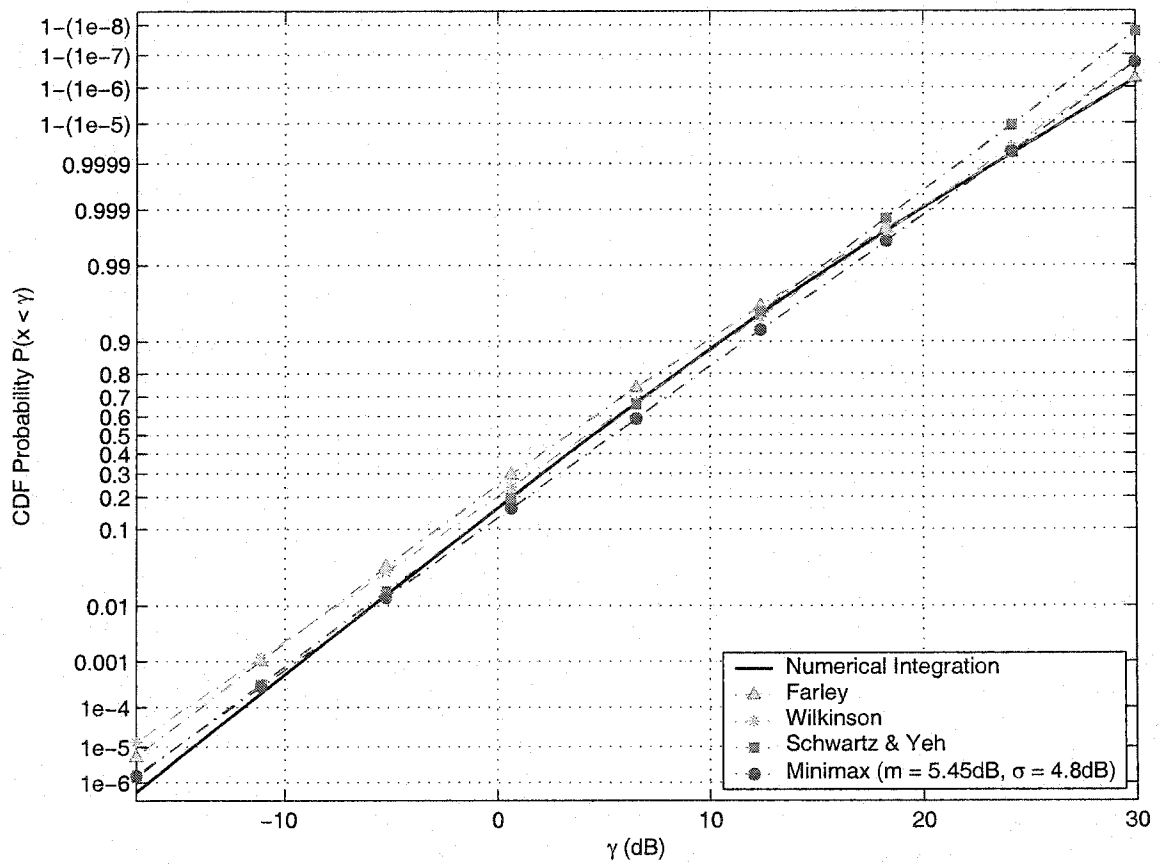


Figure 3.4. The CDF of a sum of 2 i.i.d. lognormal RV's ($m = 0$ dB, $\sigma = 6$ dB).

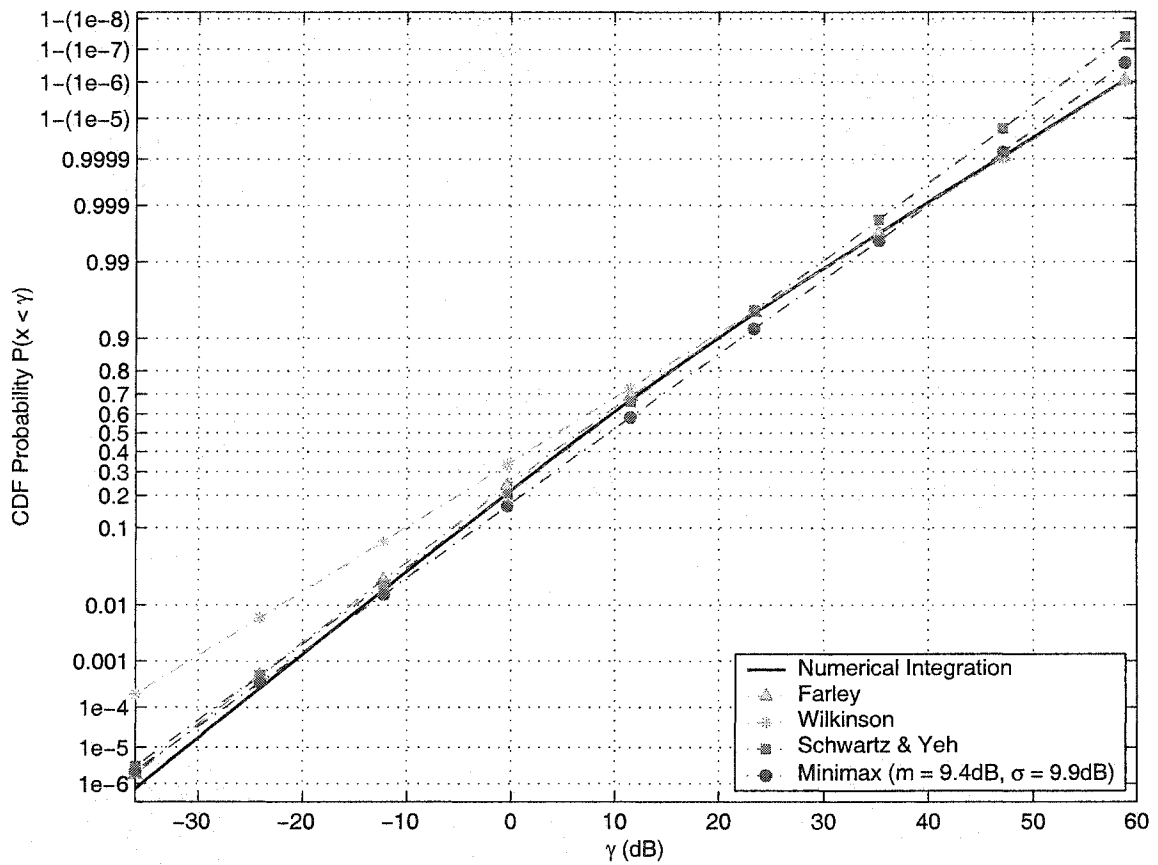


Figure 3.5. The CDF of a sum of 2 i.i.d. lognormal RV's ($m = 0$ dB, $\sigma = 12$ dB).

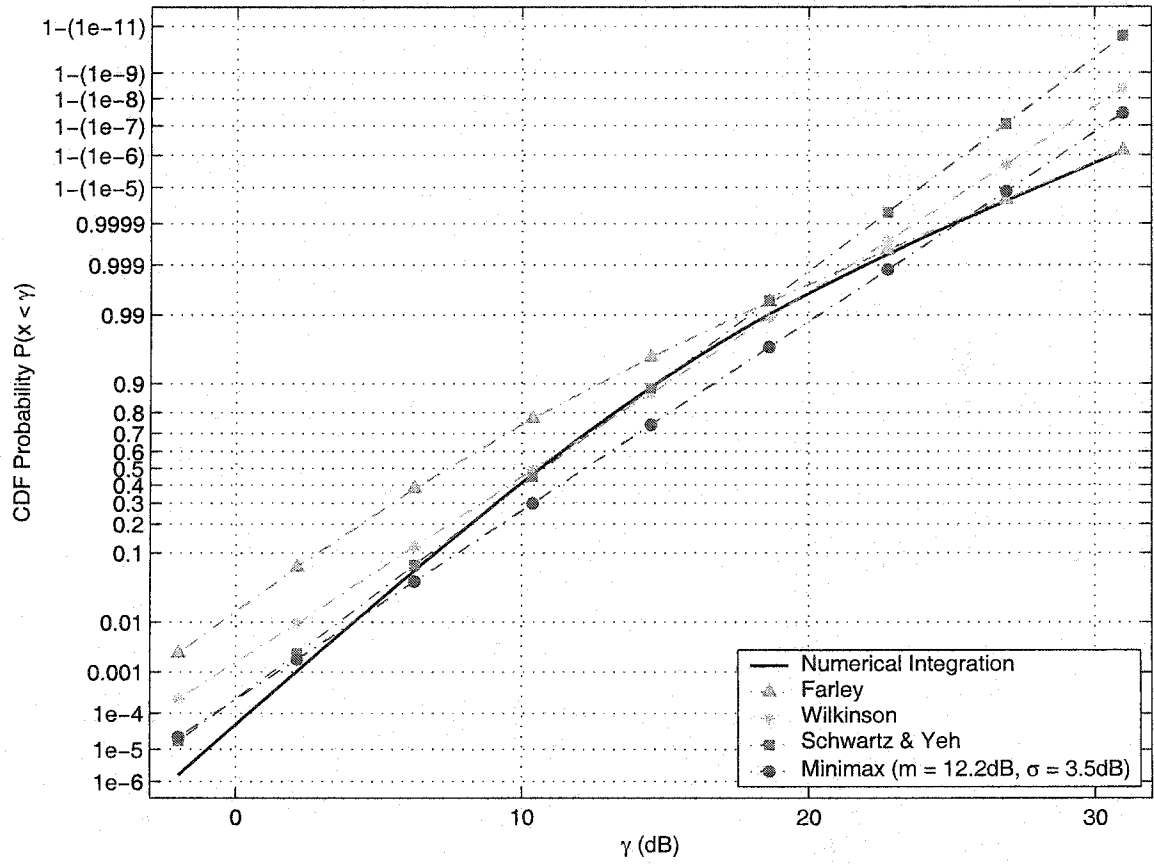


Figure 3.6. The CDF of a sum of 6 i.i.d. lognormal RV's ($m = 0$ dB, $\sigma = 6$ dB).

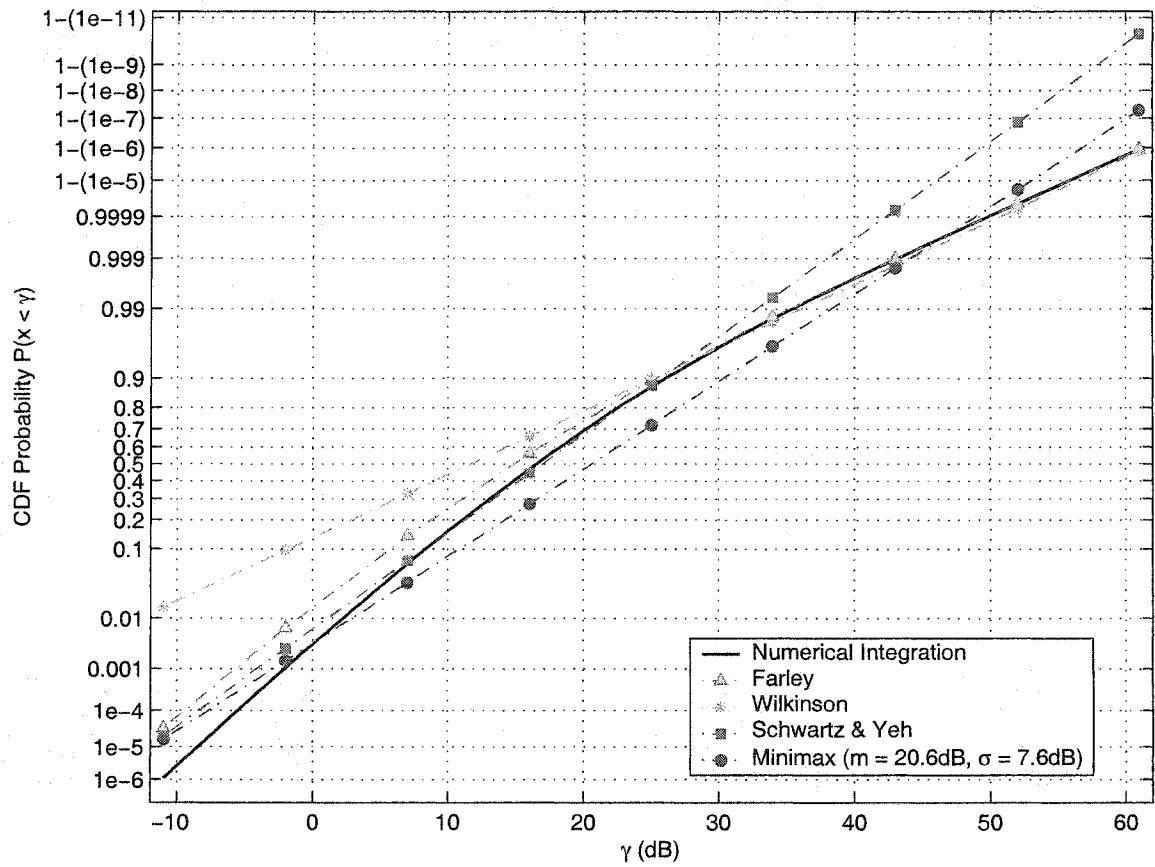


Figure 3.7. The CDF of a sum of 6 i.i.d. lognormal RV's ($m = 0$ dB, $\sigma = 12$ dB).

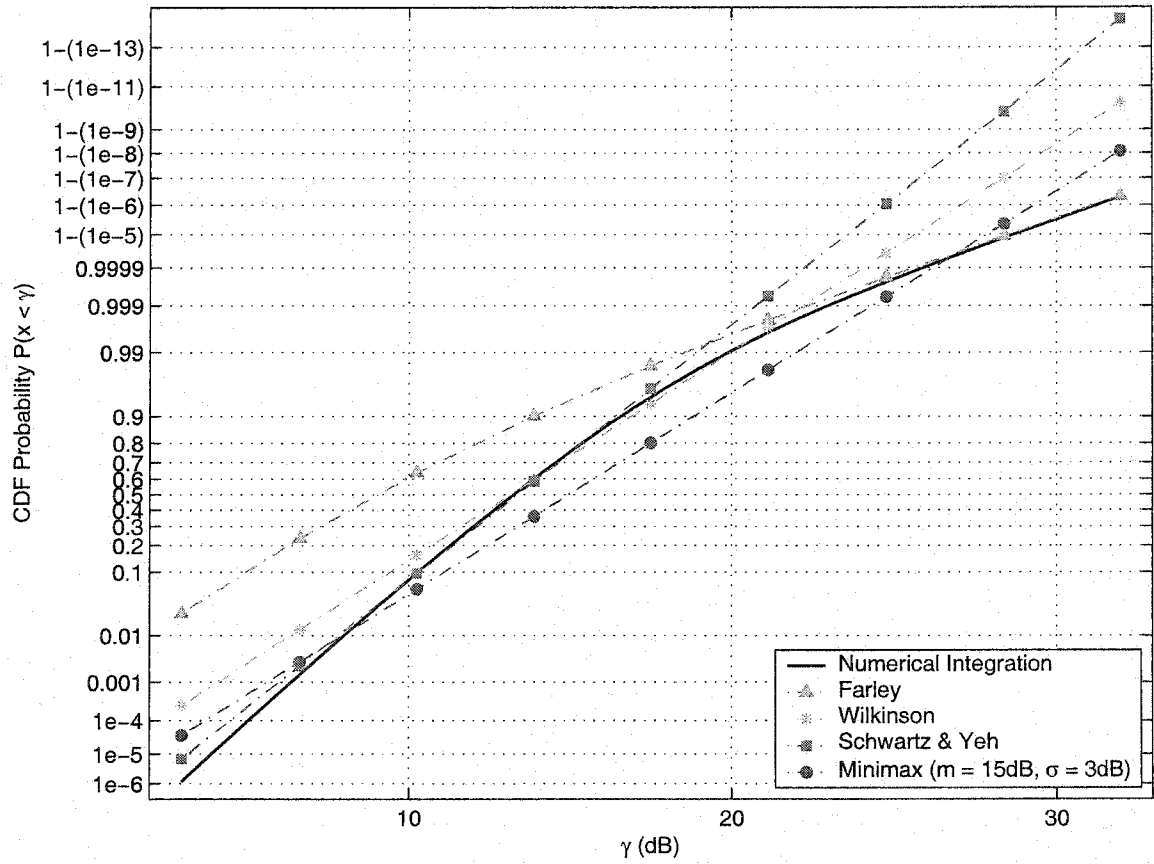


Figure 3.8. The CDF of a sum of 10 i.i.d. lognormal RV's ($m = 0$ dB, $\sigma = 6$ dB).

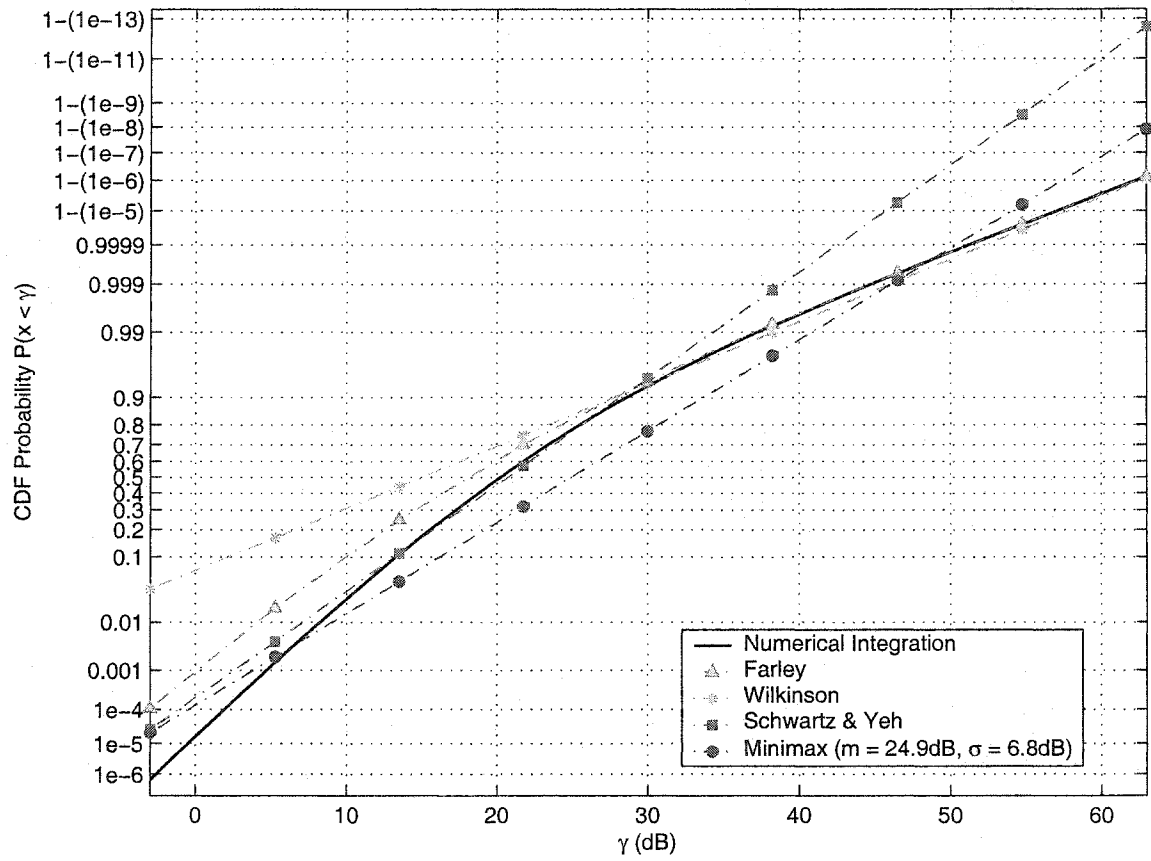


Figure 3.9. The CDF of a sum of 10 i.i.d. lognormal RV's ($m = 0$ dB, $\sigma = 12$ dB).

Table 3.1. Minimax approximation of the sums of i.i.d lognormal RV's

dB spreads of L_i	Number N	Minimax m^* (dB)	Minimax σ^* (dB)
6	2	5.45	4.8
	6	12.2	3.5
	10	15.0	3.0
7	2	6.08	5.7
	6	13.6	4.2
	10	16.5	3.7
8	2	6.62	6.5
	6	14.9	4.9
	10	18.1	4.3
9	2	7.38	7.4
	6	16.4	5.6
	10	19.7	4.9
10	2	8.0	8.2
	6	17.7	6.2
	10	21.4	5.5
11	2	8.76	9.1
	6	19.2	6.9
	10	23.2	6.2
12	2	9.44	9.9
	6	20.6	7.6
	10	24.9	6.8

Figure 3.4 - 3.9 illustrate the CDF plots and their minimax approximations of $N = 2, 6, 10$ i.i.d. lognormal sums for 6 dB and 12 dB spreads, respectively, as well as Wilkinson's, Schwartz & Yeh's and Farley's approximations for comparison. Table 3.1 summarizes the approximate values of the mean m^* and the standard deviation σ^* by using minimax approximation for sums of $N = 2, 6, 10$ i.i.d. lognormal RV's with zero mean and different dB spreads from 6 dB to 12 dB.

3.3 Discussion

The CDF's of lognormal sums on the lognormal probability paper provide us a more detailed view to look at the problem of lognormal sums and to compare previous approximate methods. From the graphs in the previous section, we found that our work agrees with the previous conclusions in many aspects. In addition, new conclusions are drawn. The following is our discussion.

1. All the methods give relative good approximation when $N = 2$ because the sum distribution of two variates is very close to a lognormal distribution.
2. Schwartz & Yeh's method always gives excellent agreements to numerical results in the range of $[0.1, 0.9]$ but has significant deviations in the tail values of complementary CDF, particularly for large summands number N . When $\sigma = 6$ dB and $N = 10$, for instance, the maximum discrepancy between Schwartz & Yeh's approximation and the numerical data reaches more than 7 orders of magnitude. Schwartz & Yeh's approximation extremely underestimates the values of the tails of complementary CDF's. Its performance for values of CDF tails is better than that for values of complementary CDF tails.

3. In contrast, the simple Wilkinson's method provides better approximation to the values of the complementary CDF's that are less than 0.1 than Schwartz & Yeh's method. Its accuracy improves when the values of dB spreads increase. For 12 dB spread, it is found that the tail values approximated by Wilkinson's method almost match with those obtained by numerical integration. On the other hand, its estimates to the tail values of the CDF's are worse than those of Schwartz & Yeh's. The maximum deviation exceeds 4 orders of magnitude for the case of 12 dB spread and $N = 10$.
4. Farley's approach is an upper bound to the CDF and strict lower bound to the complementary CDF tails but the performance becomes worse when the dB spread becomes smaller or the number N of summands becomes greater. The maximum deviation also exceeds 4 orders of magnitude when $\sigma = 6$ dB and $N = 10$.
5. If it is assumed that the sum distribution is also a lognormal RV, both Schwartz & Yeh's and Wilkinson's approximation to that lognormal distribution are not good. The straight line obtained by Schwartz & Yeh's method on the lognormal probability paper is only close to the values of CDF's in the range of $[0.1, 0.9]$, just approximately like a tangent of an arc, while the line derived by Wilkinson's method roughly looks like another tangent of this arc that touches the arc in a different place. In the global view, the minimax approximation that minimizes the maximum deviations provides more accurate approximations than Schwartz & Yeh's and Wilkinson's methods. The maximum error in our examples is less than 2 orders of magnitude.
6. Since both the CDF and the complementary CDF with values less than 10^{-1} are of practical interest, the minimax approximation provides better performance than

Schwartz & Yeh's and Wilkinson's methods on values of both CDF tails and complementary CDF tails.

In this and previous sections, we examine the sum distributions of i.i.d. lognormal RV's and provide minimax approximations to these sum distributions. In addition, this minimax approximation method can be easily extended to non-i.i.d. cases that we will examine in next two sections.

3.4 Minimax approximations of sums with different power means

Based on (2.4c) and (3.6), the same numerical integration method is used to calculate the CDF's of sums which have the same dB spread but different power means of the summands. Two examples with different power means distributed in $[-3 \text{ dB}, 3 \text{ dB}]$ and $[-25 \text{ dB}, 25 \text{ dB}]$ respectively are given for each of 6 dB spread and 12 dB spread. Therefore, the former one has smaller difference in power means of the summands than the later. All these examples are illustrated in Figures 3.10 - 3.13. We observe that three approximations, Wilkinson's, Schwartz & Yeh's and Farley's methods present similar performances to those of the i.i.d. cases. Schwartz & Yeh's method provides good approximations to CDF's in the range of $[0.1, 0.9]$ but it has great deviations in the two tails. Wilkinson's method is better than Schwartz & Yeh's method when the values of the complementary CDF's are less than 0.1. Farley's approach is a strict lower bound to the complementary CDF tail but its performance degrades for small dB spreads. When the differences in the power mean values of the summands increases, the sum distribution is more close to a straight line in the lognormal probability paper. Thus, the performance of previous methods become better. For instance,

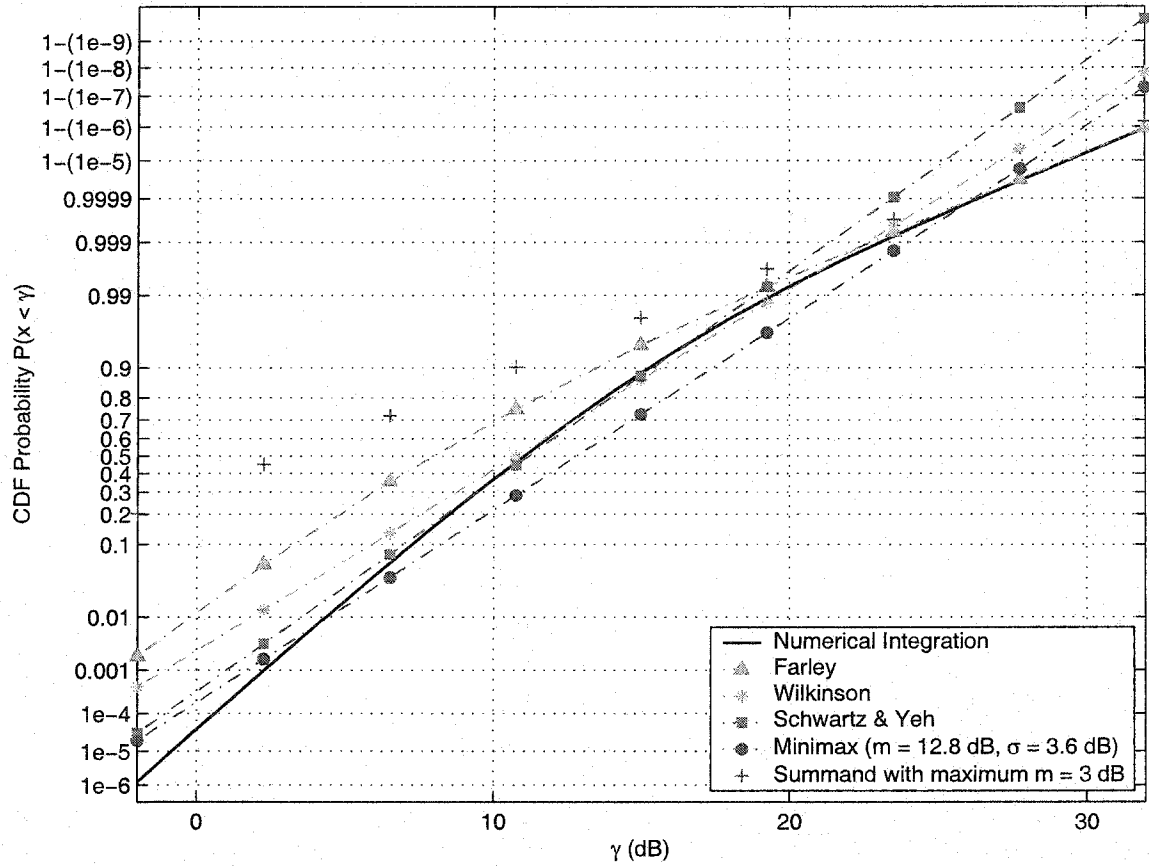


Figure 3.10. The CDF of a sum of 6 lognormal RV's with different power means ($m_1 = -3$ dB, $m_2 = -2$ dB, $m_3 = -1$ dB, $m_4 = 1$ dB, $m_5 = 2$ dB, $m_6 = 3$ dB) and the same dB spreads ($\sigma_i = 6$ dB).

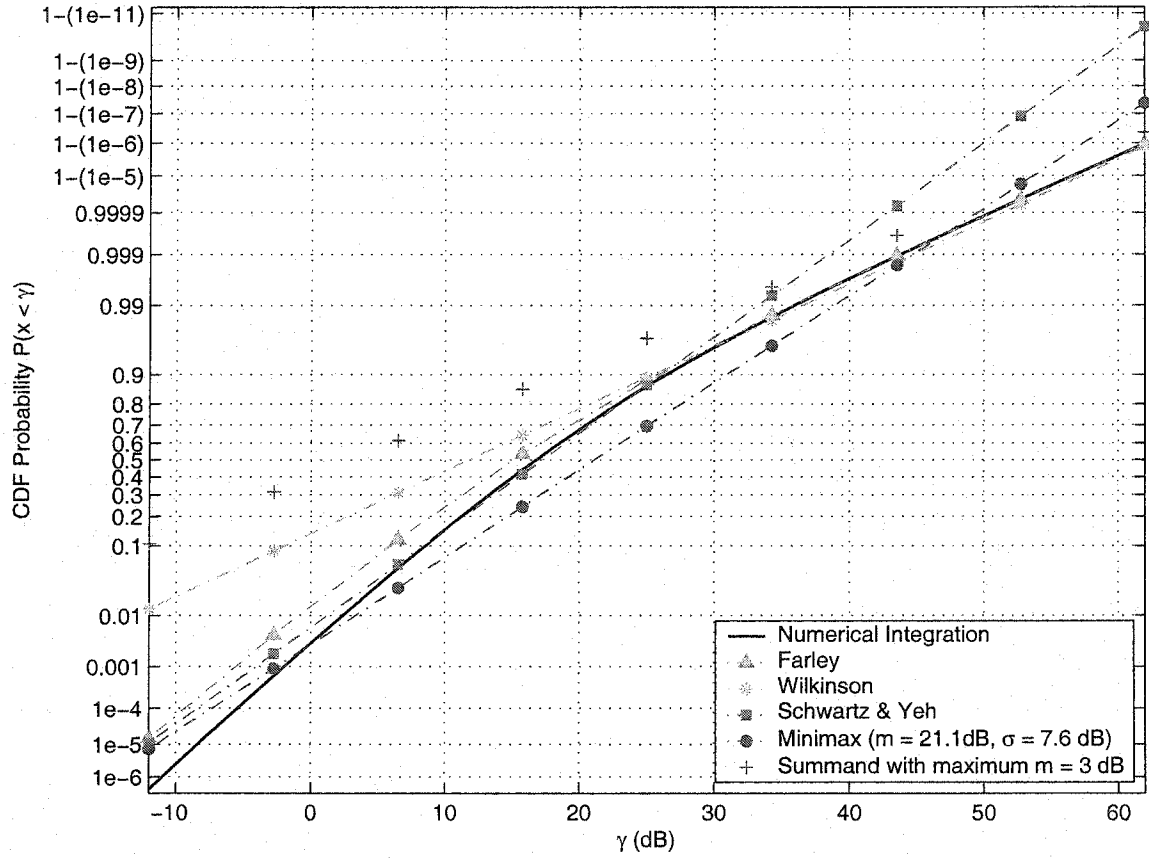


Figure 3.11. The CDF of a sum of 6 lognormal RV's with different power means ($m_1 = -3$ dB, $m_2 = -2$ dB, $m_3 = -1$ dB, $m_4 = 1$ dB, $m_5 = 2$ dB, $m_6 = 3$ dB) and the same dB spreads ($\sigma_i = 12$ dB).

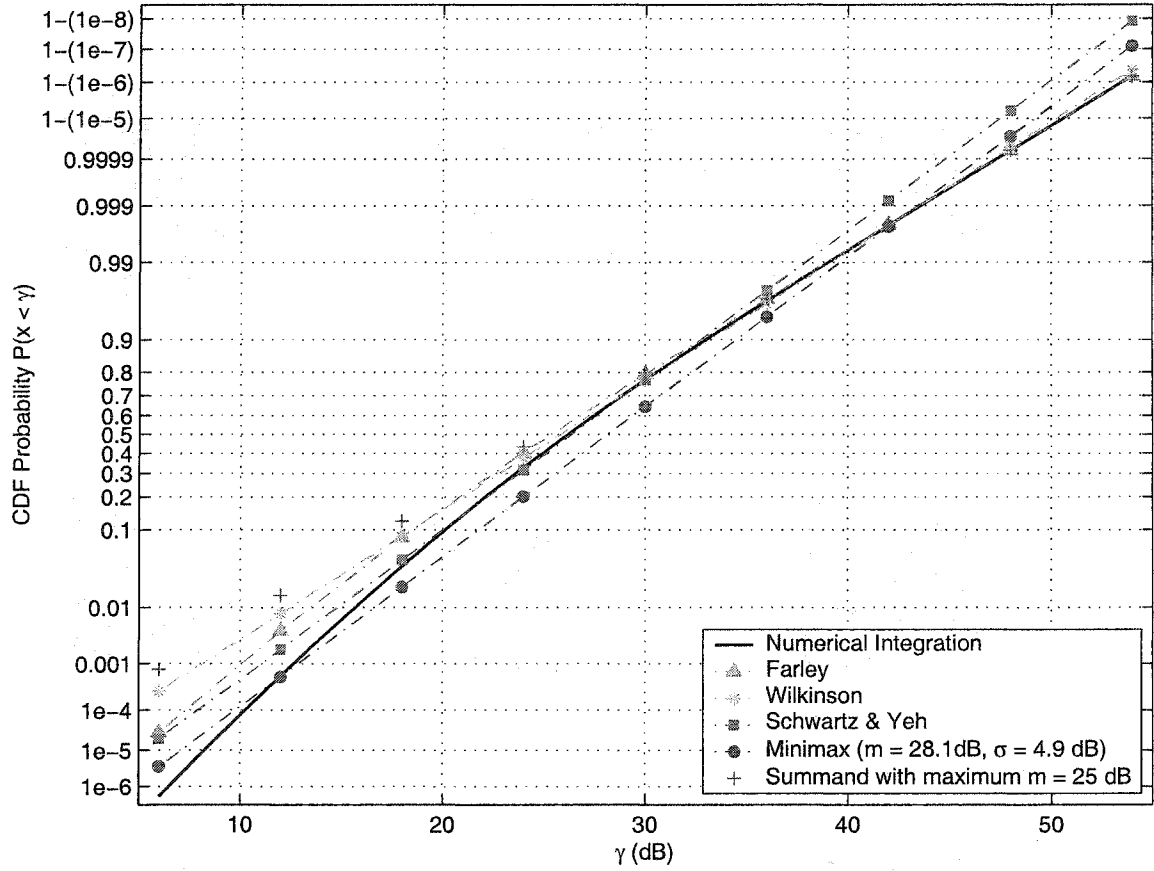


Figure 3.12. The CDF of a sum of 6 lognormal RV's with different power means ($m_1 = -25$ dB, $m_2 = -15$ dB, $m_3 = -5$ dB, $m_4 = 5$ dB, $m_5 = 15$ dB, $m_6 = 25$ dB) and the same dB spreads ($\sigma_i = 6$ dB).

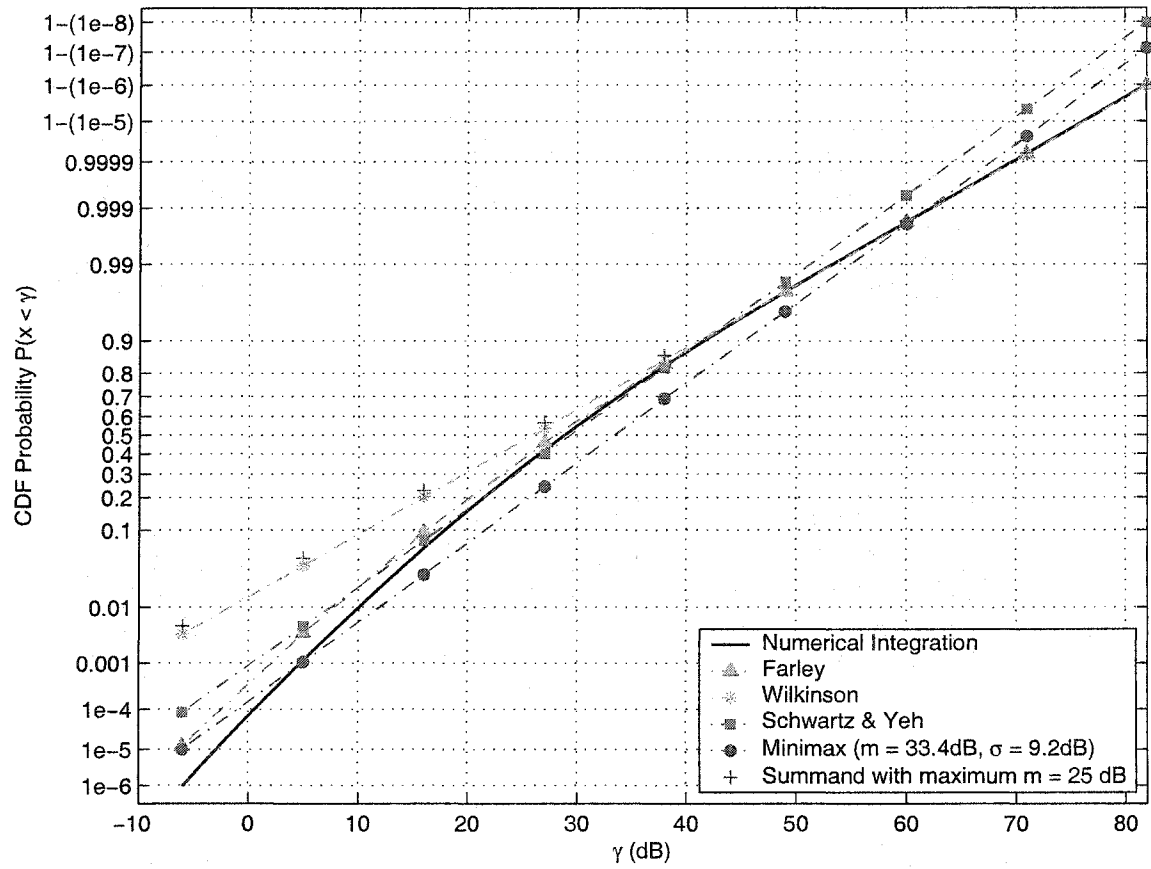


Figure 3.13. The CDF of a sum of 6 lognormal RV's with different power means ($m_1 = -25$ dB, $m_2 = -15$ dB, $m_3 = -5$ dB, $m_4 = 5$ dB, $m_5 = 15$ dB, $m_6 = 25$ dB) and the same dB spreads ($\sigma_i = 12$ dB).

the maximum deviation of Schwartz & Yeh's approximation decreases roughly from 4 orders of magnitude to 2 orders of magnitude. This is because changing the power mean of a lognormal RV is equivalent to scaling the RV. When the power means (scalings) are substantially different, the largest of the scaled RV's dominates the sum and the CF tends toward the CF of the single, dominant RV which is a lognormal RV. In the global view, the minimax approximation provides more precise estimations than other methods.

3.5 Minimax approximations of sums with different dB spreads

Figures 3.15 and 3.15 give the CDF's of two sums that have the same power mean but different dB spreads of the summand. One has the summands with different dB spreads in the range of [6 dB, 12 dB] and the other one is in [7.5 dB, 10 dB]. In these figures we plot the CDF of the summand with the greatest dB spread as well. It is found that large values of the CDF of the sum and those of the summand with the greatest dB spread overlap which clearly demonstrates the asymptotic character of the sum distribution [3]. Moreover, for the case of sums with different dB spreads, Schwartz & Yeh's method has a more significant error in the tail of the complementary CDF than that for the i.i.d. case. We take some following typical cases for example. In Figure 3.6 for the sum of 6 i.i.d. summands with 6 dB spread, the maximum error given by Schwartz & Yeh's method is about 4 orders of magnitude while the maximum error in Figure 3.15 for the sum of 6 non-i.i.d. summands with the dB spreads in [6 dB, 12 dB] is about 9 orders of magnitude. The similar phenomenon also happens to Wilkinson's method. However, the maximum deviations decrease when the difference among the dB spreads of the summands decreases.

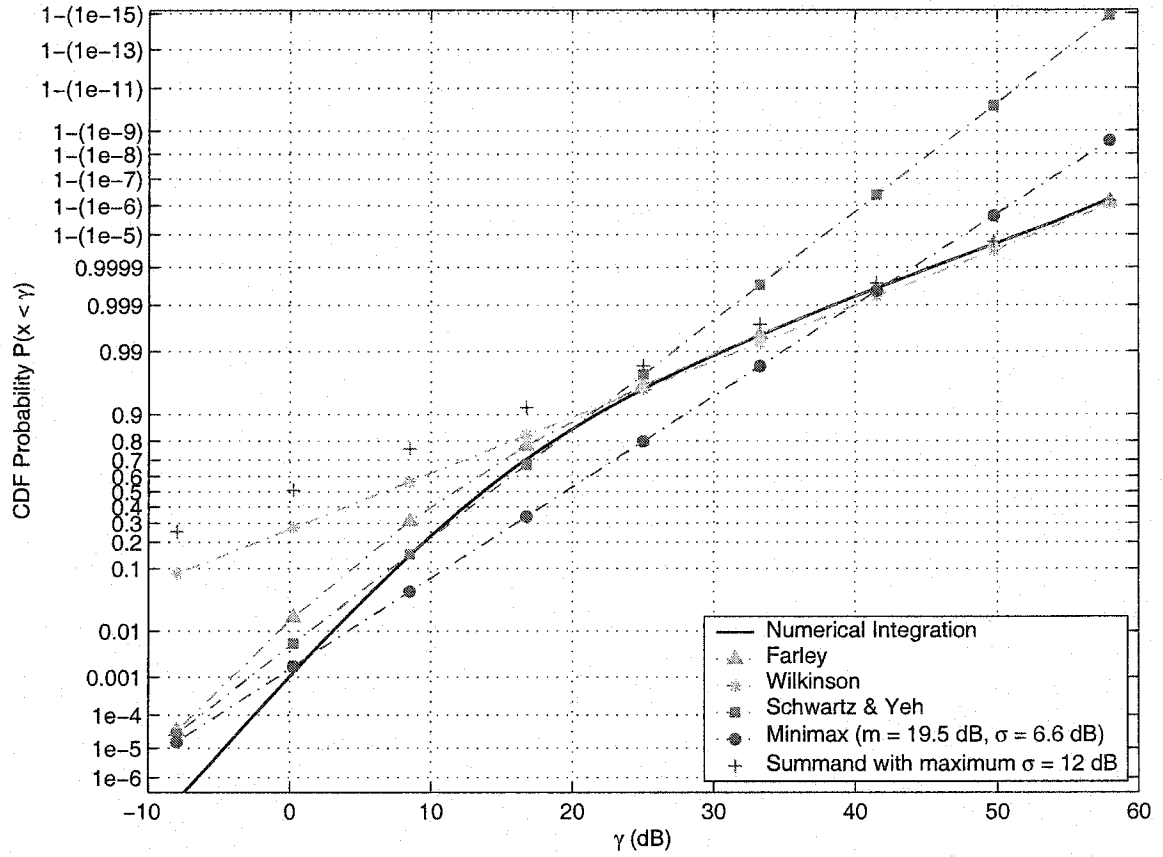


Figure 3.14. The CDF of a sum of 6 lognormal RV's with different dB spreads ($\sigma_1 = 6$ dB, $\sigma_2 = 8$ dB, $\sigma_3 = 9$ dB, $\sigma_4 = 10$ dB, $\sigma_5 = 11$ dB, $\sigma_6 = 12$ dB) and the same power means ($m_i = 0$ dB).

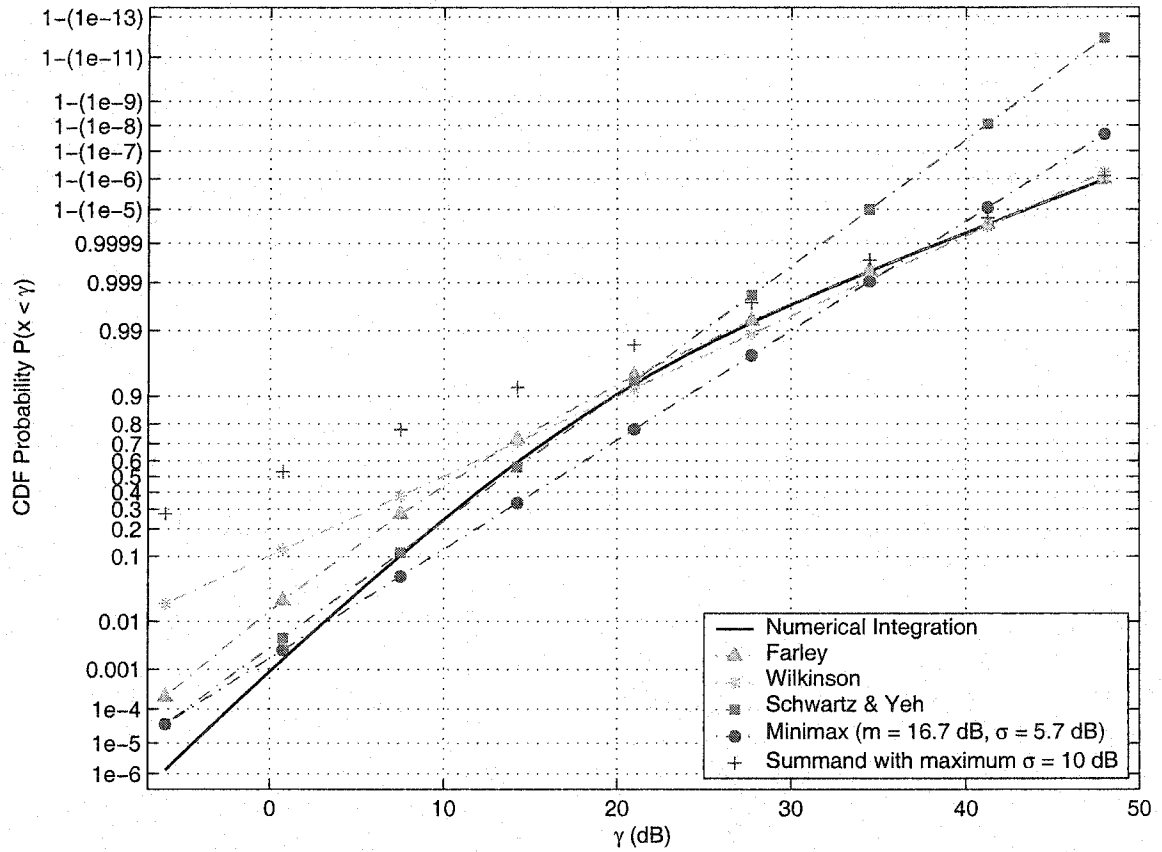


Figure 3.15. The CDF of a sum of 6 lognormal RV's with different dB spreads ($\sigma_1 = 7.5$ dB, $\sigma_2 = 8$ dB, $\sigma_3 = 8.5$ dB, $\sigma_4 = 9$ dB, $\sigma_5 = 9.5$ dB, $\sigma_6 = 10$ dB) and the same power means ($m_i = 0$ dB).

3.6 Conclusion

In conclusion, we have examined the goodness of the well-accepted assumption that a sum of independent lognormal RV's is also lognormal distributed. It was found that this assumption is good for sums of $N = 2$ i.i.d. summands but becomes worse when the number of summands increases or the difference among the dB spreads of the summands increases. Three previous approximate approaches, Schwartz & Yeh's, Wilkinson's and Farley's methods, have been compared with the results obtained by numerical computation. It was seen that none of them is valid over a wide range of parameters. The approximations obtained by Schwartz & Yeh's method deviate significantly in the tails of the complementary CDF's while the performances of Wilkinson's method are not good for tails of the CDF's. Farley's approximation is worse than others when the dB spread is small or the number of summands is large.

A new paradigm for constructing approximations to lognormal sum distributions was created in this chapter. The minimax approximation was developed to estimate a lognormal distribution to a sum distribution of independent lognormal RV's. Our work shows that this approximation is better than Schwartz & Yeh's and Wilkinson's methods in the global view.

Chapter 4

Conclusion

Determining the sum distribution of independent lognormal RV's is a longstanding problem even though it is important for assessing the capacity and system performance in cellular mobile communication systems. Many approximate solutions to this problem such as Wilkinson's, Schwartz & Yeh's, and Farley's methods have been developed. Wilkinson's and Schwartz & Yeh's approximations are based on the assumption that a sum of independent lognormal RV's is another lognormally distributed variable while Farley's method provides a lower bound to the complementary CDF of a sum of lognormal RV's. But none of them is valid over a wide range of parameters.

A standard approach for finding the distribution of a sum of independent RV's is to use characteristic functions. But an exact expression for the CF of a lognormal RV is not known. Even the numerical computation of the CF was considered to be substantially difficult [1], [9]. In this thesis, three numerical methods have been investigated and compared in terms of their efficiencies. The most efficient one, the modified Clenshaw-Curtis numerical integration, was found to evaluate a lognormal CF and the inverse transform of a CF. Additionally, this method was tested to be valid for the case of lognormal PDF in the range

of practical interests.

Furthermore, the CDF of a sum of N independent lognormal RV's was obtained by the numerical integration of the inverse transform of the CF of the sum. We found that the CDF of a lognormal sum is left-skewed relative to the lognormal distribution. This leads Wilkinson's and Schwartz & Yeh's approximations to have large discrepancy in certain areas. Schwartz & Yeh's method has significant deviations in the tails of the complementary CDF's even though it provides an excellent approximation for the CDF values in the range of 0.1 - 0.9. Wilkinson's method provides better approximation than Schwartz & Yeh's to the tails of complementary CDF values but it is worse in the CDF tails. Meanwhile, the performance of Farley's approximation degrades when the number of the summands increases or the dB spreads of the summands decreases.

We conclude that if we use a lognormal RV to approximate a sum distribution, neither Schwartz & Yeh's nor Wilkinson's approaches for determining the mean value and variance of the corresponding Gaussian distribution of the sum is good. Retaining the lognormal sum assumption, a new and more precise estimation in the global point of view, the minimax approximation, is presented in this thesis. This method was examined for the case of i.i.d. summands and the case of summands that are not i.i.d.

The contribution of this thesis is summarized as follows:

1. An efficient numerical method was found to evaluate the CF of a lognormal RV and sum distributions of independent lognormal RV's.
2. The goodness of the well-accepted assumption that a sum of independent lognormal RV's is also lognormally distributed was examined and a more detailed comparison of the previous works was given.

3. A new paradigm of constructing approximations to lognormal sum distributions, the minimax approximation, was presented for determining mean values and variances of the corresponding Gaussian distributions.

References

- [1] T. S. Rappaport, *Wireless Communications Principles and Practice*, 2nd ed. New Jersey: Prentice Hall PTR, 2002.
- [2] N. C. Beaulieu, A. A. Abu-Dayya, and P. J. McLane, "Comparison of methods of computing lognormal sum distributions and outages for digital wireless applications," in *IEEE ICC 94*, New Orleans, USA, June 1994, pp. 1270–1275.
- [3] S. C. Schwartz and Y. S. Yeh, "On the distribution function and moments of power sums with lognormal components," *Bell Syst. Tech. J.*, vol. 61, no. 7, pp. 1441–1462, Sept. 1982.
- [4] N. C. Beaulieu, A. A. Abu-Dayya, and P. J. McLane, "Estimating the distribution of a sum of independent lognormal random variable," *IEEE Trans. Commun.*, vol. 43, pp. 2869–2873, Dec. 1995.
- [5] N. C. Beaulieu, A. A. Abu-Dayya, and P. J. McLane, "Outage probabilities in the presence of correlated lognormal interferers," *IEEE Trans. Veh. Tech.*, vol. 43, pp. 164–173, Feb. 1994.

- [6] P. Cardieri and T. S. Rappaport, "Statistics of the sum of lognormal variables in wireless communications," in *IEEE Vehicular Technology Conference Proceedings*, Tokyo, 2000, vol. 3, pp. 1823–1827.
- [7] R. C. French, "The effect of fading and shadowing on channel reuse in mobile radio," *IEEE Trans. Veh. Tech.*, vol. 28, no. 3, pp. 171–181, Aug. 1979.
- [8] Y. Yeh and S. C. Schwartz, "Outage probability in mobile telephony due to multiple lognormal interferers," *IEEE Trans. Commun.*, vol. 32, no. 4, pp. 380–388, April 1984.
- [9] B. P. Lathi, *Modern Digital and Analog Communication System*, 3rd ed. Oxford: Oxford University Press, 1998.
- [10] R. Barakat, "Sums of independent lognormally distributed random variables," *J. Opt. Soc. Am*, vol. 66, no. 3, pp. 211–216, Mar. 1976.
- [11] N. C. Beaulieu, "Private communications," Dec. 2001.
- [12] R. L. Burden and J. D. Faires, *Numerical Analysis*, 7th ed. New York: Brooks/Cole, 2001.
- [13] P. J. Davis and P. Rabinowitz, *Methods of Numerical Integration*, 2nd ed. Academic Press, 1975.
- [14] A. V. Oppenheim and R. W. Schaffer, *Discrete-time Signal Processing*, 2nd ed. New Jersey: Prentice-Hall, 1999.
- [15] R. Piessens, E. de Doncker-Kapenga, C. Uberhuber, and D. Kahaner, *QUADPACK A subroutine package for automatic integration*. Springer Verlag, 1983.

- [16] P. Wynn, "On the convergence and stability of the epsilon algorithm," *J. SIAM Numer. Anal.*, vol. 3, no. 1, pp. 91–98, 1966.
- [17] S. O. Rice, "Efficient evaluation of integrals of analytic functions by the trapezoidal rule," *Bell Syst. Tech. J.*, vol. 52, no. 5, pp. 707–722, May-June 1973.
- [18] A. Papoulis, *Probability, Random Variables and Stochastic Processes*. New York: McGraw-Hill, 1991.
- [19] J. L. Devore, *Probability and Statistics for Engineering and the Sciences*, 5th ed. Duxbury, 2000.
- [20] S. B. Slimane, "Bounds on the distribution of a sum of independent lognormal random variables," *IEEE Trans. Commun.*, vol. 49, pp. 975–978, June 2001.
- [21] W. A. Janos, "Tails of the distribution of sums of lognormal variates," *IEEE Trans. Inform. Theory*, vol. IT-16, pp. 299–302, May 1970.
- [22] E. W. Cheney, *Introduction to Approximation Theory*. New York: McGraw-Hill, 1966.
- [23] P. J. Davis, *Interpolation and Approximation*. Blaisdell Publishing Company, 1963.